Spring 5-2011

Adsorbents with Chemically Bonded Saccharide Surfaces: Synthesis and Application for Stereoisomer Separation and The Synthesis of Chiral Porous Silicas using Templates Chiral Surfactant

Edwin Vega
Seton Hall University

Adsorbents with Chemically Bonded Saccharide Surfaces: Synthesis and Application for Stereoisomer Separation

And

The Synthesis of Chiral Porous Silicas using Templates Chiral Surfactant

Edwin Vega

Dissertation submitted to the Department of Chemistry and Biochemistry of Seton Hall University in fulfillment of the requirements for the degree of

Doctor of Philosophy

May 2011

South Orange, New Jersey

To my family:

My wife, Ana

My Children, Kevin, Steve and Andy

My parents, Maria and Pedro

"The whole of science is nothing more than a refinement of everyday thinking."

--Albert Einstein

We certify that we have read this dissertation and that in our opinion it is sufficient in scientific scope and quality as a dissertation for the degree of Doctor of Philosophy.

APPROVED

Cecilia H. Marzabadi, Ph.D.
Research Mentor

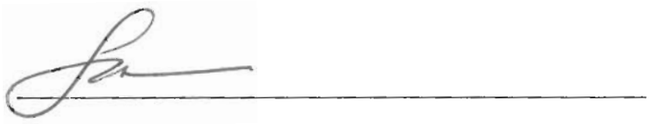

Alexander Y. Fadeev, Ph.D.
Research Mentor

Yuri Kazakevich, Ph.D.
Member of Dissertation Committee

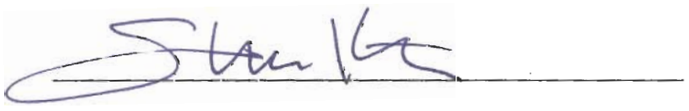

Stephen P. Kelty, Ph.D.
Chair, Department of Chemistry and Biochemistry

Acknowledgements

I would like to express my gratitude to my advisors, Dr. Cecilia Marzabadi and Dr. Alexander Fadeev, for their support, patience, and encouragement during my graduate studies. They were always available when I needed them. I will be forever grateful of the time they devoted to increasing my abilities as a chemist in this multidisciplinary research. Their scientific and editorial advice was really important to the completion of this dissertation.

I would like to thank also Dr. Yuri Kazakevich. Dr. Kazakevich donated two of his HPLC instruments for this research during residency at Seton Hall University. He also assisted me in packing all my saccharide columns and provided me with wise advice for chromatography separations.

I would like to also acknowledge Dr. Jessica Cha and Dr. Ralph Ryall from Johnson and Johnson Pharmaceutical Research Development group (JNJ PRD). Without their support, I would not be able to complete this thesis. I will always remember their encouragement to complete my doctorate.

I am thankful to Dr. Brigitte Segmuller and Dr. Alexandra Shedlow for their guidance and help in the NMR spectroscopy group at JNJ PRD. I will never forget their encouragement and their advice, especially on the spectroscopy part of my thesis. I also wish to acknowledge Gyorgy Vas and Robertson Microlit Laboratories for their assistance on the MALDI and elemental analysis respectively.

I would also like to acknowledge Dr. Frank Bernardoni, Tyler Batchelor, Ivanna Khmelynska, Sunil Sarecha, and Vikram Basava from Seton Hall University. I thank Dr.

Bernardoni for his helpful discussions in regards to surface materials science. Tyler and Ivanna were two undergraduate students whom assisted me on the pseudomorphic transformation and the co-condensation projects. Sunil assisted me with the isolation of the maltodecatriose. Vikram provided me with one of the anomeric analytes.

Lastly, I would like to thank my wife Ana and children Kevin, Steve and Andy. I admire Ana's patience with me during the past few years. Ana's and my children's support was very crucial for this dissertation. Their encouragement was in the end what made this dissertation possible.

Abstract

Adsorbents with Chemically Bonded Saccharide Surfaces: Synthesis and Application for Stereoisomer Separation

The Synthesis of Chiral Porous Silica Materials using Templated Chiral Surfactants

Edwin Vega

Doctor of Philosophy in Chemistry

Seton Hall University

Dr. Cecilia H. Marzabadi and Dr. Alexander Fadeev, Advisors

Stereoisomeric separation is a common and at times difficult problem. Using chiral materials as stationary phases for stereoisomeric separations is a common practice. Saccharides have many stereocenters making them ideal for stereoselective recognition. They are natural products that are relatively inexpensive. They typically contain numerous functional groups which are mainly hydroxyl groups. Some saccharides have at least one amino group. Our research has focused mainly on the design and synthesis of materials with defined surface structures containing saccharides and the subsequent study of their use in separating stereoisomers such as derivatized monosaccharides, Pirkle's alcohol, and *cis*- and *trans*-stilbene oxide. In addition, we have attempted pseudomorphic transformations of Prodigy and SBA-15 silica to helical silica forms using chiral surfactants.

It is known that carbon-sulfur bonding is hydrolytically stable[1-2] and carbohydrates linked to silica in this fashion have not been reported in the literature. For this reason, we have prepared a series of peracetylated-1-thiol-saccharide analogs (1, 3, 7 and 13 glucose units). The synthesis of peracetylated-1-thiol-saccharides is demonstrated in Chapter 1. These ligands were characterized by high pressure liquid chromatography (HPLC), mass spectrometry (MS), ultraviolet (UV), circular dichroism (CD), matrix-assisted laser desorption/ionization (MALDI) and nuclear magnetic resonance (NMR).

Peracetylated-1-thiol-saccharides were used as ligands on our new class of adsorbents in which a thiol group links peracetylated saccharides to silica through an epoxy-silane linker, glycido-oxypropyl trimethoxysilane. The preparation of these trimethoxysilylated saccharides are also described in Chapter 1. The saccharide stationary phases were prepared using two methods: (1) the direct incorporation of derivatized saccharides onto the silica structure in a process known as co-condensation and, (2) post-synthesis grafting-direct immobization methods.

Chapter 2 discusses the synthesis of mesoporous silica with a well-ordered network of porous materials. These materials were prepared using co-condensation of tetraethyl orthosilicate (TEOS) with trimethoxy-silylated derivatives of peracetylated glucose, maltotriose, and maltoheptaose affording ordered mesoporous SBA-15 type silicas. The post synthesis grafting method was performed by modifying Prodigy silica with analogs (1, 3, 7 and 13 glucose units) following direct immobilization and surface chemical assembly approaches. The post synthesis grafting of the saccharide Prodigy silica materials is described in detail in Chapter 3. The resulting materials from saccharide SBA-15 type and Prodigy silicas were characterized by FTIR, nitrogen

isotherms, TGA, elemental analysis and TEM (for SBA-15 type silica). The saccharide silica stationary phases prepared have been evaluated in normal phase and reverse phase HPLC stereoisomeric separations.

Chapter 4 focuses on the synthesis of chiral mesoporous silicas using the anionic chiral surfactant, N-myristoyl-L-alanine, and the cationic oligosaccharide, chitosan. In order to synthesize these silicas, co-condensation and pseudomorphic transformation techniques were used. These materials were prepared using different temperatures, aging and pH. The resulting materials were characterized by nitrogen isotherms and TEM. TEM data suggests that the new silica forms could have an ordered helical porous structure.

Table of Contents

List of Figures

List of Tables

Chapter 1: Synthesis of peracetylated-1-thiol-saccharides and their trimethoxysilyl derivatives

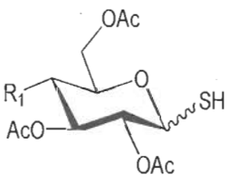

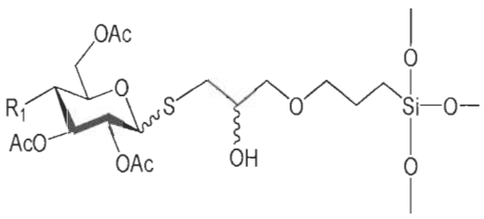

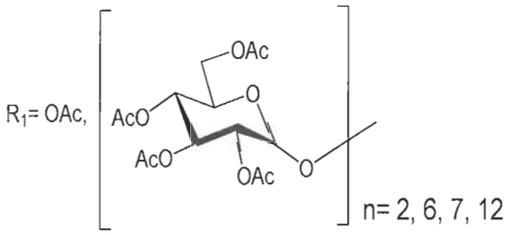

Abstract

The synthesis of a series of peracetylated-1-thiol-saccharides and their trimethoxysilyl derivatives is described in this chapter. They were prepared from the parent saccharides: glucose, maltotriose, maltoheptaose, maltooctaose and maltodextrin. Here, the anomeric thiol group of the peracetylated saccharides was reacted with a 3-glycidoxypropyl trimethoxysilane linker affording novel silane peracetylated-1-thio-saccharides after the epoxy ring opening. These previously unreported, derivatized silane saccharides contain a carbon-sulfur bond known to be hydrolytically stable. These ligands were characterized by high pressure liquid chromatography (HPLC), mass spectrometry (MS), ultraviolet (UV), circular dichroism (CD), matrix-assisted laser desorption/ionization (MALDI) and nuclear magnetic resonance (NMR). The trimethoxysilyl peracetylated-1-thio-saccharides were used as ligands for the surface of our new adsorbents.

Introduction

Carbohydrates are among the most important and abundant natural products. They play important roles in molecular recognition events and the processes that occur in inflammation and cancer metastasis[3-4] and they are known to have interactions with proteins. In addition, they have optical activity. Thus, they also can be used as ligands for enantiomeric separation. The most popular carbohydrates used for chiral stationary phases (CSPs) are cyclodextrins, cellulose and amylosic phases.[5] These saccharides are not used in their native forms due to their poor resolution capacity and problems with handling these highly polar molecules.[4] Their hydroxyl groups are typically protected with various organic functional groups such as ethers and esters.

Okamoto et al[6-10] were some of the first pioneers to synthesize polysaccharides and use them as ligands for chiral recognition. These syntheses were based on the formation of esters and carbamates of amylose and cellulose. Triphenylcarbamate derivatives of amylose and cellulose were used for the investigation of enantioseparation.[7-10] Triphenylcarbamates are typically prepared by using an excess of phenylisocyanate in dry pyridine at about 100 °C. The crude products are isolated by recrystallization from methanol. Since cellulose and cyclodextrins are well known for their chiral selectivity, it is expected that other smaller, linear saccharides will have similar behavior.[11] It is surprising that chiral recognition with these smaller saccharides has not been deeply studied since they play an important role at biological cell surfaces.[12]

Olaf Miller and Jurgen Schulze investigated the enantioselective properties of chiral stationary phases (CSPs) containing the monosaccharides D-glucose and 2-amino-2-deoxy-D-glucopyranose (glucosamine).[13-14] They chemically added the monosaccharide derivatives and bound them on aminopropyl silica gel for use as CSPs.

The selectivity of these CSPs was investigated using a series of β-blocker drugs. The β-blockers were converted into phenyl urethanes for analysis. Miller and Schulze concluded that derivatized monosaccharides could be used as an alternative for the separation of β- blockers and other secondary amine enantiomers.

Stalcup[11] took a similar approach and investigated the chiral selectivity of oligosaccharide mixtures. He derivatized these oligosaccharide mixtures as ethylcarbamates and bound them onto silica gel. With these CSPs, he was able to separate several chiral compounds such as amines and amino acids. He concluded that one of the advantages of using smaller sugars for a CSP is that it allows for a higher concentration of bonded ligand than cyclodextrin and polysaccharides and that these CSPs have a potential use for enantioselective separations.

Aburatani[15] also reported the enantioselectivity of different sizes of derivatized polysaccharides coated onto a silica gel substrate. Cellooligosaccharide, maltooligosaccharide, cyclodextrin and polysaccharide derivatives were reacted with 3, 5-dimethylphenylcarbamate. These sugars were coated onto an activated silica gel (3-aminopropylsilylated silica gel). The highly ordered structure and the chiral selectivity of the materials were compared between the different bound sugars by circular dichroism (CD). Aburatani concluded that similar ordered structures of oligosaccharides provided similar chiral recognition. In addition, he stated that the type of the alcohol protecting group on the sugars influenced the enantioselectivity of the stationary phase. The importance of the sugar derivative on the stereoselectivity had to do with the type of chemical interaction between the derivatives and the enantiomeric analytes, such as hydrogen bonding, dipole-dipole and π- π interactions.

There have been many reports in the literature of derivatized oligosaccharides covalently bound to modified silica using the allylamino[16] functionality, and even by a Schiff base.[17] The drawback of derivatizing surfaces using carbon-nitrogen double bonds is the potential instability of these functional groups under hydrolytic conditions. To the best of our knowledge, thioglycosides have never been investigated in regards to their role in stereoisomer separation. Our goal was to have a novel thiol group on the anomeric carbon of a derivatized sugar and covalently bind it to an activated silica gel for stereoisomeric recognition. A thiol group is a good nucleophile and can react with an epoxy-linker, glycido-oxypropyl trimethoxysilane. This reaction makes a hydrolytically stable carbon-sulfur-carbon bond after ring opening.

In this thesis, the synthesis of the three major components of our new chiral adsorbents is described. The first component is a peracetylated-1-thiol-saccharide used as a chiral selector. The synthesis of a series of these compounds is described in detail in this chapter. The second component is a glycido-oxypropyl trimethoxysilane linker. The reaction between the thiol saccharide and this second component is also discussed in this chapter. The modification of silica, the third component, is described in detail in Chapter 2, Chapter 3 and Chapter 4.

Experimental

Chemicals and Materials

2,3,4,6-tetra-*O*-acetyl-1-thiol-glucopyranose, maltotriose, maltohepatose, maltodextrin (dextrose equivalent 4.0-7.0), 3-glycidoxypropyl-trimethoxysilane (GOPTMS), Chromosolv plus grade acetone (dry with molecular sieve), thiourea, acetic anhydride, 33% HBr in acetic acid, sodium pyrosulfite, and potassium phosphate dibasic were obtained from Sigma Aldrich Chemical Company. Maltooctaose was obtained from Carbosynth (UK).

Instruments

^{1}H and 2D-COSY ^{1}H-^{1}H correlation experiments were recorded with Varian Inova 500 MHz (5 mm Varian BB Direct Observe probe) and Bruker Avance 600 MHz (5mm z-gradient TCI cryoprobe) spectrometers. Mass spectrometry was performed with an ion trap mass spectrometer (Thermo Scientific Instruments, Finnigan LCQ Deca XP MAX), MALDI (Bruker autoflex matrix-assisted laser desorption/ionization - time-of-flight Mass spectrometer). Elemental analyses were performed by Robertson Microlit Laboratories (Madison, NJ). Preparative scale, chromatography was conducted with Agilent 1100 preparative LC-MS. ESI+ reverse phase HPLC (Phenomenex Gemini C18, 10 μm, 21.2 X 250 mm). HPLC conditions: flow rate 22 mL/min; 30 °C; mobile phase (A) 5 mM ammonium formate aqueous, (B) acetonitrile; gradient: 0-25 min, 90 → 10% A, 10 → 90% B. HPLC analytical experiments were performed with an HP Agilent 1110 series, DAD detector interfaced to ChemStation software and MS interfaced to Xcalibur software (Atlantis T3, dC18 columns, 4.6 X 150 mm, 3 μm). HPLC conditions: flow rate 1.0 mL/min; 35 °C; mobile phase (A) 5 mM ammonium formate aqueous, (B)

acetonitrile; gradient: 0-25 min, 80 →0% A, 20 →100% B. HPLC-circular dichroism experiments were performed with an Agilent 1100–Jasco CD-1595 circular dichroism detector interfaced to Empower II software.

Synthesis of peracetylated-1-thiol-saccharides series (n=1, 3, 7, 8, 13)

The synthetic pathway for the preparation of the peracetylated-1-thiol-saccharides (PA-1-thiol-Sac) series is shown in Figure 1-1. These derivatized saccharides were prepared following the procedure reported in the literature[18-20] with some minor modifications. 2,3,4,6-tetra-O-acetyl-1-thiol-glucopyranose (thiol Glc) is commercially available (Sigma-Aldrich). However, the thiol Glc was synthesized once to find the optimum conditions for preparing larger saccharides. The structures of the derivatized saccharides are shown in Figures 1-2, 1-3, 1-4, 1-5 and 1-6

Figure 1-1: Synthesis of peracetylated-1-thiol-saccharides

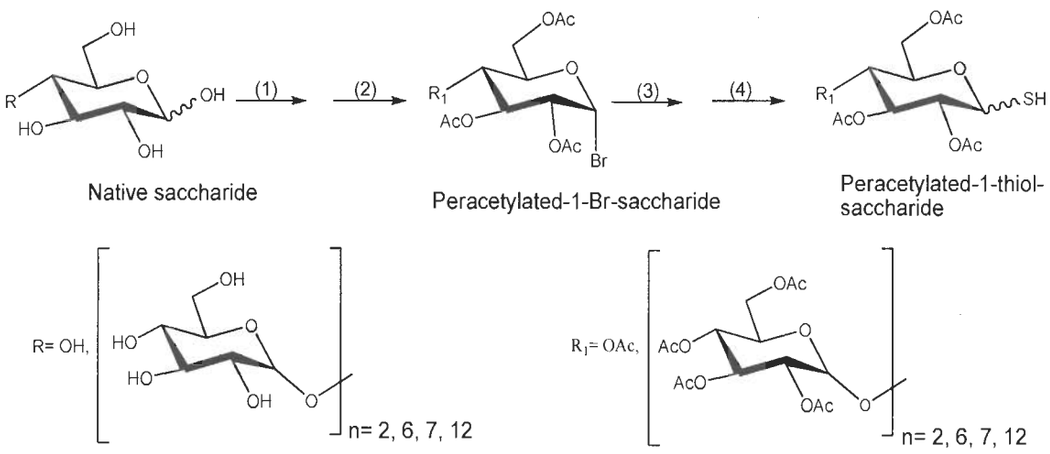

(1) Acetic anhydride, 33% HBr/acetic acid; (2) 33% HBr/acetic acid, dichloromethane; (3) acetone, thiourea, reflux; and (4) sodium pyrosulfite/water (0.1g/mL), reflux.

Synthesis of 2,3,4,6-tetra-O-acetyl-glucopyranosyl bromide (2)

Penta-*O*-acetyl-β-D-glucopyranose (3.2 g, 8.2 mmol) **1** was dissolved in dichloromethane (40 mL). While stirring in an ice-water bath, a solution of HBr in acetic acid was added slowly (33% HBr/acetic acid, 8 mL) to the mixture. After 30 minutes, the reaction was quenched with cold dichloromethane and washed with ice-water followed by a cold, saturated $NaHCO_3$ solution. The organic solvent was dried (Na_2SO_4), filtered and concentrated *in vacuo* affording crude **2** (3.3 g, 8.0 mmol, 96% yield) as an-off-white solid. ^{1}H-NMR data was consistent with the data reported by Aldrich.[21]

Synthesis of 2,3,4,6-tetra-O-acetyl-1-thiol-glucopyranose (4)

2,3,4,6-tetra-*O*-acetylglucopyranosyl bromide **2** (2.5 g, 6.1 mmol) was dissolved in dry acetone (5 mL). Thiourea (0.5 g, 6.6 mmol) was then added to the solution and it was heated to reflux. The mixture was maintained at reflux temperature under nitrogen for 35 minutes (precipitation occurred). The solid mixture was recrystallized from isopropanol to afford **3** (2,3,4,6-tetra-*O*-acetyl-pseudothio-glucopyranose) as an off-white solid. The disappearance of the starting material **2** was monitored by HPLC-UV-CD and ^{1}H-NMR (500 MHz, $CDCl_3$). 2,3,4,6-tetra-*O*-acetyl-pseudothio-glucopyranose (3.0 g) was then dissolved in dichloromethane (30 mL) and a solution of sodium pyrosulfite (1.5 g) in water (15 mL) was added. Next, the mixture was heated at 40 $^\circ$C for 45 minutes. After cooling, the organic layer was separated and washed with water (30 mL) and with brine (30 mL). The organic mixture was dried (Na_2SO_4), filtered and concentrated *in vacuo* to afforded the crude thiol product **4**. The crude 2,3,4,6-tetra-*O*-acetyl-1-thiol-glucopyranose **4** was recrystalized from methanol to afford pure **4** (2.0 g, 5.5 mmol, 90%

yield) as an-off-white solid. ^{1}H-NMR, ^{13}C-NMR and FTIR data were consistent with the spectra in the Aldrich.[22]

Figure 1-2: Structures of monosaccharide derivatives

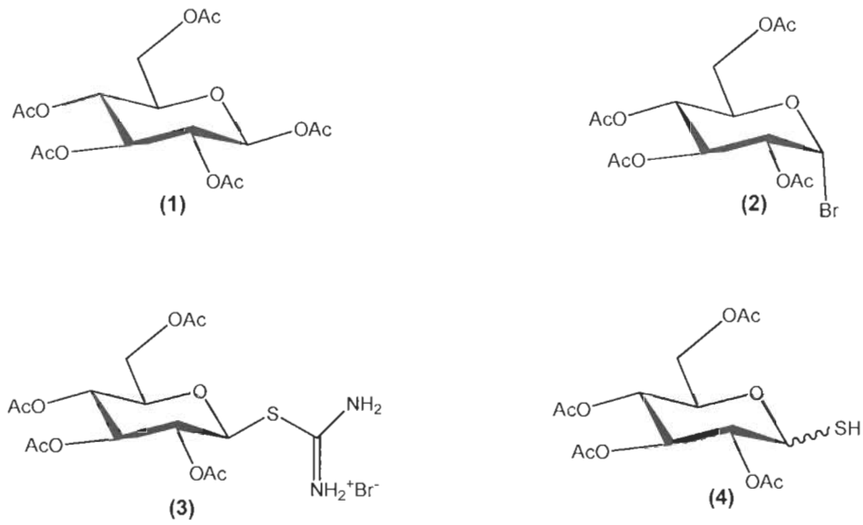

Synthesis of peracetylated-1-Br-maltotriose (7)

Maltotriose **5** (3.0 g, 5.9 mmoles) was dissolved in acetic anhydride (30 mL). While stirring in an ice-water bath, a solution of HBr in acetic acid was added slowly (33% HBr/acetic acid, 13 mL) to the mixture. A clear colorless/faint yellow solution indicated completion of peracetylation after 90 minutes. The reaction was quenched with cold dichloromethane (30 mL) and washed with ice-water (30 mL) and cold saturated $NaHCO_3$ solution (30 mL). The organic solvent was dried (Na_2SO_4), filtered and concentrated *in vacuo*. The crude, peracetylated maltotriose (5.5 g, 5.7 mmol) was dissolved in dichloromethane (70 mL). While stirring in an ice-water bath, a solution of HBr in acetic acid was added slowly (33% HBr/acetic acid, 13 mL) to the mixture. After

60 minutes, the solution was washed with ice-water and cold saturated $NaHCO_3$ solution. The organic solvent was dried (Na_2SO_4), filtered and concentrated *in vacuo* to afford **7** (5.6 g, 5.7 mmol, 96% yield) as an off-white solid. ^{1}H-NMR data was consistent with the literature values.[23]

Synthesis of peracetylated-1-thiol-maltotriose (9)

The peracetylated-1-Br-maltotriose **7** (5.3 g, 5.4 mmol) was dissolved in dry acetone (12 mL). Thiourea (0.83 g, 10.9 mmol) was then added to the solution and it was brought to reflux. The mixture was maintained at reflux temperature under nitrogen for 60 minutes (precipitation occurred). The solid mixture was recrystallized from isopropanol to afford **8** (peracetylated-1-pseudothio-maltotriose) as an off-white solid. The disappearance of the starting material **7** was monitored by HPLC-UV-CD and ^{1}H-NMR (500 MHz, $CDCl_3$). The peracetylated-1-pseudothio-maltotriose **8** (6.2 g) was dissolved in dichloromethane (60 mL) and a solution of sodium pyrosulfite (3 g) in water (30 mL) was added. The mixture was heated at 45 °C for 45 minutes. After cooling, the organic layer was separated and washed with water (30 mL) and with brine (30 mL). It was dried (Na_2SO_4), filtered and concentrated *in vacuo*. Recrystallization from methanol afforded the crude thiol product **9**. The crude peracetylated-1-thiol-maltotriose was further purified by preparative elution chromatography (2.9 g, 3.1 mmol, 57% yield) to afford the thiol maltotriose as white solid. ^{1}H-NMR (600 MHz, $CDCl_3$): δ 4.61 (dd, 1H, $J_{1,2}$ = 11.5 Hz, $J_{1,SH}$ = 9.6 Hz, H-1), 2.27 (d, 1H, $J_{SH,1}$ = 9.6 Hz, SH), 2.20-2.00 (cluster of s, 10 OAc); ^{13}C-NMR (151 MHz, $CDCl_3$): δ 170.66, 170.60, 170.55, 170.51, 170.35, 169.96, 169.90, 169.82, 169.70, 169.46, 95.87, 95.69, 78.18, 76.47, 75.95, 74.38, 73.74, 72.55,

71.67, 70.44, 70.10, 69.37, 69.04, 68.52, 67.88, 63.13, 62.29, 61.37, 21.00-20.50 (cluster of s, 10 OCH_3).

Figure 1-3: Structures of maltotriose and its derivatives

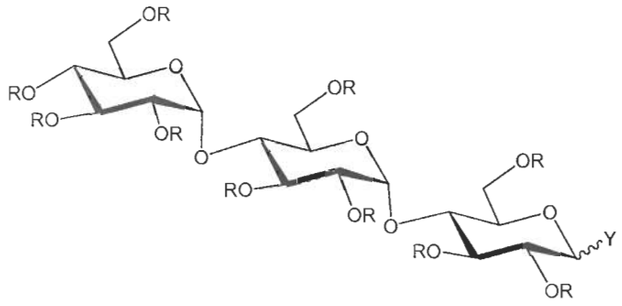

5 R= H, Y=OH
6 R=Ac, Y= OAc
8 R= Ac, Y= $SC(NH_2)Br$
9 R= Ac, Y= SH

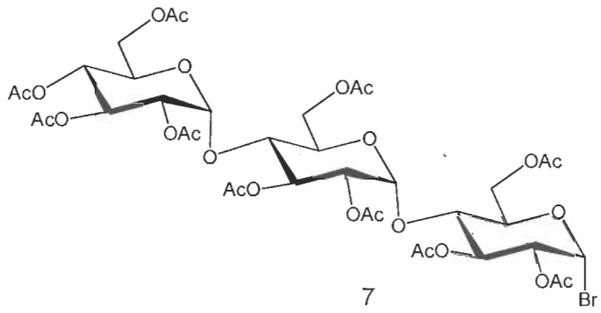

7

Synthesis of peracetylated-1-Br-maltoheptaose (12)

Maltoheptaose **10** (1.0 g, 0.87 mmol) was dissolved in acetic anhydride (28 mL). While stirring, a solution of 33% HBr in acetic acid (3 mL) was added slowly to the mixture. A clear, colorless/faint yellow solution indicated completion of peracetylation after 8 hours. The crude mixture solution was quenched with cold dichloromethane (30 mL) and washed with ice-water (30 mL) and cold saturated $NaHCO_3$ solution (30 mL). The organic solvent was dried (Na_2SO_4), filtered and concentrated *in vacuo*. The crude, peracetylated maltoheptaose **11** (1.8 g, 0.85 mmol) was dissolved in dichloromethane (36 mL). While stirring in an ice water bath, a solution of HBr in acetic acid was added slowly (33% HBr/acetic acid, 5 mL) to the mixture. After 90 minutes, the solution was washed with ice –water and cold saturated $NaHCO_3$ solution. The organic layer was dried (Na_2SO_4), filtered and concentrated *in vacuo* to afford **12** (1.7 g, 0.79 mmol 91% yield) as an off-white solid. ^{1}H-NMR data was consistent with the literature values.[23]

Synthesis of peracetylated-1-thiol-maltoheptaose (14)

The peracetylated-1-Br-maltoheptaose (1.45 g, 0.68 mmol) was dissolved in dry acetone (7 mL). Thiourea (0.28 g, 3.7 mmol) was then added to the solution and it was brought to reflux. The mixture was maintained at reflux temperature under nitrogen for 3 h (some precipitation occurred). The crude mixture was filtered and concentrated *in vacuo*. The solid, crude mixture was recrystallized from isopropanol to afford **13** (peracetylated-1-pseudothio-maltoheptaose) as an off-white solid. The disappearance of the starting material **12** was monitored by HPLC-UV-CD and ^{1}H-NMR (500 MHz, $CDCl_3$). The peracetylated-1-pseudothio-maltoheptaose (1.8 g) was dissolved in dichloromethane (20 mL) and a solution of sodium pyrosulfite (1.0 g) in water (10 mL) was added. The

mixture was heated at 45 °C for 45 minutes. After cooling, the organic layer was separated and washed with water (15 mL) and with brine (15 mL). The organic layer was dried (Na_2SO_4) and filtered. The mixture was then concentrated *in vacuo* and the crude product was recrystallized from methanol to afford the thiol product **14**. The crude thiol maltoheptaose **14** was further purified by preparative elution chromatography (0.8 g, 0.9 mmol, 56% yield) to afford the peracetylated-1-thiol maltoheptaose as white solid. ^{1}H-NMR (600 MHz, $CDCl_3$): δ 4.59 (dd, 1H, $J_{1,2}$ = 11.5 Hz, $J_{1,SH}$ = 9.6 Hz, H-1), 2.25 (d, 1H, $J_{SH,1}$ = 9.6 Hz, SH), 2.20-2.00 (cluster of s, 22 OAc); ^{13}C-NMR (151 MHz, $CDCl_3$): δ 170.74 (3), 170.67 (3), 170.55, 170.44, 170.42, 170.38 (2), 170.37 (2), 169.96, 169.89, 169.76, 169.60, 169.55, 169.51, 169.45 (3), 95.74 (3), 95.70, 95.64, 95.62, 78.19, 76.40-67.50 (cluster of s, 28 CH), 63.08, 62.46, 62.38, 62.33 (2), 62.14, 61.35, 21.00-20.40 (cluster of s, 22 OCH_3).

Figure 1-4: Structures of maltoheptaose and its derivatives

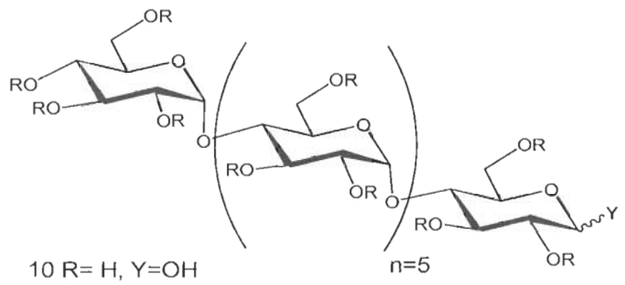

10 R= H, Y=OH
11 R=Ac, Y= OAc
13 R= Ac, Y= $SC(NH_2)Br$
14 R= Ac, Y= SH

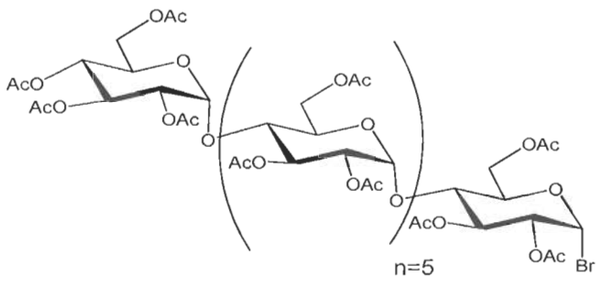

12

Synthesis of peracetylated-1-Br-maltooctaose (17)

Maltooctaose **15** (0.9 g, 0.68 mmoles) was dissolved in acetic anhydride (28 mL). While stirring, a solution of HBr in acetic acid was added slowly (33% HBr/acetic acid, 3 mL) to the mixture. A clear, colorless/faint yellow solution indicated completion of peracetylation after 10 hours affording a crude mixture of peracetylated maltooctaose **16**. The reaction was quenched with cold dichloromethane (25 mL) and washed with ice-water (25 mL) followed by cold saturated $NaHCO_3$ (25 mL). The organic layer was dried (Na_2SO_4), filtered and concentrated *in vacuo*. The crude peracetylated maltooctaose (1.7 g, 0.71 mmol) was dissolved in CH_2Cl_2 (35 mL). While stirring in an ice bath, a solution of HBr in acetic acid was added slowly (33% HBr/acetic acid, 5 mL) to the mixture. After 2 hours, the solution was washed with ice–water (35 mL) and cold saturated $NaHCO_3$ solution (35 mL). The organic solvent was dried (Na_2SO_4), filtered and concentrated *in vacuo* to afford **17** (1.5 g, 0.61 mmol, 89% yield) as an off-white solid. ^{1}H-NMR data was consistent with the literature values.[23]

Synthesis of peracetylated-1-thiol-maltooctaose (19)

The peracetylated-1-Br-maltooctaose **17** (1.4 g, 0.58 mmol) was dissolved in dry acetone (8 mL) and thiourea (0.30 g, 3.9 mmol) was added. The mixture was refluxed under nitrogen for 3 hours (no precipitation occurred). The crude mixture was filtered and concentrated *in vacuo*. The solid crude product was recrystallized from isopropanol to afford **18** (peracetylated-1-pseudothio-maltooctaose) as an off-white solid. The disappearance of the starting material **17** was monitored by HPLC-UV-CD and ^{1}H-NMR (500 MHz, $CDCl_3$). The peracetylated-1-pseudothio-maltooctaose **18** (1.7 g) was dissolved in dichloromethane (20 mL) and a solution of sodium pyrosulfite (1.0 g) in

water (10 mL) was added. The mixture was heated at 45 °C for 45 minutes. After cooling, the organic layer was separated and washed with water (15 mL) and with brine (15 mL). The organic layer was dried (Na_2SO_4) and filtered. The mixture was then concentrated *in vacuo* and the crude product was recrystallized from methanol to afford the thiol product **19**. Crude **19** was further purified by preparative elution chromatography (0.7 g, 0.29 mmol, 50% yield) as a white a solid. ^{1}H-NMR (600 MHz, $CDCl_3$): δ 4.60 (dd, 1H, $J_{1,2}$ = 11.5 Hz, $J_{1,SH}$ = 9.6 Hz, H-1), 2.25 (d, 1H, $J_{SH,1}$ = 9.6 Hz, SH), 2.20-2.00 (cluster of s, 25 OAc); ^{13}C-NMR (151 MHz, $CDCl_3$): δ 170.95 (3), 170.89 (3), 170.77, 170.66, 170.63, 170.60 (3), 170.17, 170.10, 170.02, 169.97, 169.83 (2), 169.82, 169.77, 169.83, 169.82, 169.77, 169.68 (2), 169.66, 96.08, 95.95 (2), 95.92, 95.84 (3), 78.41, 76.80- 68.00 (cluster of s, 32 CH), 63.29, 62.86, 62.65, 62.59, 62.51 (2), 62.35, 61.56, 21.20-20.40 (cluster of s, 25 OCH_3).

Figure 1-5: Structures of maltooctaose and its derivatives

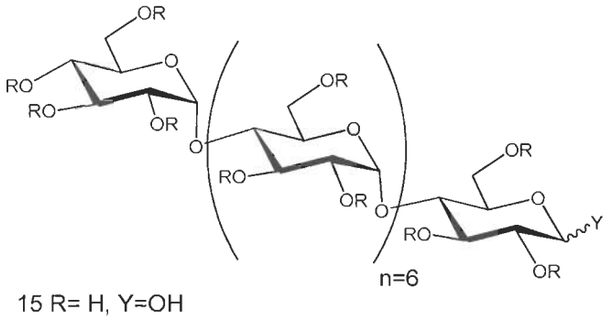

15 R= H, Y=OH
16 R=Ac, Y= OAc
18 R= Ac, Y= SC(NH_2)Br
19 R= Ac, Y= SH

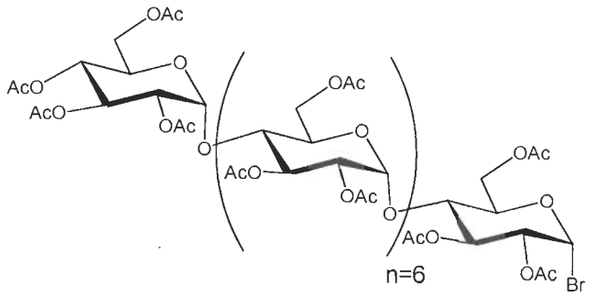

17

Synthesis of peracetylated-1-Br-maltodecatriose (22)

Crude maltodextrin **20** (3.0 g, 1.41 mmol) was dissolved in acetic anhydride (150 mL). While stirring, a solution of HBr in acetic acid was added slowly (33% HBr/acetic acid, 20 mL) to the mixture. A clear, colorless/faint yellow solution indicated completion of peracetylation after 2 days. The reaction was quenched with cold dichloromethane (300 mL) and was washed with ice-water (400 mL) and cold saturated $NaHCO_3$ solution (250 mL). The organic layer was dried (Na_2SO_4), filtered and concentrated *in vacuo*. The crude peracetylated maltodecatriose (2.8 g, 0.73 mmol) was dissolved in dichloromethane (40 mL) and was cooled to 5 °C. A solution of HBr in acetic acid was added slowly (33% HBr/acetic acid, 6 mL) to the mixture. After 2 hours, the solution was washed with ice – water and cold saturated $NaHCO_3$ solution. The organic layer was dried (Na_2SO_4), filtered, and concentrated *in vacuo* to afford **22** (1.8 g, 0.47 mmol, 33% yield) as an off-white solid. ^{1}H-NMR (600 MHz, $CDCl_3$): δ 6.60 (d, 1H, $J_{1,2}$ = 4.0 Hz, H-1), 2.20-1.90 (cluster of OAc); ^{13}C-NMR (151 MHz, $CDCl_3$): δ 171.00-169.00 (cluster of C=O), 96.00-95.50 (cluster of anomeric CH), 86.06 (2), 73.00- 67.50 (cluster of s, CH), 21.00-20.20 (cluster of OCH_3).

Synthesis of peracetylated-1-thiol-maltodecatriose (24)

The peracetylated-1-Br-maltodecatriose (1.8 g, 0.47 mmoles) was dissolved in dry acetone (9 mL). Thiourea (0.38 g, 4.3 mmoles) was then added to the solution. The mixture was maintained at reflux temperature under nitrogen for 3 hours (no precipitation occurred). The crude mixture was filtered and concentrated *in vacuo*. The solid mixture was recrystalized in isopropanol to obtain **23** (peracetylated-1-pseudothio-maltodecatriose) as an off-white solid. The disappearance of the starting material **22** was monitored by HPLC-UV-CD and ^{1}H-NMR (600 MHz, $CDCl_3$). The peracetylated-1-pseudothio-maltodecatriose (2.2 g) was dissolved in dichloromethane (22 mL) and a solution of sodium pyrosulfite (1.1 g) in water (11 mL) was added. The mixture was heated at 45 °C for 45 minutes. After cooling, the organic layer was separated and washed with water (25 mL) and with brine (25 mL). The organic layer was dried (Na_2SO_4) and filtered. The mixture was then concentrated *in vacuo* and the crude product was recrystallized in methanol to afford the thiol product **24**. The crude peracetylated-1-thiol-maltodecatriose was further purified by preparative elution chromatography (0.8 g, 0.21 mmol, 45%) as white solid. ^{1}H-NMR (600 MHz, $CDCl_3$): δ 4.60 (m, 1H, $J_{1,SH}$ = 9.6 Hz, H-1), 2.25 (d, 1H, $J_{SH,1}$ = 9.6 Hz, SH), 2.20-1.90 (cluster OAc); ^{13}C-NMR (151 MHz, $CDCl_3$): δ 171.00-169.00 (cluster of C=O), 96.00-95.50 (cluster of anomeric CH), 78.23 (2), 21.00-20.20 (cluster of OCH_3).

Figure 1-6: Structures of maltodecatriose and its derivatives

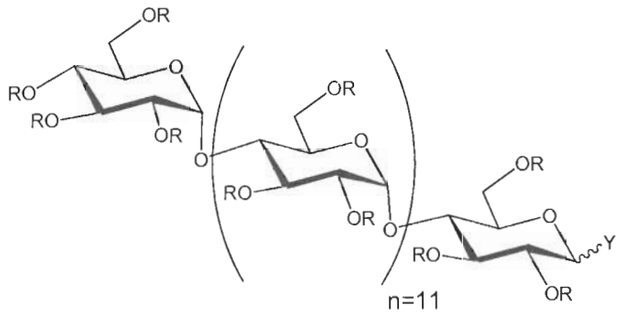

20 R= H, Y=OH
21 R=Ac, Y= OAc
23 R= Ac, Y= $SC(NH_2)Br$
24 R= Ac, Y= SH

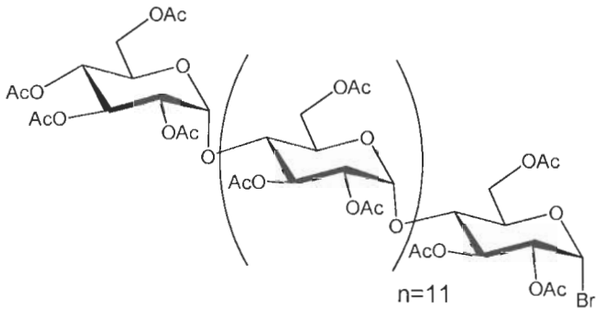

22

Synthesis of trimethoxysilyl peracetylated-1-thio-saccharides series (n=1, 3, 7, 13)

The synthetic pathway for the preparation of the trimethoxysilyl peracetylated-1-thio saccharides (Sil PA-1-thio-Sac) series is shown in Figure 1-7. The thiol functional group from the PA-1-thiol-Sac, reacted with the epoxy group of glycido-oxypropyl trimethoxysilane (GOPTMS) forming a carbon-sulfur-carbon bond after ring opening. In brief, peracetylated-1-thiol-saccharides were reacted with the GOPTMS (2-5 equivalents) in acetonitrile containing aqueous 10 mM dibasic potassium phosphate (3:1 ratio). The reaction was completed within 10 to 12 hours. The crude products from the reactions were then extracted with ethyl acetate and concentrated *in vacuo*. The structures of the trimethoxysilyl peracetylated-1-thio-saccharides are shown in Figures 1-8.

Figure 1-7: Synthesis of the trimethoxysilyl peracetylated-1-thio-saccharides

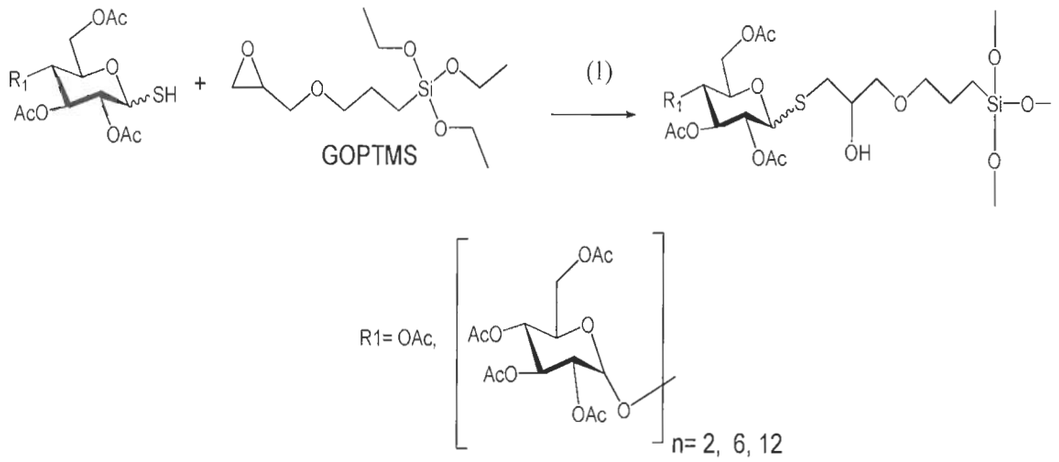

(1) acetonitrile, 10 mM K_2HPO_4 in water, RT for 12 hours.

Synthesis of trimethoxysilyl 2,3,4,6-tetra-O-acetyl-1-thio-glucopyranose (25)

The 2,3,4,6-tetra-*O*-acetyl-1-thiol-glucopyranose (thiol Glc) (1.0 g, 2.7 mmol) **4** was dissolved in acetonitrile (30 mL). While stirring, GOPTMS (1.2 g, 5.0 mmol) and aqueous 10 mM dibasic potassium phosphate (10 mL) were added to the solution. After 8 hours, the solution was concentrated *in vacuo*. The crude product in aqueous solution was immediately extracted with ethyl acetate (2X, 25 mL). The organic solvent was dried (Na_2SO_4), filtered and concentrated *in vacuo* to afford crude **25** (1.7 g, 2.7 mmol 100% yield) as a pale-yellow oil. ^{1}H-NMR (500 MHz, CD_3SOCD_3): δ 5.26 (dd, 1H, J = 10.7, 9.4 Hz, H-2), 2.10-1.90 (s, 4 OAc), 3.5 (s, OCH_3); ^{13}C-NMR (126 MHz, CD_3SOCD_3): δ 170.69, 170.20, 169.96 (2), 169.76 (2), 82.98, 82.75, 75.02(2), 73.97, 73.90, 73.69, 73.20, 73.14, 71.82, 70.58, 70.40, 69.77, 69.71, 68.85, 62.62, 51.02, 50.66 (2), 44.08, 34.43, 34.16, 23.19, 23.14, 21.13, 21.10, 21.08, 21.05, 20.96, 5.48.

Synthesis of trimethoxysilyl peracetylated-1-thio-maltotriose (26)

Peracetylated-1-thiol-maltotriose (thiol triose) (0.90 g, 0.96 mmol) **9** was dissolved in acetonitrile (30 mL). While stirring, GOPTMS (0.64 g, 2.72 mmol) and aqueous 10 mM dibasic potassium phosphate (10 mL) were added to the solution. After 10-12 hours, the solution was concentrated *in vacuo*. The crude product in aqueous solution was immediately extracted with ethyl acetate (2X, 25 mL). The organic solvent was dried (Na_2SO_4), filtered and concentrated *in vacuo* to afford crude **26** (1.1 g, 0.94 mmol, 98% yield). ^{1}H-NMR (500 MHz, CD_3SOCD_3): δ 5.31 (dd, 1H, J = 10.7, 9.0 Hz, H-2), 2.10-1.90 (cluster of s, 10 OAc), 3.56 (s, OCH_3); ^{13}C-NMR (126 MHz, CD_3SOCD_3): δ 170.76 (2), 170.67, 170.63, 170.57, 170.23, 170.18, 170.12, 169.88, 169.84, 96.22,

96.16, 82.57, 82.37, 75.69, 75.61, 75.18, 73.99, 73.94, 73.90, 73.20, 71.75 (2), 71.60, 71.31, 71.13, 70.51, 70.10, 69.75, 69.70, 69.57, 69.49, 68.70, 68.42, 63.95, 63.21, 62.05, 51.02 (2), 50.67, 44.08 (2), 21.25, 21.23, 21.21, 21.17, 21.08 (2), 21.02 (2), 2.96 (2), 5.48.

Synthesis of trimethoxysilyl peracetylated-1-thio-maltoheptaose (27)

Peracetylated-1-thiol-maltoheptaose (1.0 g, 0.48 mmol) **14** was dissolved in acetonitrile (30 mL). While stirring, glycido-oxypropyltrimethoxysilane (0.54 g, 2.26 mmol) and aqueous 10 mM dibasic potassium phosphate (10 mL) were added to the mixture. After 10-12 hours, the solution was concentrated *in vacuo*. The crude product in aqueous solution was immediately extracted with ethyl acetate (2X, 25 mL). The organic solvent was dried (Na_2SO_4), filtered and concentrated *in vacuo* to afford crude **27** (1.14 g, 0.48 mmol, 99% yield). ^{1}H-NMR (500 MHz, $CDCl_3$): δ 5.10 (dd, 1H, J = 11.0, 10.0 Hz, H-3), 2.20-1.90 (cluster of OAc), 3.56 (s, OCH_3). ^{13}C-NMR (126 MHz, $CDCl_3$): δ 170.93 (3), 170.89 (3), 170.85, 170.76, 170.65, 170.62, 170.58 (3), 170.20, 169.97, 169.87, 169.84, 169.79, 169.76, 169.67 (2), 169.5, 96.20-95.60 (cluster of anomeric CH), 84.00, 83.66, 76.46, 76.36, 73.77 (2), 73.61, 73.39 (2), 73.13, 72.54, 71.94 (2), 71.89 (2), 71.60, 70.64 (3), 70.26, 70.21, 69.58, 69.28, 69.15 (2), 68.67, 68.16, 62.95, 62.55 (4), 62.37, 61.58, 51.10, 50.77, 50.75, 44.55, 23.02, 21.20-20.60 (cluster of OCH_3), 5.61, 5.48.

Synthesis of trimethoxysilyl peracetylated-1-thio-maltodecatriose (28)

Peracetylated-1-thiol-maltodecatriose (0.9 g, 0.23 mmol) **24** was dissolved in acetonitrile (27 mL). While stirring, glycido-oxypropyltriethoxysilane (0.48 g, 2.04 mmol) and aqueous 10 mM dibasic potassium phosphate (9 mL) was added to the mixture. After 12

hours, the organic solvent was concentrated *in vacuo*. The crude product in aqueous solution was immediately extracted with ethyl acetate (2X, 25 mL). The organic solvent was dried (Na_2SO_4), filtered and concentrated *in vacuo* to afford crude **28** (1.1 g, 98% yield). ^{1}H-NMR (500 MHz, $CDCl_3$): δ 5.10 (dd, 1H, J = 11.1, 9.9 Hz), 2.20-1.90 (cluster of OAc), 3.56 (s, OCH_3). ^{13}C-NMR (126 MHz, $CDCl_3$): δ 171.00-169.00 (cluster of C=O), 96.50-95.50 (cluster of anomeric CH), 74.00-61.00 (cluster of s, CH), 51.10 (2), 50.75, 44.55, 23.19, 21.20-20.50 (cluster of OCH_3), 5.45.

Figure 1-8: Structures of trimethoxysilyl peracetylated-1-thio-saccharides

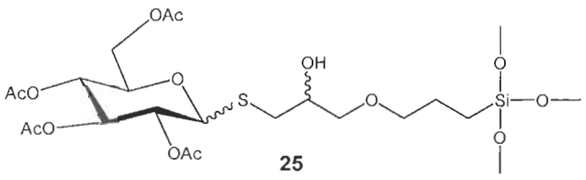

25

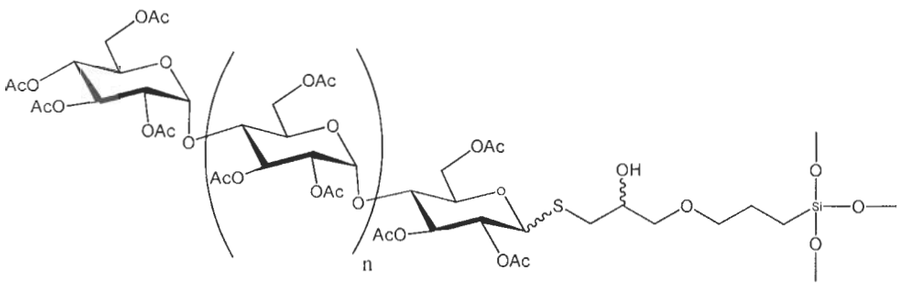

	n
26	**1**
27	**5**
28	**11**

Results and Discussion

Characterization of 2,3,4,6-tetra-O-acetyl-1-thiol-glucopyranose and its trimethoxysilyl derivative

The chemical characterization of the 2,3,4,6-tetra-*O*-acetyl-1-thiol-glucopyranose (thiol Glc) and its trimethoxysilyl derivative (silane thio Glc) was performed using HPLC-charged aerosol detector (CAD), circular dichroism (CD), UV, MS, and NMR. These glucose derivatives are the simplest ligands prepared in this thesis. They can be used to identify some important chemical characteristics of the larger saccharide ligands. Thus, extensive NMR experiments were conducted on these sugar derivatives. The two major fingerprints observed clearly from the thiol Glc in the ^{1}H-NMR spectrum are the doublet of doublet from the anomeric proton at 4.55 ppm and the doublet from the thiol proton at 2.25 ppm. In addition, it is clearly observed that there are chemical shift differences once the thiol Glc reacted with the epoxy-silane linker. For example, the chemical shift of the anomeric proton of the thiol Glc was changed from 4.55 ppm to 5.10 ppm (downfield) when trimethoxysilyl thio glucose is prepared. (Figure 1-9 (c)). The ^{1}H-^{1}H COSY experiment was another NMR experiment performed. It shows the proton spin-spin coupling and connectivity of protons on the thiol Glc and Silane thio Glc. The 2D COSY NMR experiments are shown in Figure 1-10.

Figure 1-9: 1D ^{1}H-NMR, experiments monitoring the reaction of glucose derivatives and the trimethoxysilyl linker.

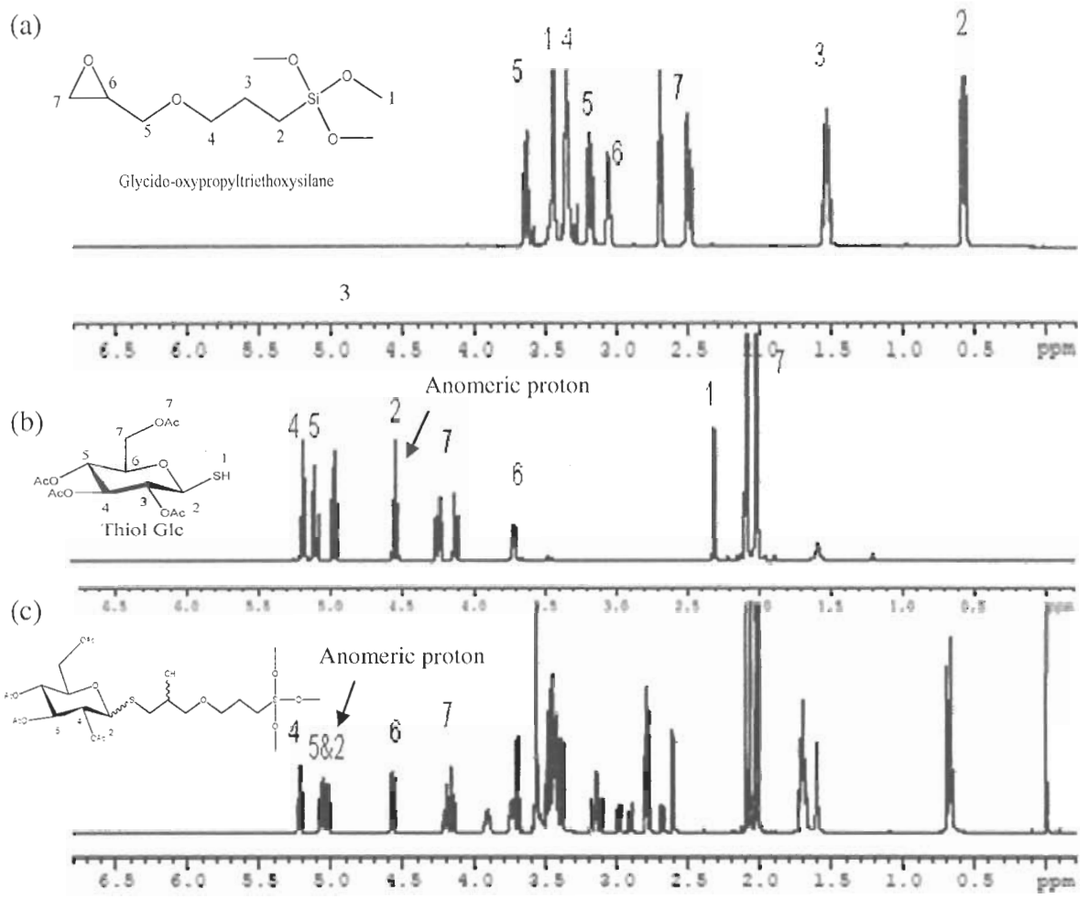

Figure 1-10: ^{1}H-^{1}H correlation, 2D COSY, experiments for compounds thiol Glc **4** and trimethoxysilyl derivative **25**

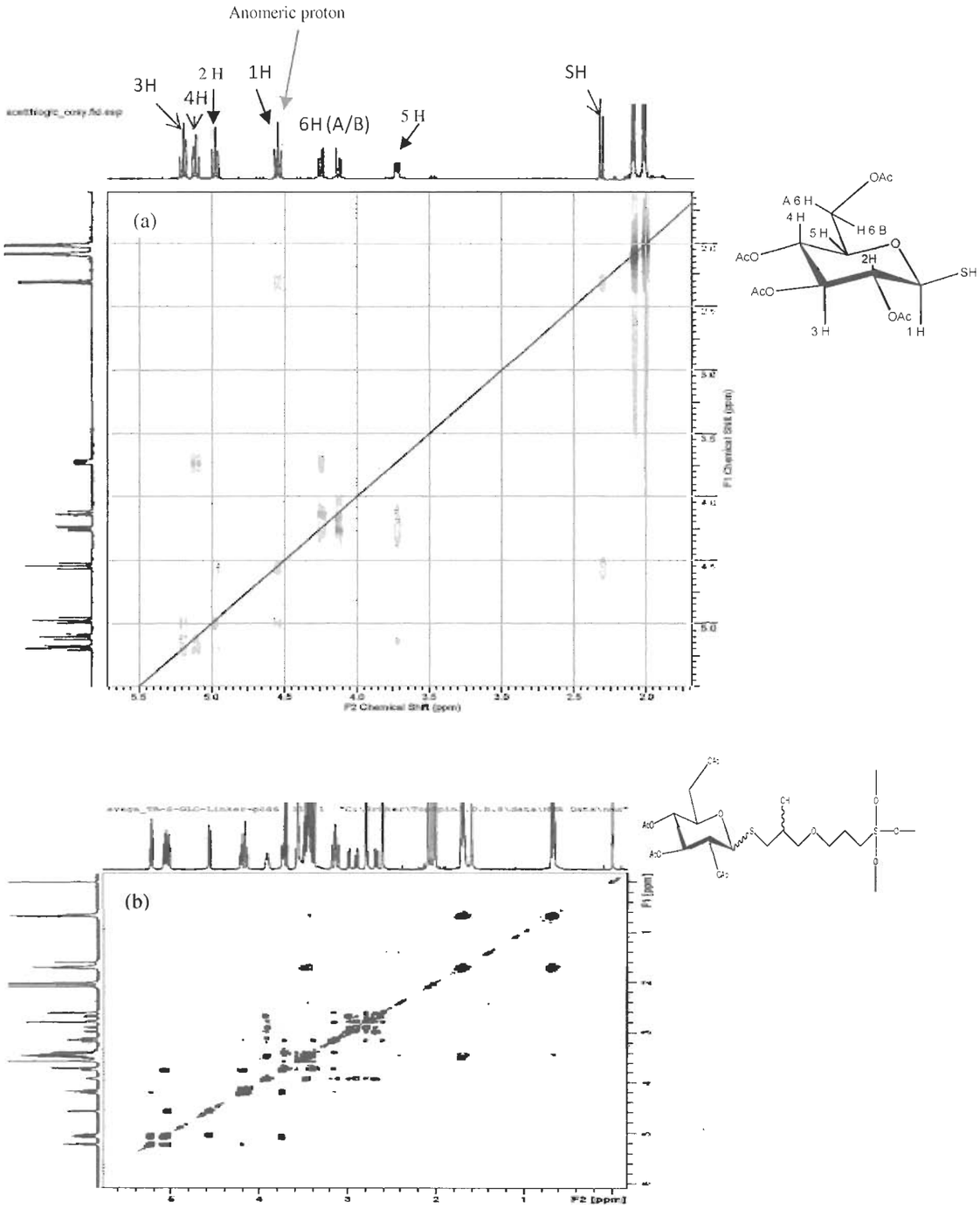

(a) Varian 500 MHz (d) Bruker 600 MHz (CDCl3).

The chirality of compounds thiol Glc **4** and trimethoxysilyl thio Glc **25** was demonstrated by circular dichroism as seem in Figure 1-11. Among all the silane thio sugar ligands only trimethoxysilyl thio Glc showed a negative signal. The signal changed from a positive signal after the achiral epoxy silane linker reacted with the thiol Glc suggesting a change in sugar conformation. This phenomenon was not observed with the larger ligands, probably due to their increased bulk keeping their conformation intact.

Figure 1-11: Chiral conformation of the thiol Glc and trimethoxysilyl thio Glc by circular dichroism (CD).

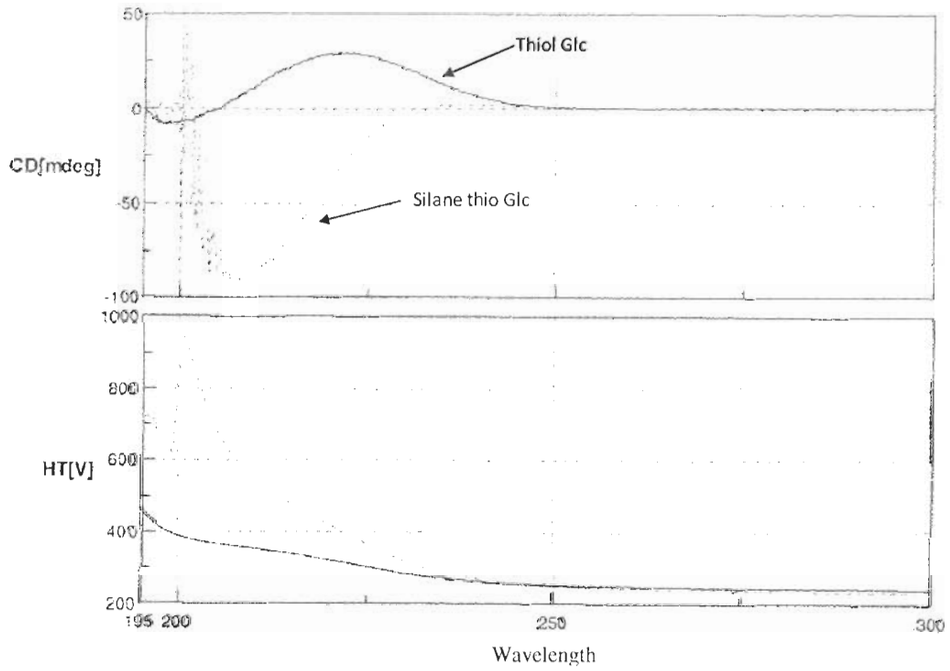

During the initial synthesis of thiol glucose and bromo maltotriose, HPLC with charged aerosol detector (CAD) was used to monitor the reactions. CAD is a universal detector, which uses an evaporative technique. It involves measurement of charged particles and provides responses independent of chemical structure. UV detection was not suitable due to the absence of a chromophore in the starting materials. Figure 1-12 shows an example of a chromatographic separation of a spike sample solution. It contains the saccharide starting materials and their derivatives. In addition, the molecular weight of the thiol glucose and its trimethoxysilyl derivative were determined using HPLC with an electrospray ionization mass spectrometry (ESI MS). As it is observed in Figure 1-13, the glucose derivatives form adducts with sodium and ammonium ions.

Figure 1-12: Chromatographic separation of glucose derivatives by HPLC-charged aerosol detector (CAD)

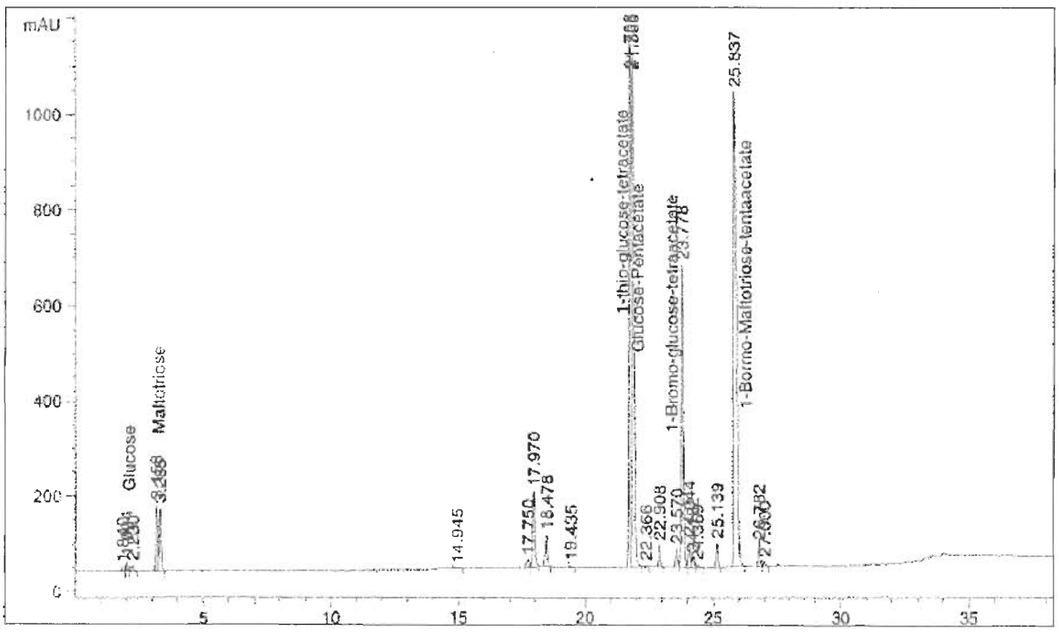

(Atlantis T3, dC18 columns, 3.0 X 150 mm, 3 µm). Conditions: flow rate 1.0 mL/min; 35 °C; mobile phase (A) 5 mM ammonium formate aqueous, (B) acetonitrile; gradient: 0-30 min, 95 →0% A, 5 →100% B.

Figure 1-13: HPLC-ESI+-MS for thiol Glc (a) and trimethoxysilyl thio Glc (b).

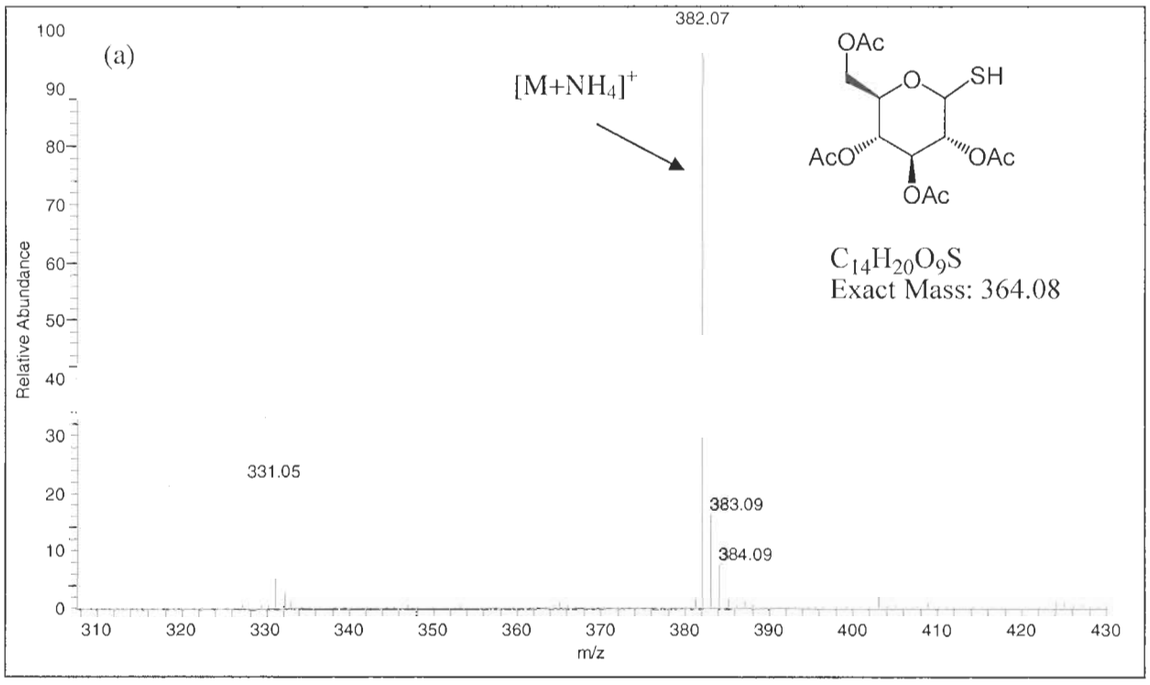

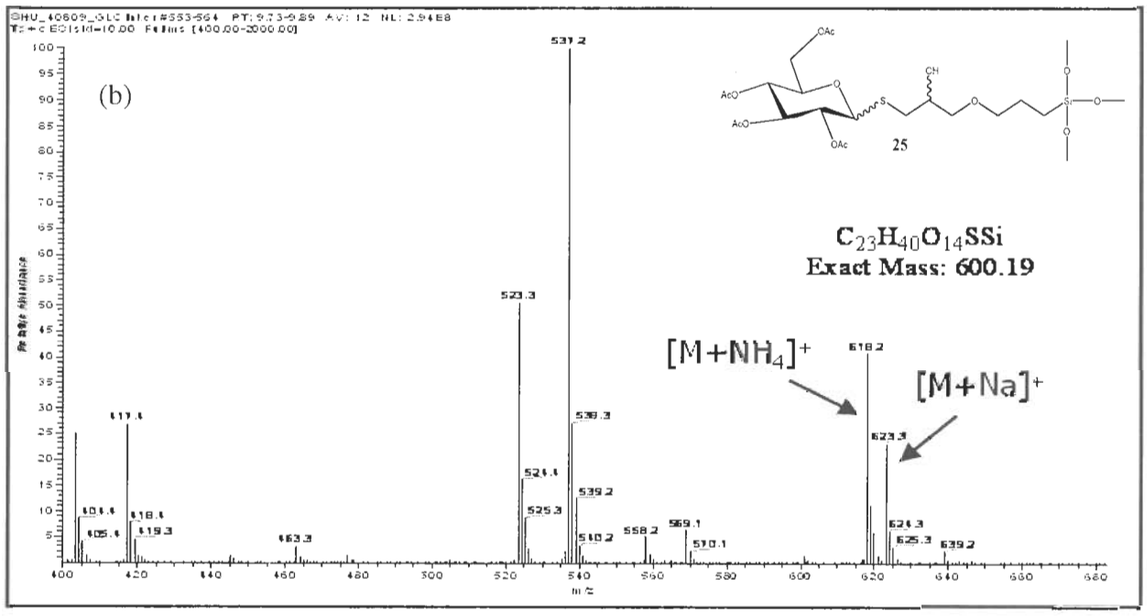

The reaction kinetics for the preparation of the silane thio Glc was demonstrated using HPLC-UV. The reaction was conducted at ambient temperature and the details of the reaction procedures was previously described in this chapter (synthesis section). As observed in Figure 1-14 the reaction is complete within 12 hours and it never goes to 100% completion. In fact, a significant increase of by-products are observed after 6 hours. However, the formation of the silane thio Glc is at its maximum (86%) after 8 hours. Thus, it is recommended to react the thiol Glc with trimethoxysilyl (silane) for at least 8 hours.

Figure 1-14: Reaction kinetics for the synthesis of trimethoxysilyl -1-thio-Glc.

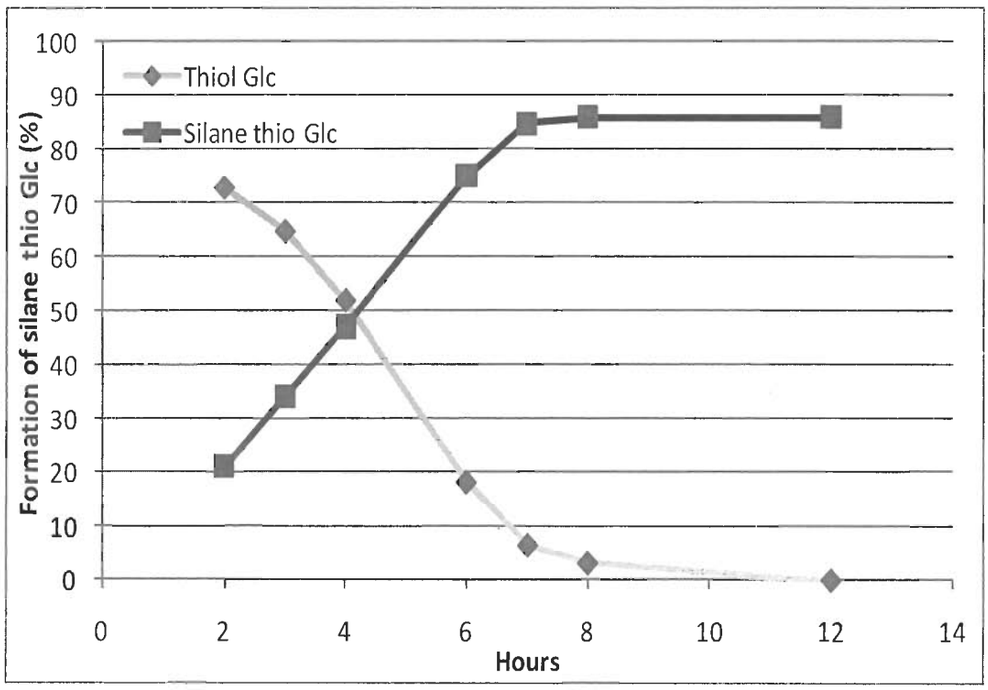

Characterization of peracetylated-1-thiol-maltotriose and its trimethoxysilyl derivative.

The chemical characterization of the peracetylated-1-thiol-maltotriose (thiol triose) and its trimethoxysilyl derivative (silane thio maltotriose) was performed using HPLC, circular dichroism (CD), UV, MS, and NMR. The maltotriose derivatives are observed to share some important characteristics with the glucose derivatives. For example, as it is observed in the 2 D COSY experiment, the thiol maltotriose shows an anomeric proton correlation at 4.60 ppm with the proton from the thiol group at 2.25 ppm as seem in Figure 1-15. A similar proton-proton correlation between the anomeric proton and the proton from the thiol group was observed on the thiol Glc (shown in Figure 1-10).

Figure 1-15: 2D COSY, experiments illustrating 1H-1H correlation between the anomeric proton and the thiol components-Bruker 600 MHz (CDCl3)

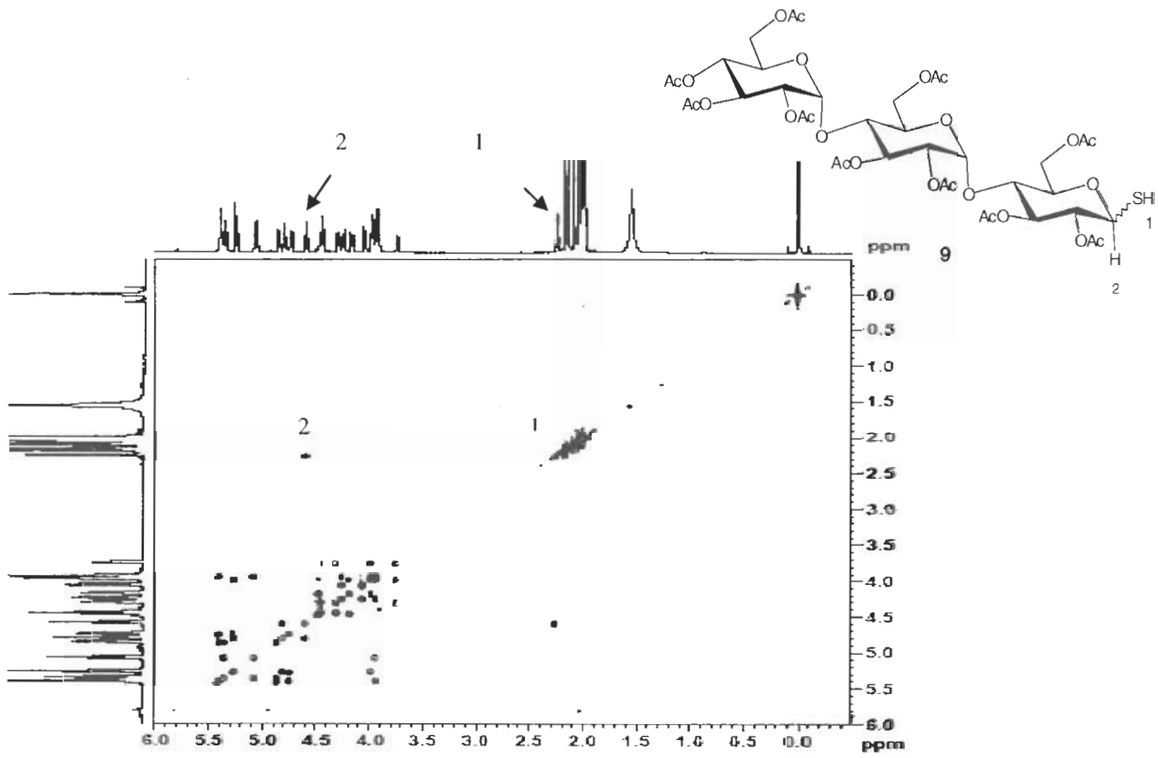

^{1}H-NMR was one of the techniques used to monitor the synthesis of silane thio maltotriose. As it is observed in Figure 1-16, the doublet from the thiol proton at 2.25 ppm disappeared after the formation of the silane thio maltotriose.

Figure 1-16: 1D-^{1}H-NMR, experiments monitoring the reaction of thiol triose with the silane linker

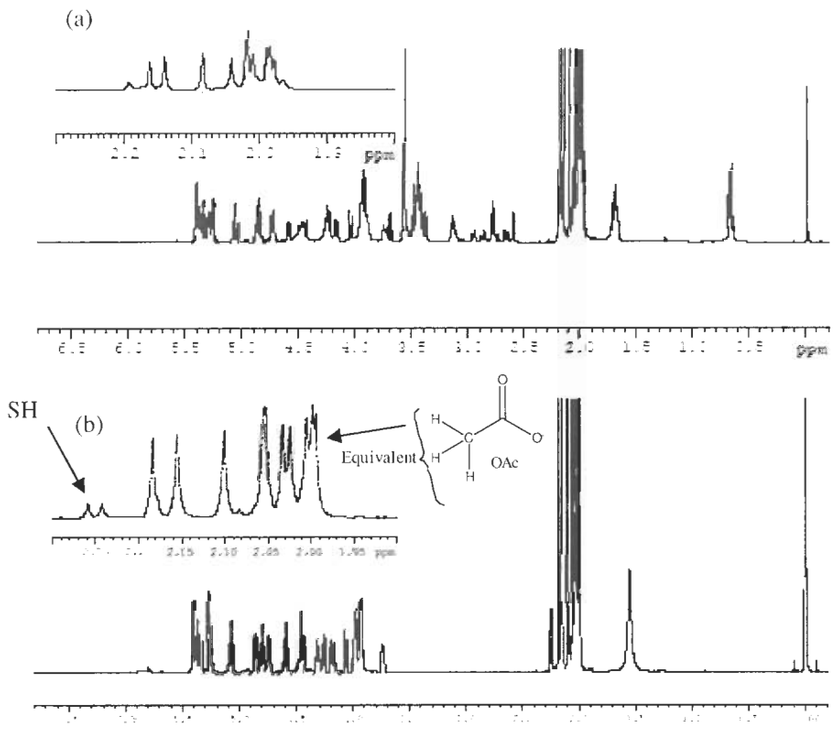

(a) Silane thio maltotriose, Varian 500 MHz; (b) Thiol triose, Bruker 600 MHz ($CDCl_3$)

The chirality of the peracetylated-1-thiol-maltotriose and its intermediates was demonstrated by HPLC-circular dichroism (Figure 1-17). Among all the intermediates, only the peracetylated maltotriose showed a negative signal. The signal changed from a negative to a positive signal after the preparation of the peracetylated-1-Br-maltotriose. It is suspected that the electrostatic environment between the acetate group of the anomeric center and the acetate group of the C-2 in the peracetylated maltotriose changes the orientation of transition dipole moments, which affects the chiral conformation.

Figure 1-17: Demonstration of chirality of the peracetylated-1-thiol-maltotriose and its intermediates by HPLC-CD

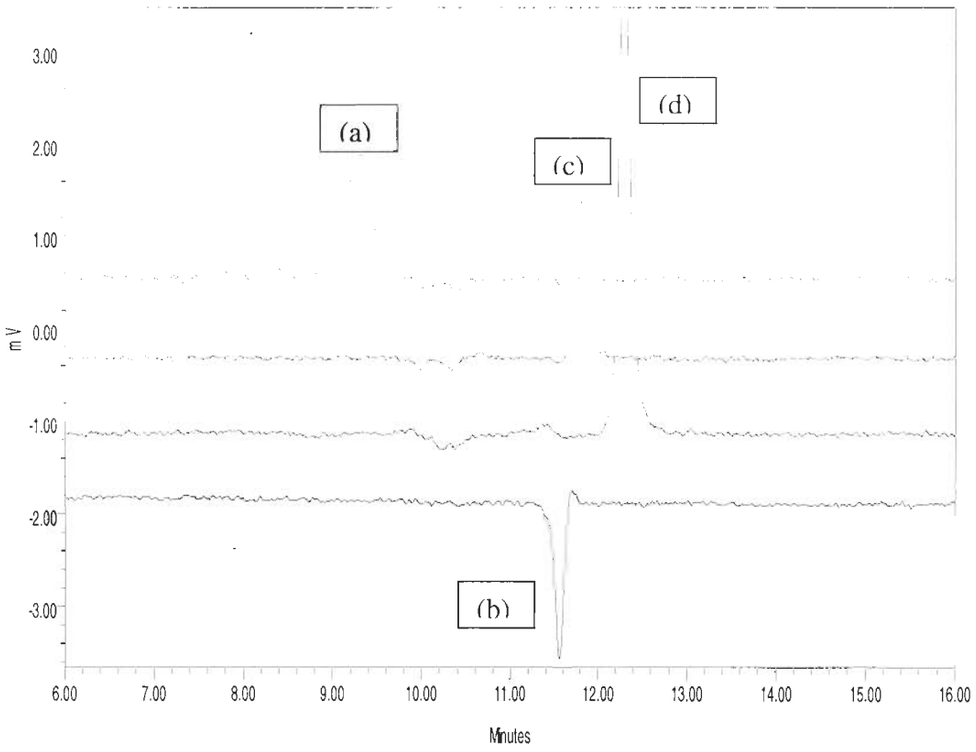

(Atlantis T3, dC18 columns, 3.0 X 150 mm, 3 μm). (a) Pseudothiomaltriose; (b) Peracetylated maltotriose; (c) Peracetylated-1-thiol-maltotriose (d) Peracetylated-1-Br-maltotriose. Conditions: flow rate 1.0 mL/min; 35 °C; mobile phase (A) 5 mM ammonium formate aqueous, (B) acetonitrile; gradient: 0-25 min, 80 →0% A, 20 →100% B.

For the verification of the molecular mass of the thiol maltotriose and the silane thio maltotriose, HPLC-ESI MS was conducted. As it is observed in Figure 1-18, the maltotriose derivatives form adducts with ammonium ions.

Elemental analyses

Peracetylated-1-thiol-maltotriose: Anal. Calcd for $C_{38}H_{52}O_{25}S$: C, 48.51; H, 5.57; S, 3.41. Found: C, 48.45; H, 5.55; S, 3.65.

Figure 1-18 : HPLC-ESI+-MS for thiol maltotriose (a) and silane thio maltotriose (b).

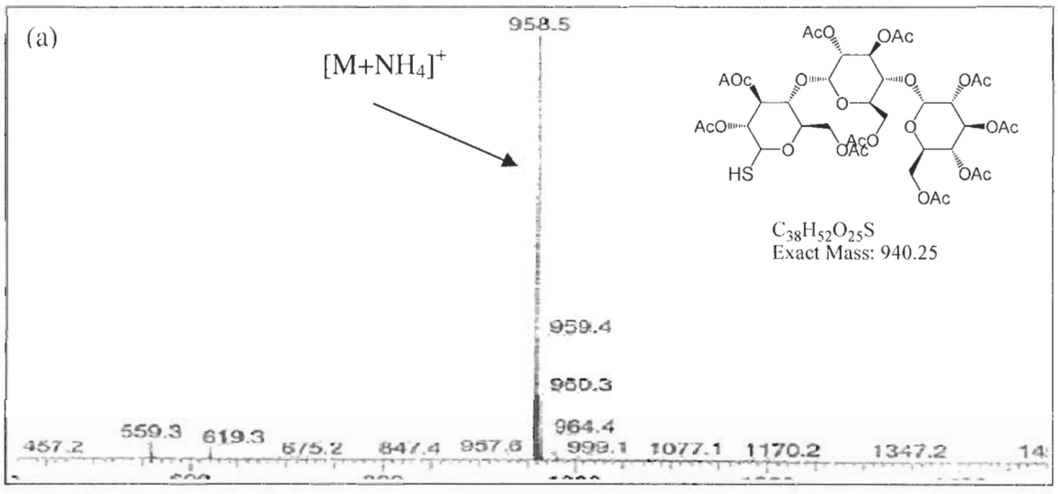

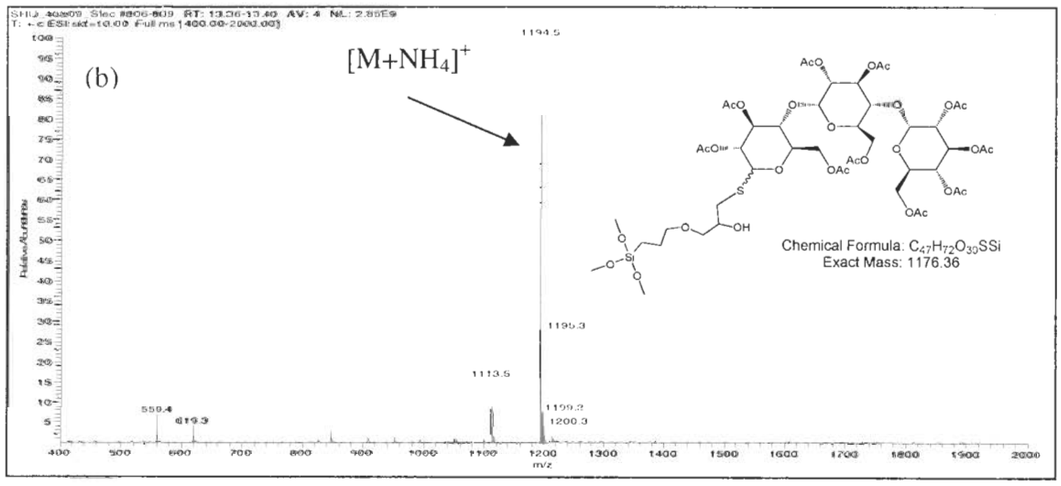

Characterization of peracetylated-1-thiol-saccharides and their trimethoxysilyl derivatives (analogs n=7, 8 and 13-glucose units)

These analogs were characterized by mass spectrometry, NMR and elemental analysis. Figure 1-19 shows the ^{1}H-NMR ($CDCl_3$) spectrum using a Bruker 600 MHz system with a cryoprobe. As was pointed out with the analogs n=1 and 3, the three major fingerprints observed clearly for the analogs n=7 and 8 in the ^{1}H-NMR are the doublet of doublet from the anomeric proton at 4.60 ppm, the doublet from the thiol proton at 2.25 ppm and the acetate groups at 2-2.1 ppm. Next, in order to illustrate the disappearance of the proton from the thiol group after the formation of the carbon-sulfur-carbon bonds, 2D COSY experiments were performed. Figure 1-20 shows the ^{1}H-^{1}H COSY experiments using the analog(s) n=1 and n=13 as reference.

Peracetylated-1-thiol-maltoheptaose, MALDI MS m/z 2115.1 $(M + Na)^{+}$. Anal. Calcd for $C_{86}H_{116}O_{57}S$: C, 49.33; H, 5.58; S, 1.53. Found: C, 49.21; H, 5.63; S, 1.69.

Peracetylated-1-thiol-maltooctaose, MALDI MS m/z 2403.4 $(M + Na)^{+}$.

PA-1-thiol-maltodecatriose, MALDI MS m/z 3843.98 $(M + Na)^{+}$. Anal. Calcd for $C_{158}H_{212}O_{105}S$: C, 49.63; H, 5.59; S, 0.84. Found: C, 49.94; H, 5.61; S, 1.00.

Figure 1-19: ^{1}H-NMR spectra for peracetylated-1-thiol-saccharides

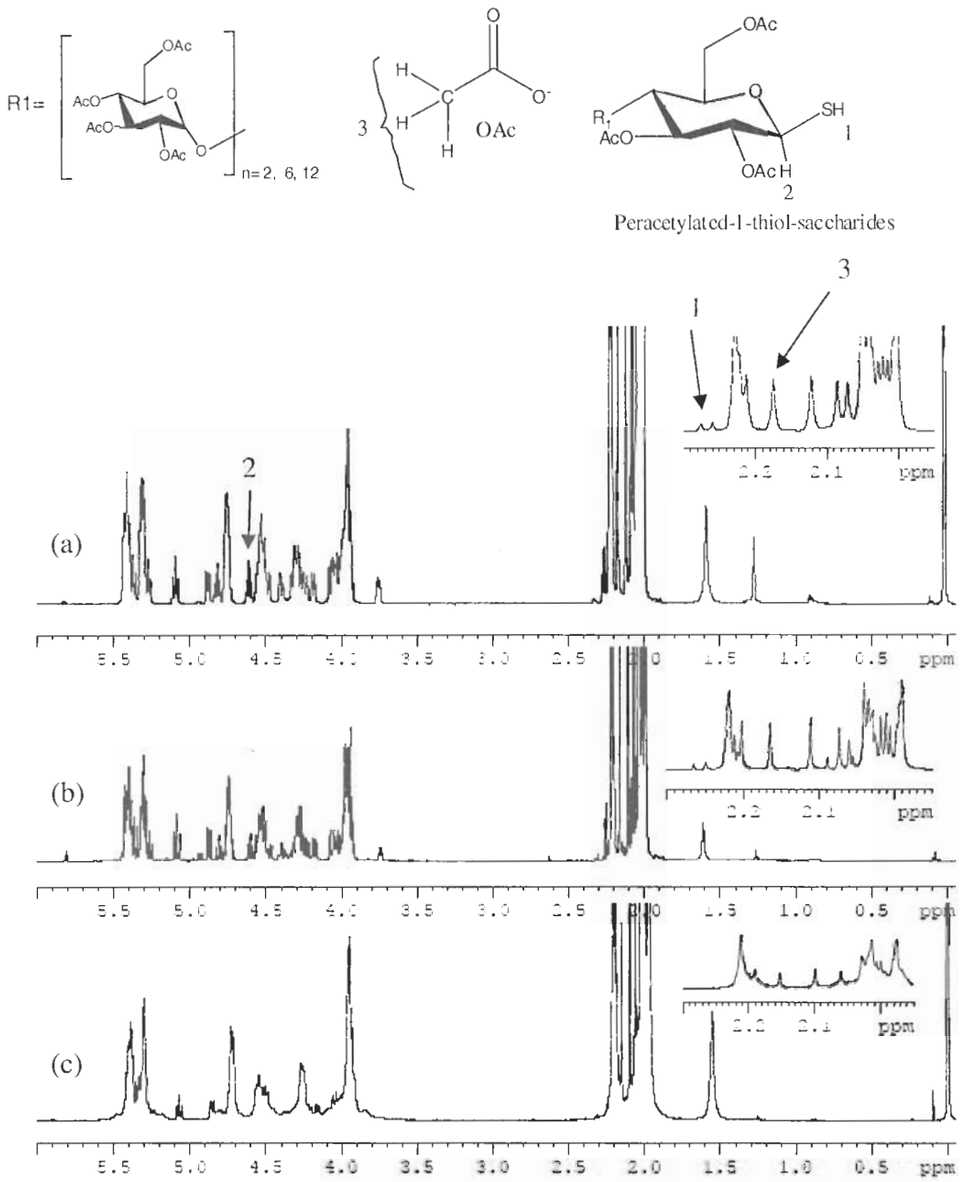

(a) Peracetylated-1-thiol-maltoheptaose; (b) Peracetylated-1-thiol-maltoctaose; (c) Peracetylated-1-thiol-maltodecatriose. Bruker 600 MHz ($CDCl_3$).

Figure 1-20: ^{1}H-^{1}H correlation, 2D COSY, glucose and maltodecatriose derivatives

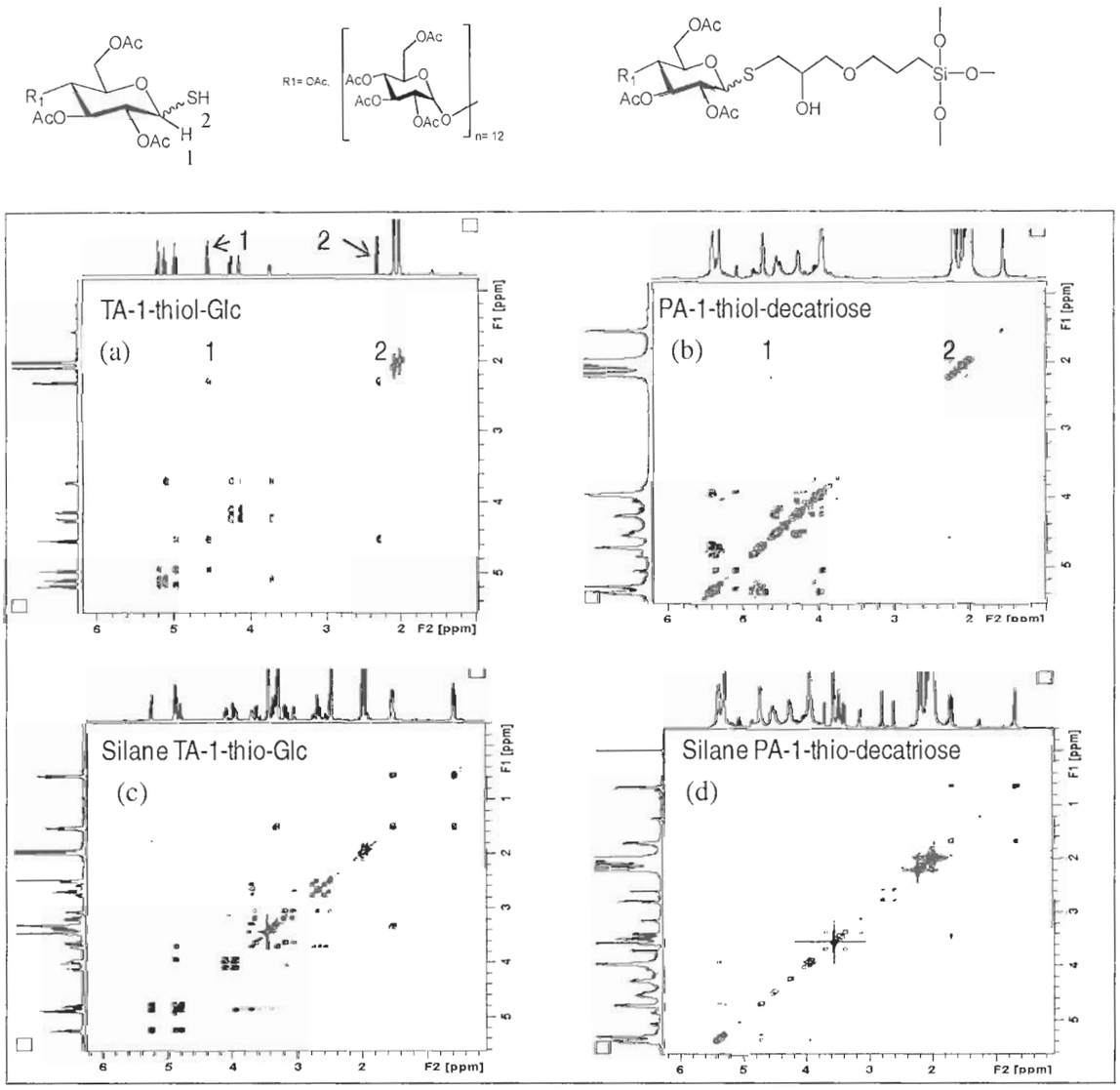

NMR experiments illustrate the disappearance of the proton from the anomeric thiol group after ring opening (a) Varian 500 MHz: (b); (c); (d) Bruker 600 MHz. ($CDCl_3$).

Chiral conformation of trimethoxysilyl thio saccharides by circular dichroism

The chirality of the silane thio saccharides (analogs n=1, 3, 7 and 13 glucose units) were demonstrated by HPLC-circular dichroism (CD) (Figure 1-21). Among all the sugar trimethoxysilyl derivatives only the signal for silane thio Glc changed from a positive signal to a negative signal (Refer to Figure 1-11 and Addendum B). The signal changed from a positive signal after the achiral GOPTMS reacted with the thiol Glc. This phenomenon was not observed with the larger sugars, probably due to their increased bulk keeping their conformations intact.

Figure 1-21: Demonstration of chirality of silane thio saccharides by HPLC-CD

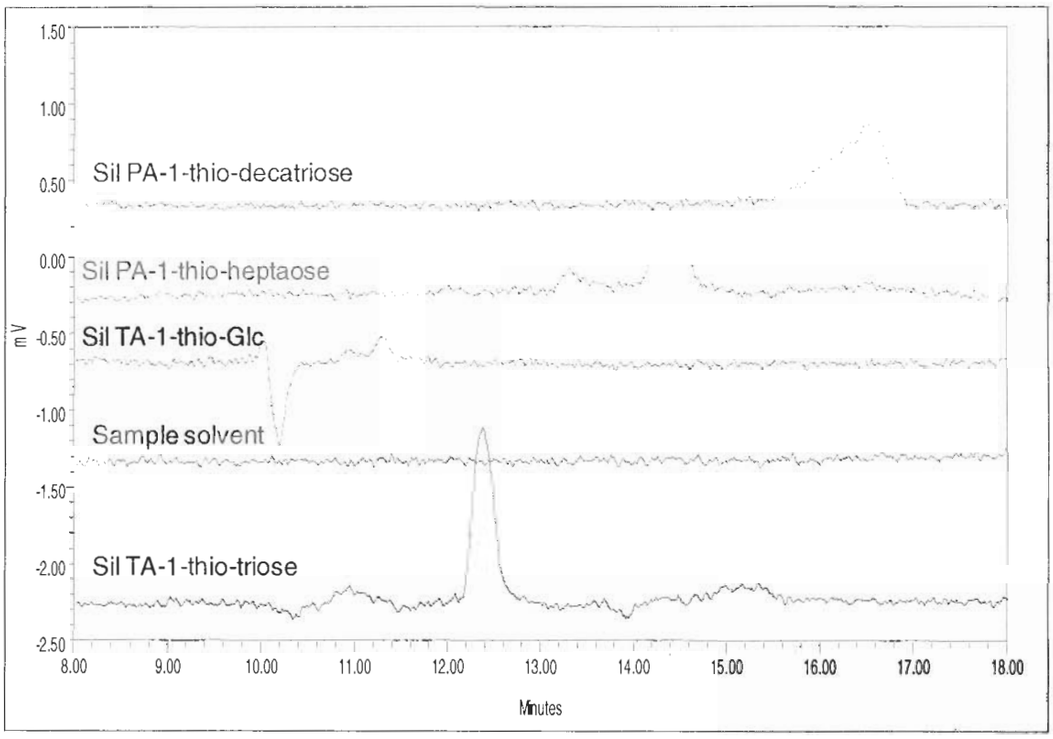

(Atlantis T3 HPLC column). Conditions: flow rate 1.0 mL/min: 35 °C; Mobile phase (A) 5 mM ammoium formate aqueous, (B) acetonitrile: gradient: 0-25 min, 80→0% A, 20 →100% B.

Conclusions

A series of thiol saccharides and their trimethoxysilyl derivatives have been successfully synthesized. The starting materials for these thiol saccharides were glucose, maltotriose, maltoheptaose, maltooctaose and maltodextrin. The anomeric thiol group on the sugar was carefully selected for its nucleophilic properties. Here the thiol saccharides were used to react with the epoxy group of the 3-glycidoxypropyl trimethoxysilane (GOPTMS) linker to afford novel silane peracetylated-1-thio-saccharides after the ring opening. To the best of our knowledge, the peracetylated-1-thiol-maltodecatriose and the trimethoxysilyl saccharides derivatives have not been reported in the literature. The use of the trimethoxysilyl linker ensured bonding of the saccharides to the organosilane moiety via a robust and hydrolytically stable carbon-sulfur bond. As demonstrated in Chapters 2 and 3, the trimethoxysilyl peracetylated-1-thio-saccharides were used as ligands for new adsorbents to be used for stereoisomer separations.

Addendum A (NMR Spectra)

This supplement provides additional NMR spectra (including ^{13}C APT spectra) of the saccharide derivatives. In the APT experiment, quaternary carbons (C) and methylene (CH_2) groups have opposite phase to the methine (CH) and methyl (CH_3). Here the APT spectra of the derivatized saccharides show quaternary (C) and methylene (CH_2) positive while CH and CH_3 groups give negative signals.

^{13}C-NMR (500 MHz, $CDCl_3$)

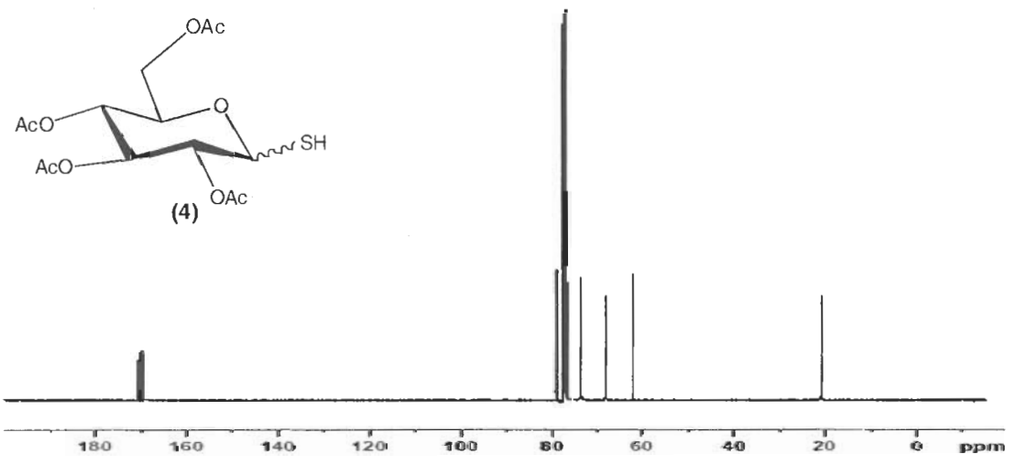

^{13}C-APT NMR (600 MHz, $CDCl_3$)

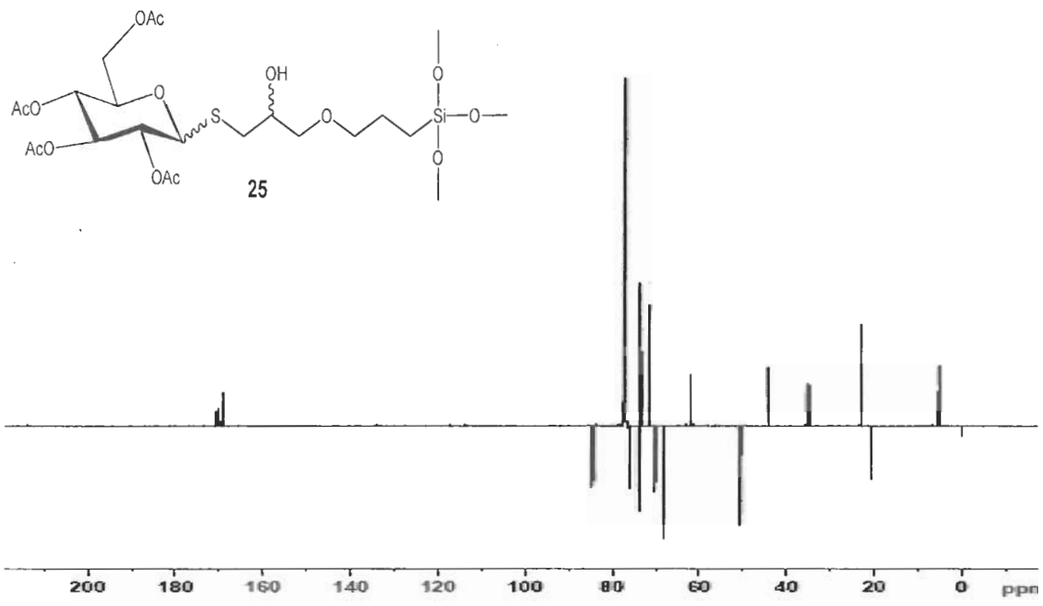

25

^{13}C-APT NMR (600 MHz, $CDCl_3$)

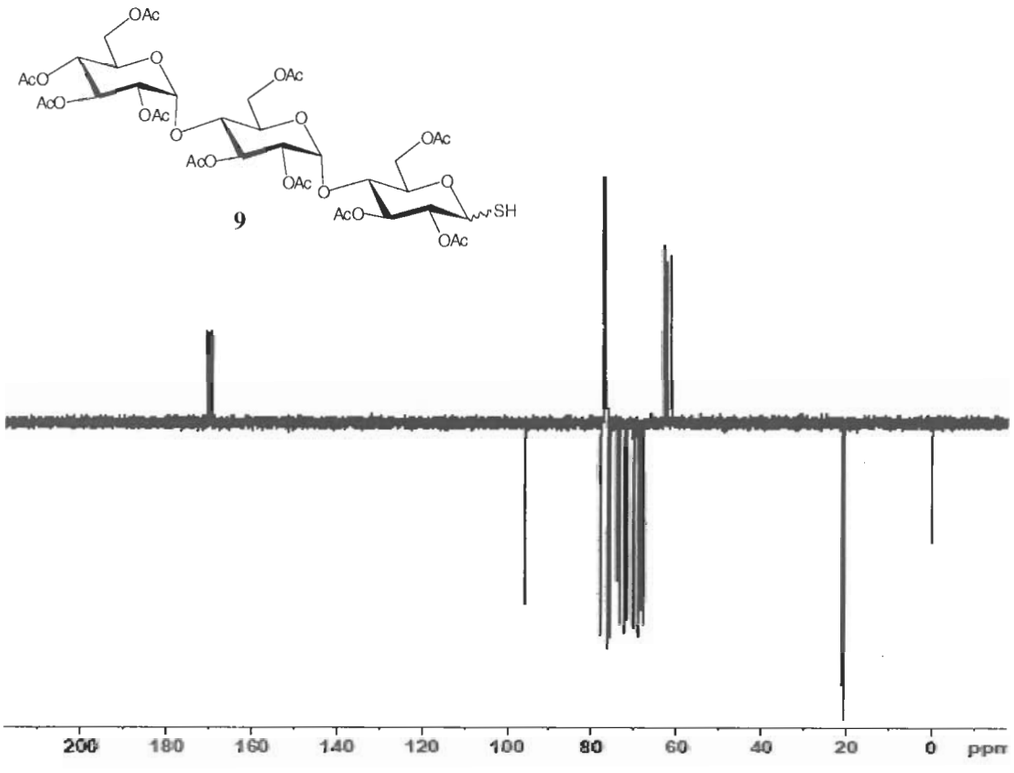

9

^{13}C-NMR (500 MHz, $CDCl_3$)

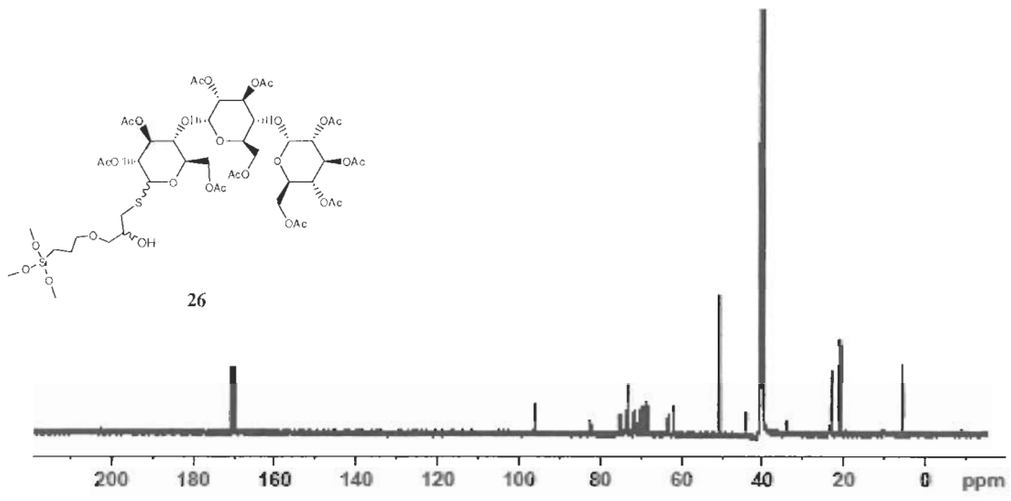

^{13}C-APT NMR (600 MHz, $CDCl_3$)

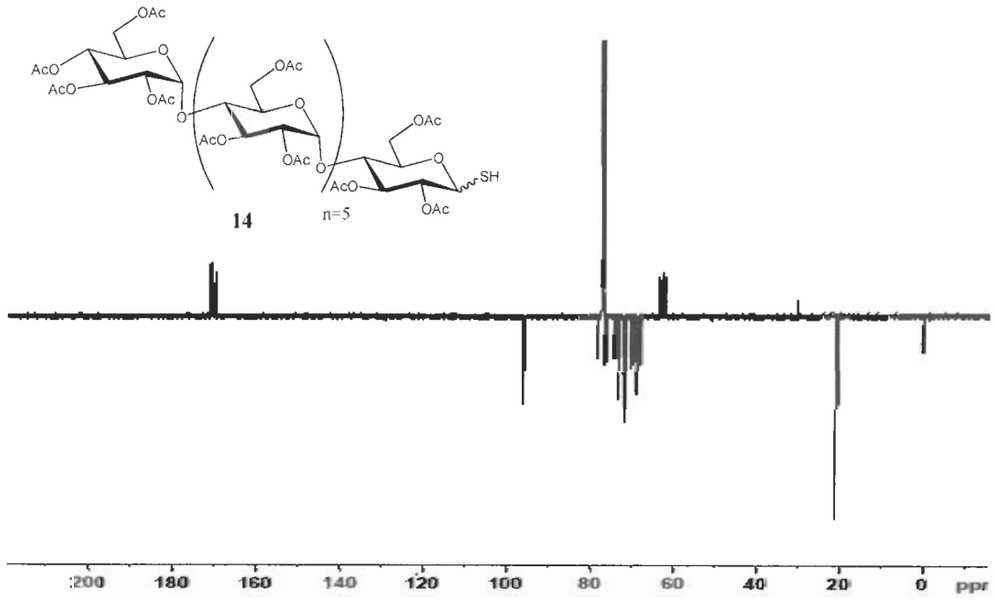

^{13}C-NMR (500 MHz, $CDCl_3$)

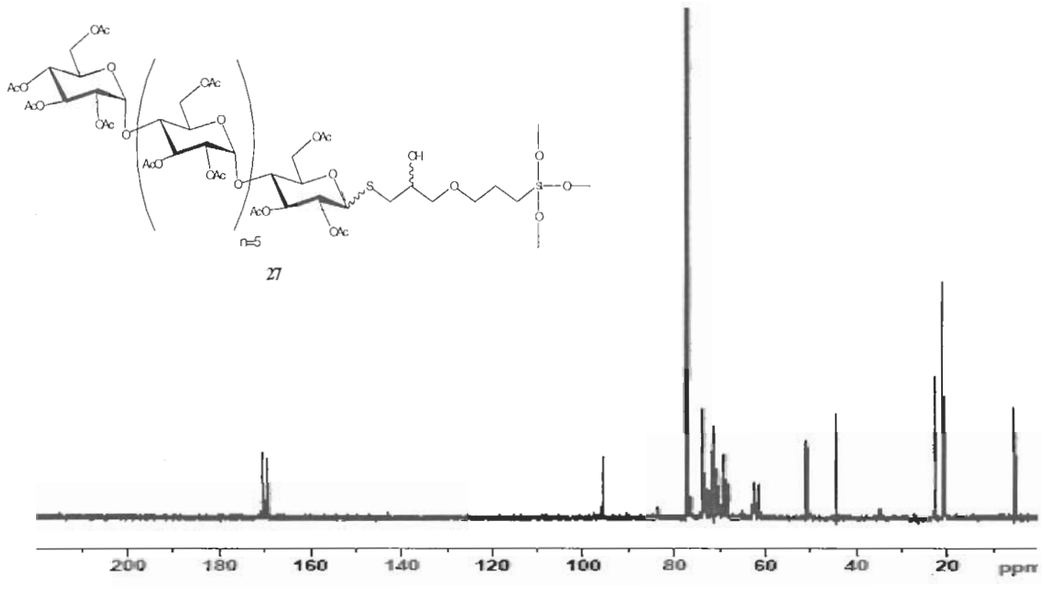

27

^{13}C-APT NMR (600 MHz, $CDCl_3$)

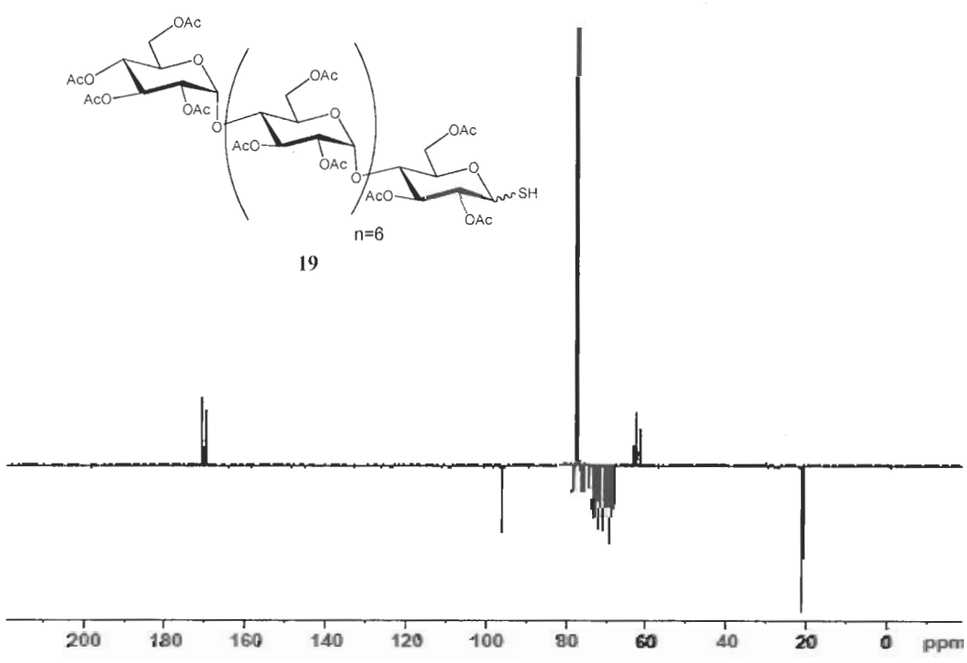

19

^{13}C-APT NMR (600 MHz, $CDCl_3$)

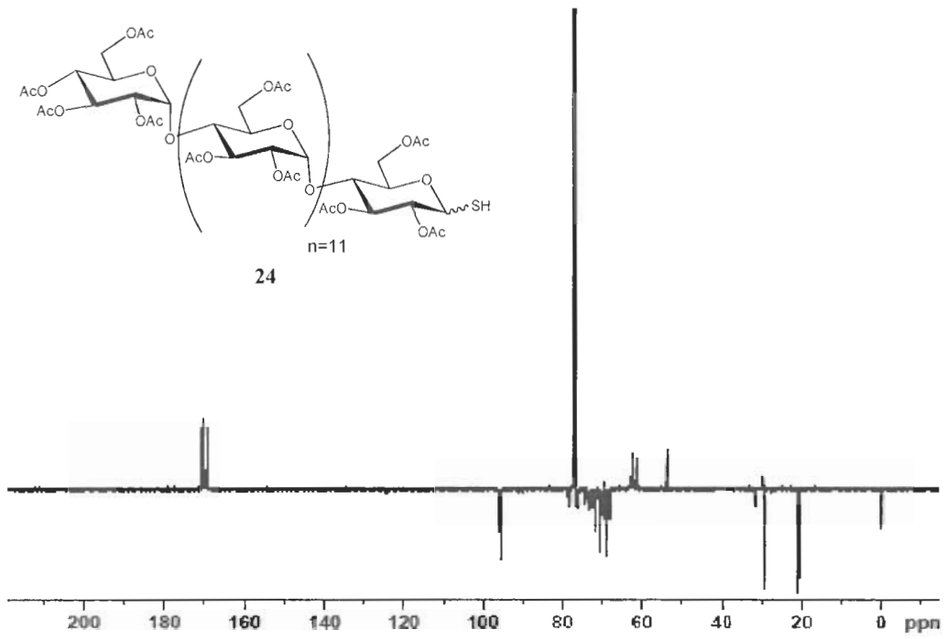

^{13}C-NMR (500 MHz, $CDCl_3$)

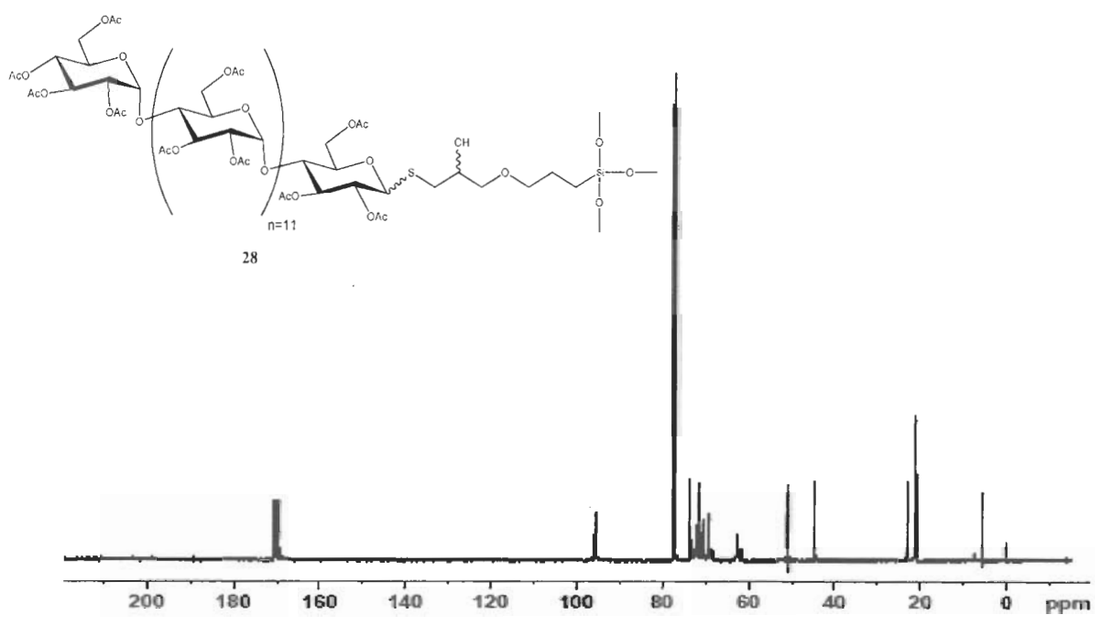

^{1}H-^{1}H-COSY NMR (600 MHz, $CDCl_3$)

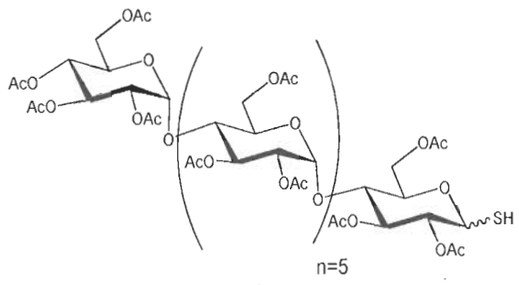

14

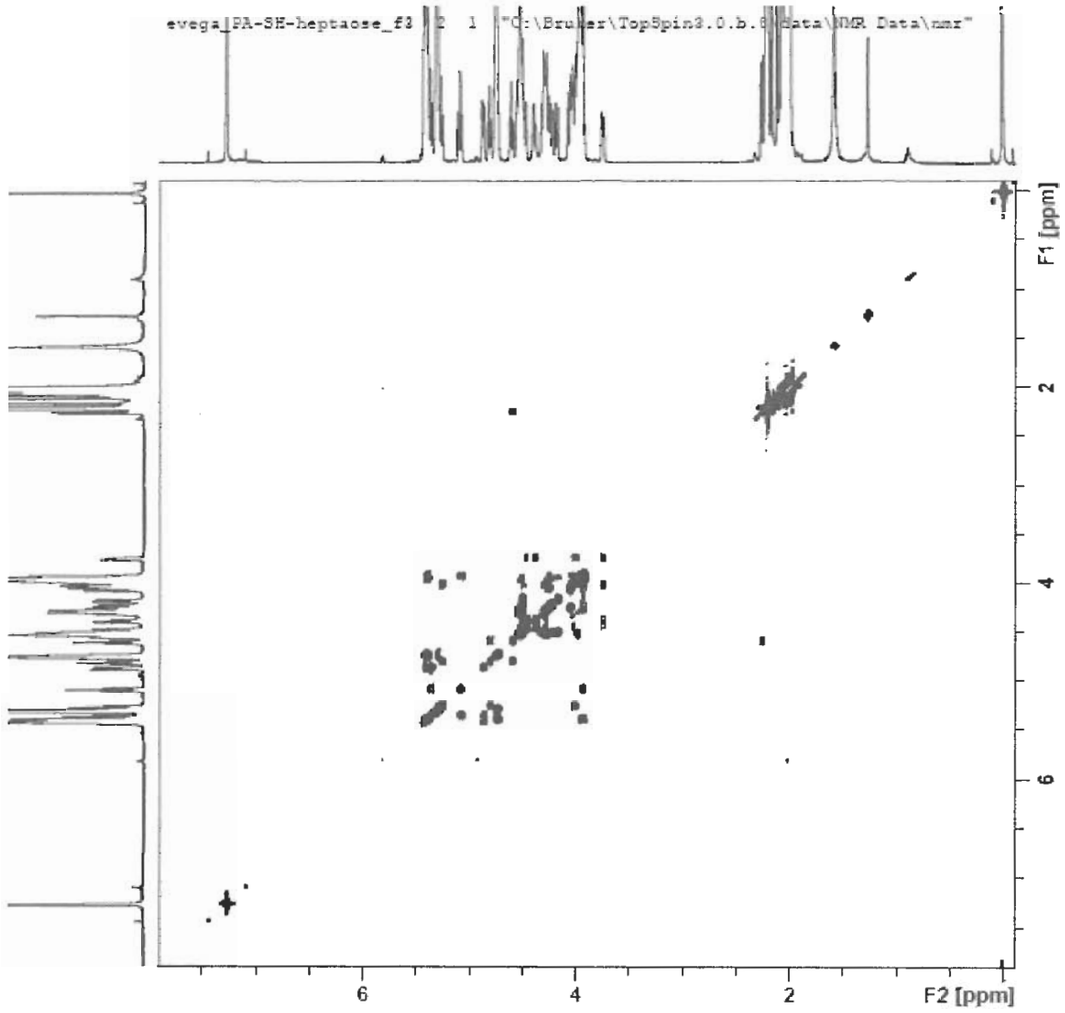

^{1}H-^{1}H-COSY NMR (600 MHz, $CDCl_3$)

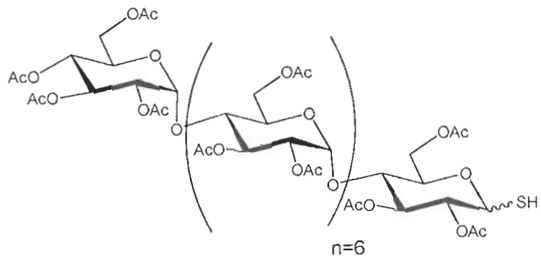

19

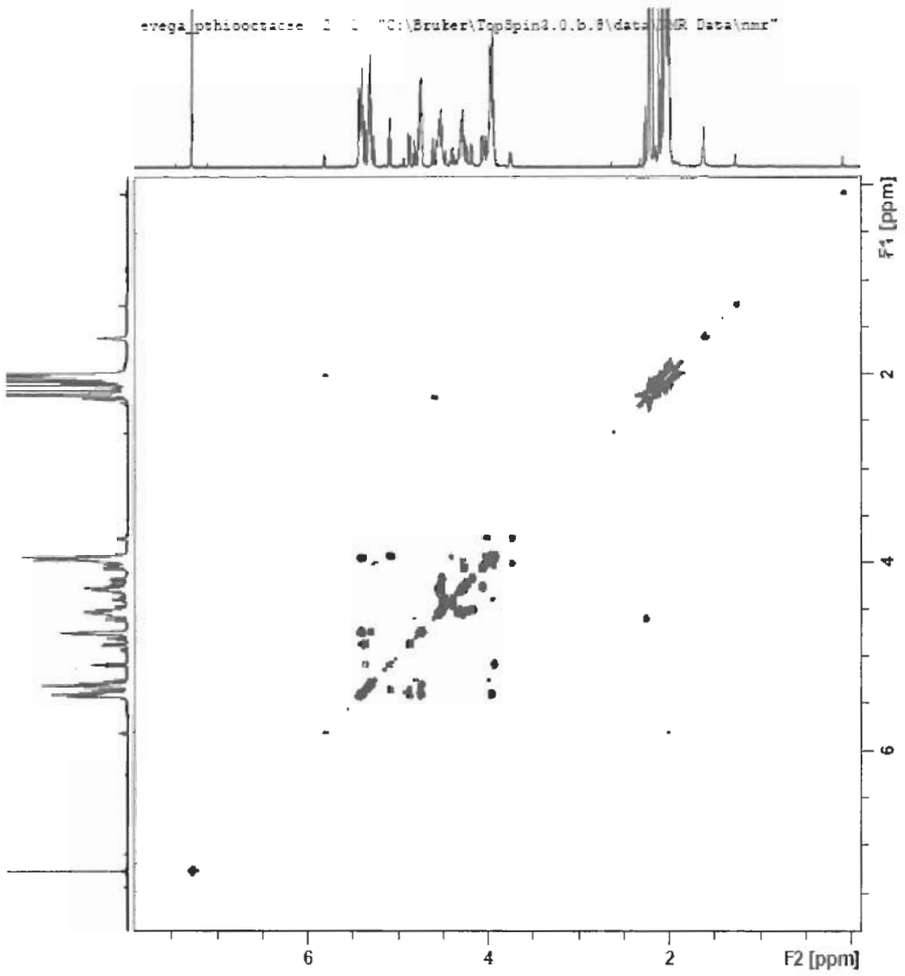

Addendum B (FTIR Spectra)

This supplement provides additional FTIR spectra and (HPLC) high pressure liquid chromatography- circular dichroism (CD) spectra of the saccharide derivatives

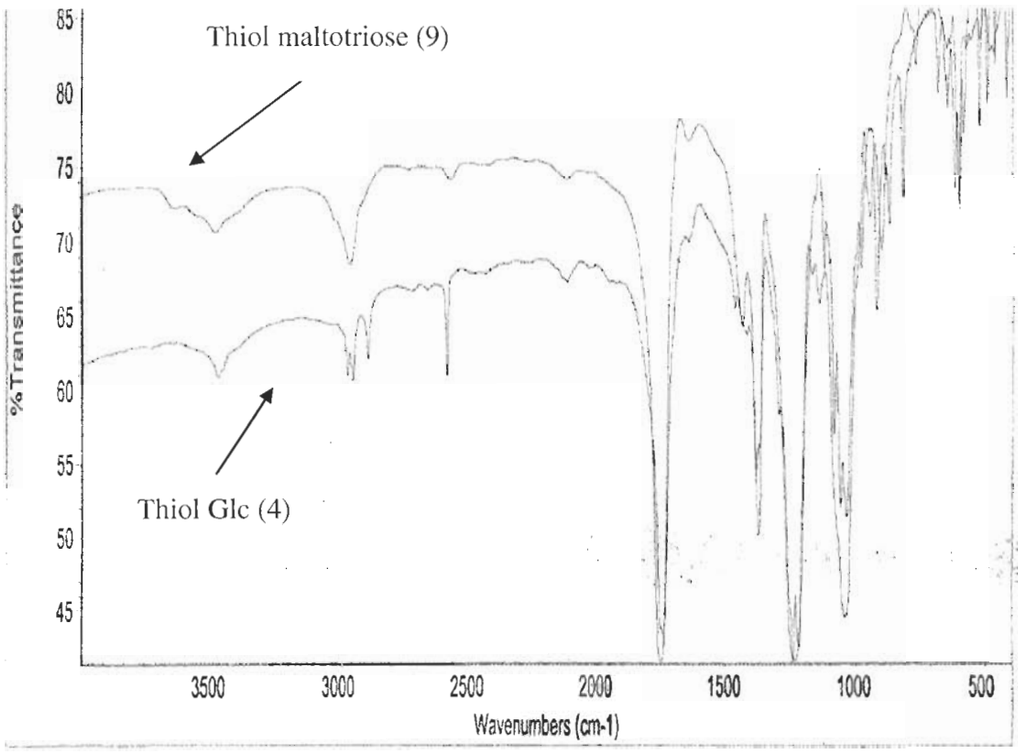

HPLC-circular dichroism: Thiol heptaose (14) and its intermediates

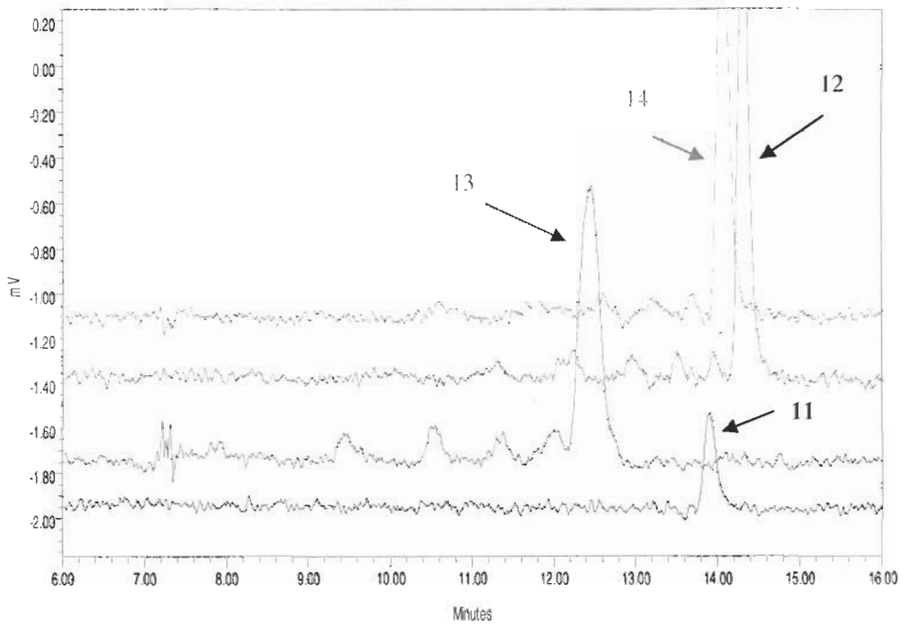

HPLC-Circular dichroism: Thiol saccharides

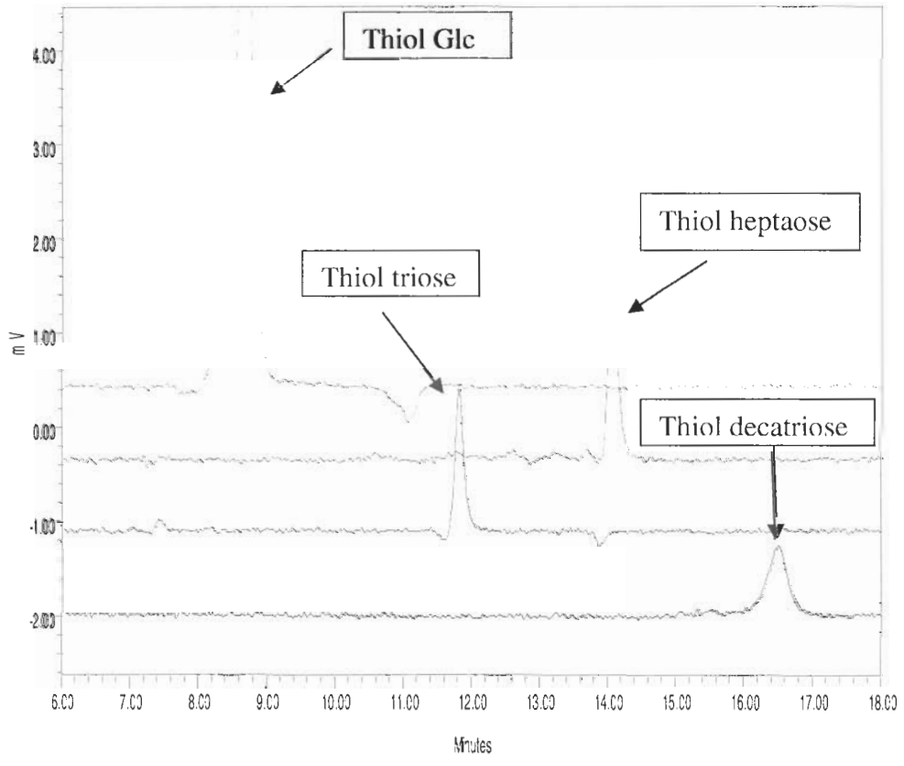

Chapter 2: Synthesis of chiral mesoporous silicas with saccharide surfaces and their use in separation of stereoisomers

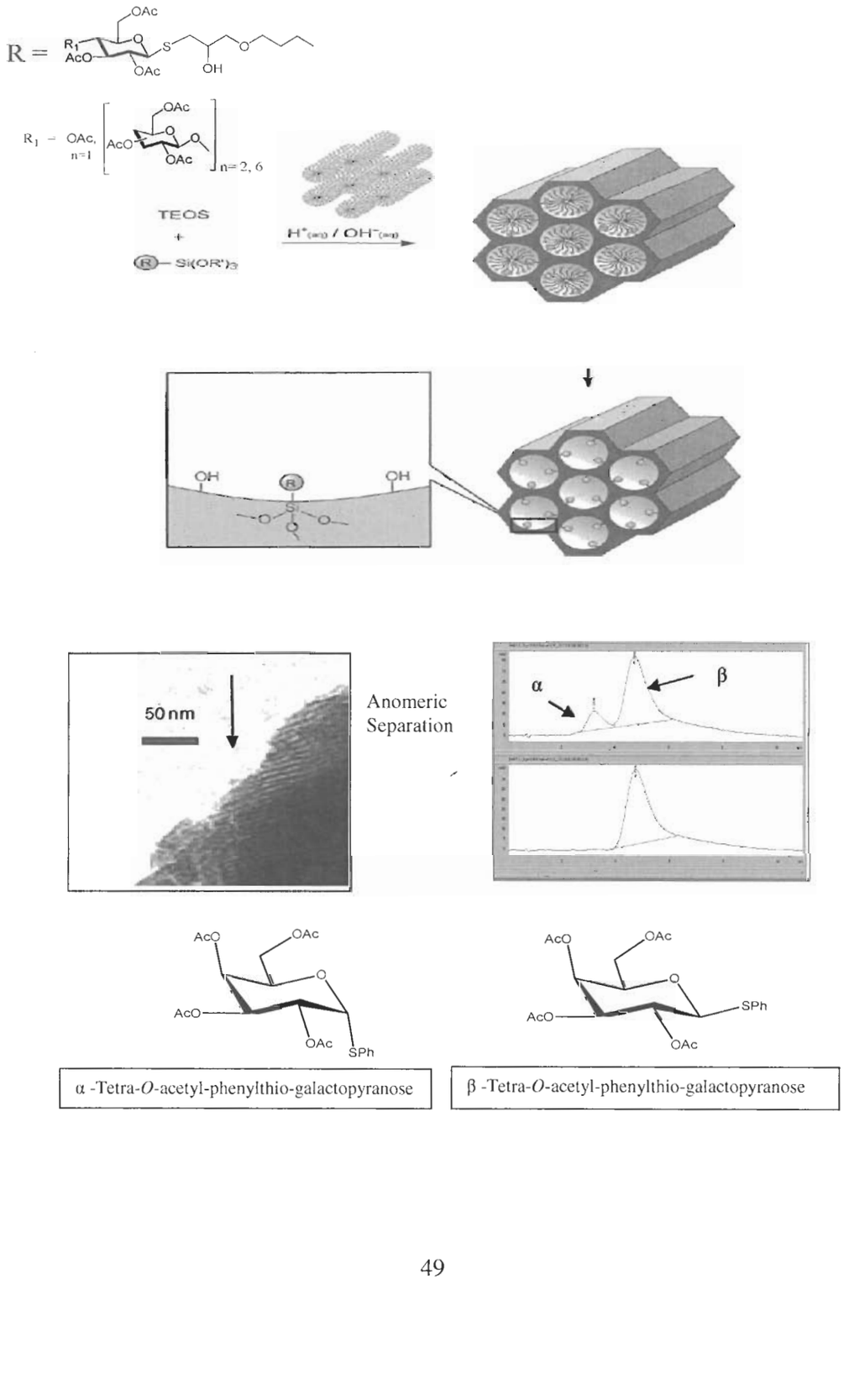

α -Tetra-*O*-acetyl-phenylthio-galactopyranose

β -Tetra-*O*-acetyl-phenylthio-galactopyranose

Abstract

Novel chiral mesoporous silicas (SBA-15 motif) with chemically bonded saccharides (1, 3, and 7 glucose units) were obtained through the co-condensation reactions. This one pot synthesis involved the reaction of organosilicon derivatives of the saccharides and tetraethyl orthosilicate (TEOS) in the presence of a P123 surfactant template under mild acidic conditions. The pore order and structure of the materials prepared were characterized by TEM and nitrogen adsorption studies. The best quality SBA-15 type silica was prepared using glucose and maltotriose derivatives. The transmission electron microscopy (TEM) images and nitrogen adsorption isotherms indicated that the pore uniformity of SBA-15 thio glucose and SBA-15 thio maltotriose were preserved. However, the SBA-15 maltoheptaose showed disordered pores. The disorder might be attributed to the larger size of maltoheptaose. Materials prepared were also characterized by elemental analysis, FTIR and TGA (thermogravimetric analysis). The application of the saccharide-grafted SBA-15 silicas in the HPLC separations of stereoisomers was demonstrated for the first time.

Introduction

Since it was discovered that ordered mesoporous silicas M41S,[24-25] KIT-1,[26]FSM-16[27] and SBA-15[28] could be obtained using a surfactant as a template, scientists became very interested in studying these materials. The synthesis of mesoporous silica with an organic functional surface was another advance in this field.[29] It was thought then that the organic-inorganic hybrid materials could play an important role in many applications such as adsorption, ion exchange, and catalysis. In general, there are two approaches to prepare mesoporous silica with organic functional surfaces: post-grafting and direct synthesis.[30] Post-grafting is typically carried out by reacting an organosilane of the type $(R'O)_3$ SiR with the free silanol groups of the mesoporous surfaces. The direct synthesis, one pot reaction, involves the co-condensation of tetraalkoxysilanes (TEOS or TMOS) with terminal trialkoxyorganosilanes in the presence of structure-directing agents affording materials with organic groups anchored chemically to the pore walls. Thus, this one pot reaction provides a high and uniform surface coverage of functional groups. Some of the examples of organic functional groups attached to mesoporous materials are vinyl,[30] aliphatic hydrocarbon,[31] thiol,[32-33] phenyl,[34-35] amine,[36-38] and sulfonic acid ligands.[39-40]

In addition, the sol-gel synthesis performed in the presence of chiral media enables the preparation of chiral mesoporous silicas[41] (CMSs) – the emerging new group of materials with prominent applications in stereoselective adsorption, recognition, and catalysis. The preparation of CMSs with chirality present at different length scales have been reported through the use of chiral surfactant templates, chiral directing agents, and additives.[41-44] As with the achiral organic functionalized mesoporous silica stated above, the CMSs with chirality embeded in the pore walls can be obtained through the direct co-

condensation of silica precursors (TEOS) and chiral organosilanes in the presence of the appropriate surfactant or polymer templates. The most researched routes utilize CTAB surfactant (MCM-41 family) and P123 polymer (SBA-15 family) yielding the organosilica hybrid materials with ordered mesopores, tailored pore size, and diverse surface chemistry.[45-50]

Polysaccharides and their derivatives are very popular chiral selectors due to their ability to interact with a wide variety of stereoisomers. In particular, polysaccharide-based stationary phases are the most efficient and popular for HPLC stereoseparations.[48] However, the use of saccharides for the preparation of the CMSs has not been explored. Also, the use of CMSs (of any kind) in the HPLC separation of stereoisomers has not been demonstrated. In the work presented here, we report: (1) the preparation of ordered CMSs functionalized with saccharides containing glucose, maltotriose, and maltoheptaose groups, and (2) the direct application these materials in the HPLC separations of stereoisomers. The materials prepared demonstrated high stereoselectivity in the HPLC separation of anomers and this is reported for the first time to the best of our knowledge. The saccharide SBA-15 type materials prepared were thoroughly characterized by nitrogen adsorption, TEM, chemical analysis, FTIR, and TGA.

Experimental

Materials

Trimethoxy-silylated thio saccharides were prepared in our laboratories (Refer to chapter 1). Tetraethyl orthosilicate and Pluronic P123 surfactant were obtained from Sigma Aldrich Chemical Company (St. Louis, MO, USA). All other chemicals and solvents were of analytical or HPLC grade.

Synthesis

The saccharide functionalized SBA-15 silicas were prepared through the co-condensation of the trimethoxy-silylated derivatives of peracetylated glucose, maltotriose, and maltoheptaose with TEOS. Figure 2-1 represents the structures of the molecules and the reaction scheme used. The trimethoxysilylated saccharides were obtained via the reaction of the corresponding peracetylated-1-thiol-saccharides with glycido-oxypropyl trimethoxysilane (GOPTMS). The use of the GOPTMS linker ensured bonding of the saccharides to the organosilane moiety via a robust and hydrolytically stable carbon-sulfur bond. The synthesis of thiol-saccharides and their silylated derivatives was described in details in Chapter 1 and it is briefly described below.

Synthesis of peracetylated-1-thio-saccharides and their triethoxysilyl derivatives

Each saccharide was peracetylated by using an excess of acetic anhydride and about 10 equivalents of a hydrogen bromide solution (33% HBr in glacial acidic acid). After isolation, the peracetylated saccharide was converted to the anomeric bromide using additional 33% hydrogen bromide /glacial acidic (10 equivalent HBr) in methylene chloride. Then, an anomeric thiourea salt ("Pseudothiosaccharide") was prepared from the glycosylbromide using thiourea in refluxing acetone. The pseudothiosaccharides

were hydrolyzed using aqueous sodium pyrosulfite to afford the desired crude peracetylated-1-thio-saccharides that were purified by preparative elution chromatography. Once isolated, peracetylated-1-thio-saccharides were reacted with the glycido-oxypropyltrimethoxysilane (2 equivalents) in acetonitrile containing aqueous 10 mM dibasic potassium phosphate (3:1 ratio). The reaction was completed within 10 to 12 hours. The crude products from the reactions were then extracted with ethyl acetate and concentrated *in vacuo*. The structures of the peracetylated-1-thio-saccharides and their trimethoxysilyl derivatives were confirmed by chemical analysis, ^{1}H- and ^{13}C-NMR, and mass-spectrometry.

Figure 2-1: The reaction scheme used for the preparation of trimethoxysilylated saccharides and their co-condensation with TEOS

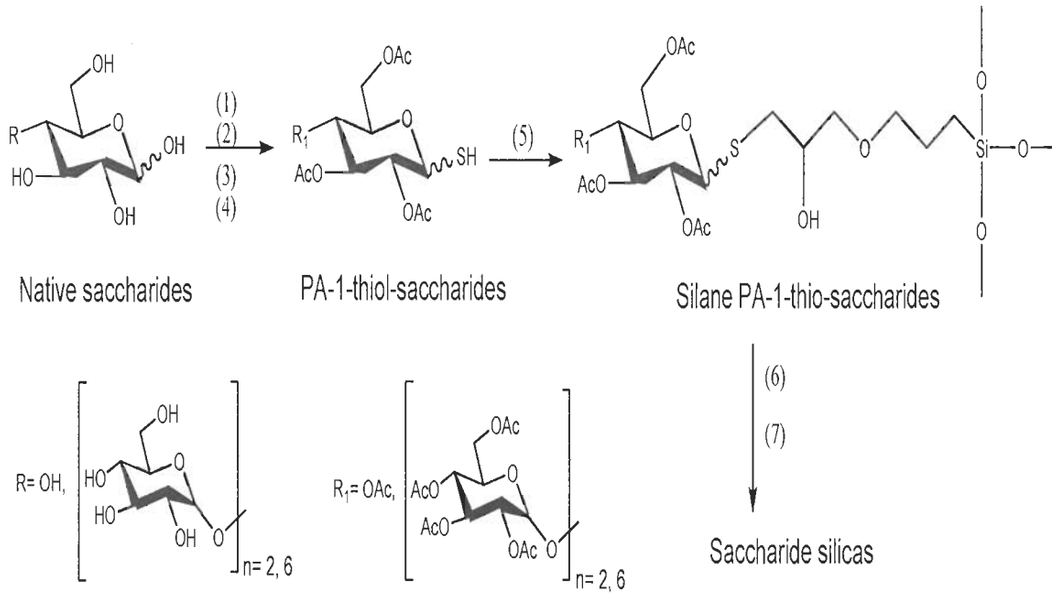

(1) Acetic anhydride, 33% HBr/acetic acid; (2) 33% HBr/acetic acid, CH_2Cl_2; (3) acetone, thiourea, reflux (4) $Na_2S_2O_5$/water, reflux; (5) $(OMe)_3Si(CH_2)_3OCH(O)CH_2$, CH_3CN, 10 mM K_2HPO_4 (3:1) (6) EtOH (7) TEOS, P123, aqueous HCl (pH=2.8)

Synthesis of SBA-15 type silicas by co-condensation of TEOS and trimethoxysilyl peracetylated-1-thio-saccharides (analogs 1, 3 and 7 Glc units)

Briefly, the co-condensation of the trimethoxysilyl-saccharides with TEOS was carried out in presence of Pluronic P123 surfactant under mild acidic conditions to avoid hydrolysis of the acetyl protecting groups of the saccharides. In a typical synthesis, Pluronic P123 [poly-ethylene-glycol-block-polypropylene-glycol-block-polyethylene-glycol ($EO_{20}PO_{70}EO_{20}$)] (600 mg) was dissolved in deionized water (30 mL) at 40 °C. TEOS (3.0 g, 12.7 mmol) was pre-hydrolyzed with aqueous HCl solution (1.5 g, pH=2.8) for two hours at 40 °C, then transfered into the P123 solution. After one hour, the corresponding trimethoxysilyl derivative of the saccharide (previously dissolved in warm ethanol) was added to the P123-TEOS solution and stirred for 20 h at 40 °C. It was aged in an oven for additional 24 h at 80 °C. The precipitated silica was collected and thoughly washed (to remove P123) using the following sequence of washes : 1) warm deionized water; 2) 2N HCl; 3) 2% (wt) HCl in ethanol; 4) water and 5) finally acetone. A significant amount of washing was required to remove the Pluronic P123 from the silicas: typically, ~1 L of each solvent was required for every gram of modified silica produced. Finally, the materials prepared were dried at 90 °C.

Characterization

Carbon analysis was performed with a Perkin Elmer 2400 CHN Analyzer. Elemental Analysis was performed by Robertson Microlit Laboratories (Madison, NJ) using the ASTM method. The chemical structures of the saccharide moieties incorporated in the silicas were confirmed by FTIR (PerkinElmer Spectrum One) : ~1760 cm^{-1} (C=O stretch in acetyl groups); the full spectra are shown in Figure 2-2. The surface area, pore size

distributions, and pore volumes were done by nitrogen adsorption. The order structures of the SBA-15 saccharides were further examined using transmission electron microscopy (TEM).

Infrared spectroscopy. Infrared spectra were recorded with a Perkin Elmer Spectrum One FTIR instrument using a mercury cadmium telluride detector. The spectra were obtained using a Harrick Seagull accessory (reflectance mode, 45° angle of incidence, 128 scans, and resolution 4 cm^{-1}). Figure 2-2 shows an overlay of the spectra for glucose-, maltotriose-, and maltoheptaose-modified silicas. Peaks at ~2920, 2850 cm^{-1} (C-H stretches), and ~1760 cm^{-1} (C=O stretch) were attributed to methyl, methylene, and carbonyl groups in the acetylated saccharides. Peaks at ~1000-1100 cm^{-1} were attributed to Si-O stretches from silica matrix. A broad peak at ~3200-3300 cm^{-1} was O-H stretching from the surface water.

Figure 2-2: Infrared spectra for bare SBA-15 and SBA-15 saccharides

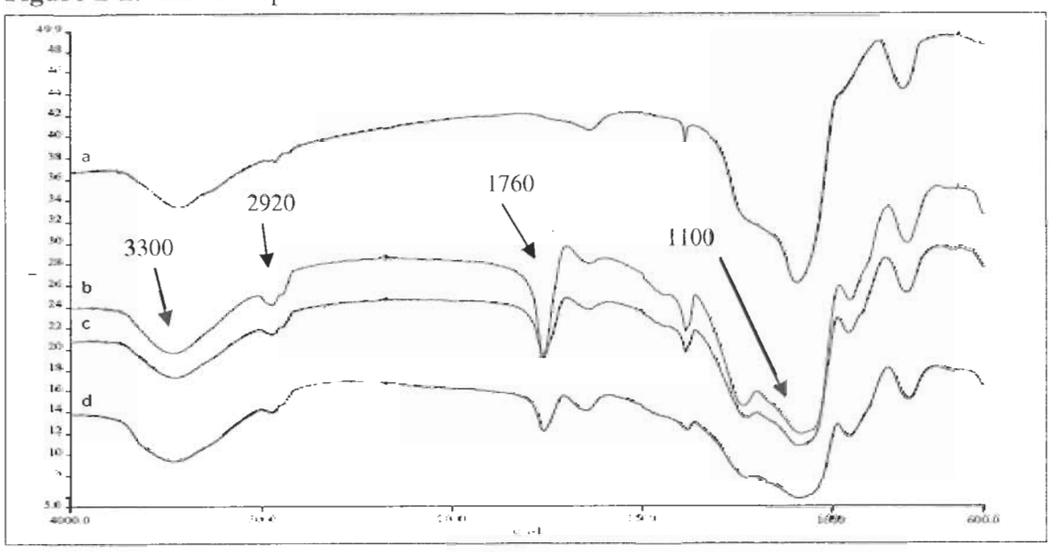

Bare SBA-15 (a) and SBA-15 modified with glucose (b); maltotriose (c); and maltoheptaose (d).

Nitrogen adsorption

Nitrogen adsorption-desorption isotherms (77K) were measured using an Autosorb-1 analyzer (Quantachrome Instruments, Boynton Beach, FL, USA). The adsorption isotherms were measured over a relative pressure p/p_o range extending from 10^{-2} to 0.995. Desorption isotherms were measured over a relative pressure range from 0.995 to 0.2-0.3 respectively. Prior to analysis, the materials were degassed at 60 $^{\circ}$C overnight using the out-gassing port of the instrument. A relatively low outgassing temperature was chosen to avoid the degradation of the saccharide groups grafted to silica. The surface area was calculated via the Brunauer-Emmett-Teller (BET) method in the range of relative pressure from 0.06 to 0.20. The cumulative volume of the pores was determined as the volume of the adsorbed liquid nitrogen at 0.98 p/p_o. The micropore volume was determined using the t-plot method using software provided by the instrument's vendor. The pore size distribution (PSD) and average pore diameter was

calculated with the Barrett-Joyner-Halenda (BJH) algorithm using the adsorption branch of the adsorption-desorption hysteresis. It is recommended to use the adsorption branch to obtain PSD for the SBA-15 silicas due to their small pores and well-ordered network of porous materials.

Thermal gravimetric analyses (TGA)

Thermal analyses of the modified silicas were performed in air and in nitrogen using a TA Instruments Hi-Res 2950 Thermogravimetric Analyzer using a heating rate of 10 °C per min.

Results and Discussion

The organic solvents play an important role in the synthesis of the saccharide SBA-15 silicas. When acetonitrile was used to dissolve the saccharide, it was noticed that saccharide silicas had a very a wide pore size distribution by nitrogen isotherms (Addendum C). This was attributed to the acetonitrile solvent used during the co-condensation reaction of TEOS with silane saccharides. It was suspected then that the acetonitrile solvent inhibited the properties of the structure directing agent, P123. Thus, it was decided to use ethanol instead of acetonitrile to dissolve the saccharide derivatives affording a well-order PSD.

The TEM images of the SBA-15 thio glucose and SBA-15 thio maltotriose prepared by co-condensation are presented in Figures 2-3 and 2-4, respectively. Silicas prepared showed an ordered structure with a hexagonal pattern of pores similar to that of bare[51] SBA-15.

Figure 2-3: TEM images for the glucose-SBA-15 silica

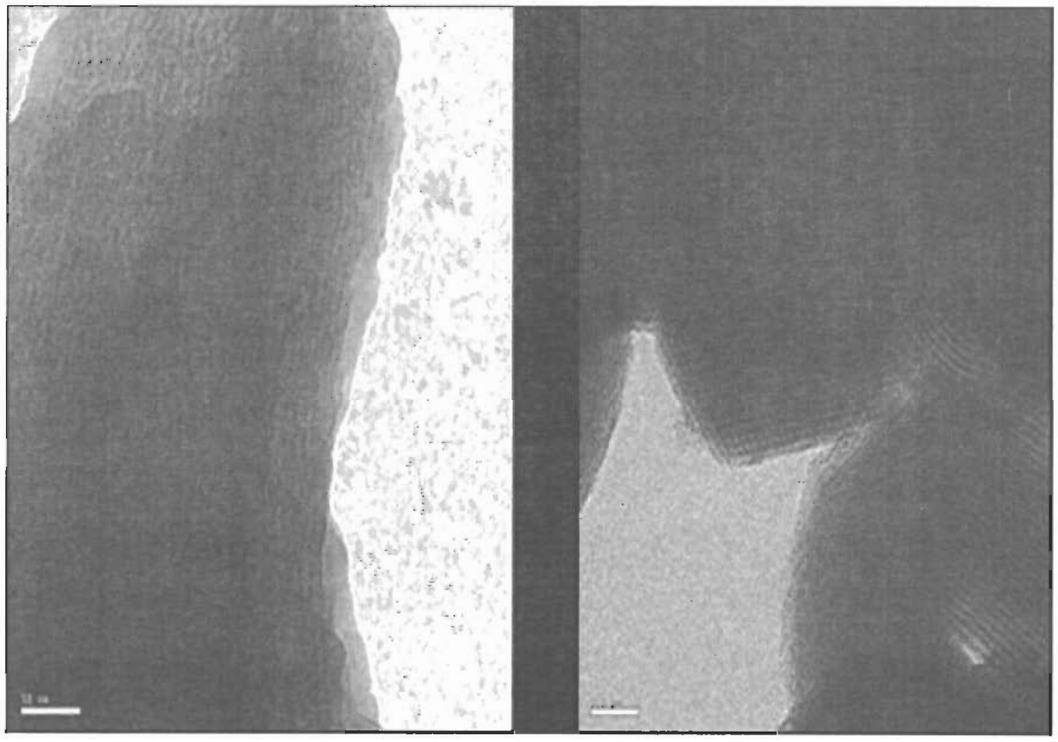

Scale bar - 50 nm (left) and 200 nm (right).

Figure 2-4: TEM images for the maltotriose-SBA-15 silica.

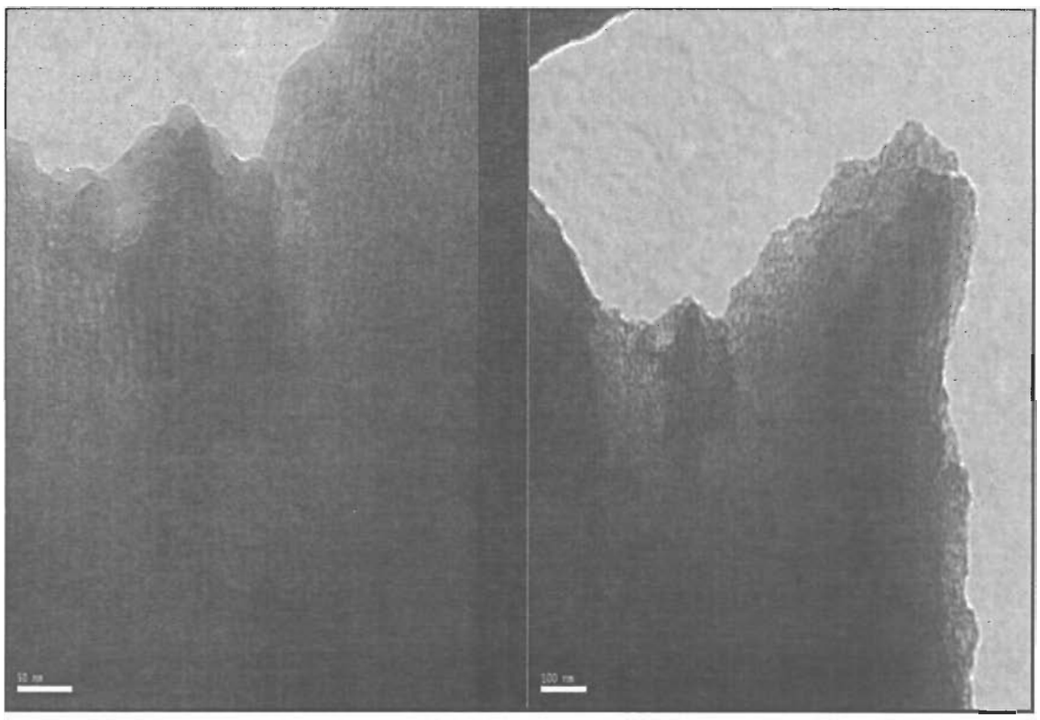

Scale bar - 50 nm (left) and 100 nm (right).

The ordered structure of silicas observed by TEM was further corroborated by nitrogen adsorption-desorption isotherms (Figure 2-5). The isotherms were type IV isotherms with a capillary condensation hysteresis at ~0.5-0.7 p/p_0 indicating mesoporous materials.[52] For the glucose- and maltotriose-modified silicas, (PSD) curves were symmetrical and narrow showing uniform pores with mean radii of ~3.8 and 3.3 nm respectively. For the maltoheptaose-silica, the mean pore radius was ~ 2.5 nm and the PSD was notably wider which was attributed to the disordering effect of the larger sized saccharide moiety. The surface areas and the pore volumes of the silicas demonstrated substantial decreases as the size of the saccharide group increased (Table 2-1).

Figure 2-5: N_2 adsorption-desorption isotherms of SBA-15 saccharides

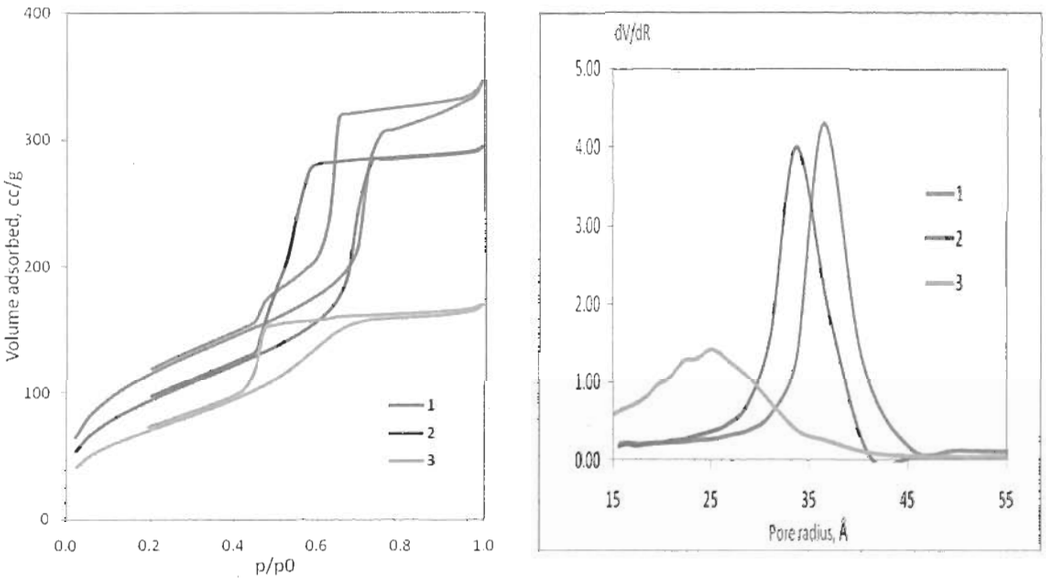

Nitrogen isotherms (left) and pore-size distribution curves (right) for SBA-15 silicas modified with glucose (1); maltotriose (2); and maltoheptaose (3).

Grafting density of saccharide ligands

The grafting density was obtained from the results of carbon (%C) and sulfur (%S) analysis of the saccharide-silicas as follows:

$$\rho[\mu mole/m^2] = \frac{10^6(\%C)}{[1200 \cdot n_C - MW \times (\%C)]} \cdot \frac{1}{S_{SiO2}}$$

$$\rho[\mu mole/m^2] = \frac{10^6(\%S)}{[3200 \cdot n_S - MW \times (\%S)]} \cdot \frac{1}{S_{SiO2}}.$$

MW was the molecular weight of the saccharide-silane group, n_C and n_S were the numbers of carbon or sulfur atoms in the grafted group, S_{SiO2} was the surface area of the corresponding silica after the calcination (Table 2-1).

The surface concentration (grafting density, ρ) of the saccharides was estimated independently from carbon and sulfur analyses. For glucose-modified silicas, the

grafting density was ~1.6 μmole/m^2, which corresponded to ~100 $Å^2$ per molecule demonstrating surfaces with close packing of glucose groups. As one can see (Table 2-1), the grafting densities decreased with the increase of the size of the saccharide. The surface coverage (calculated as number of glucose units per nm^2), however, did not change much and was comparable for all the saccharide surfaces. We noted that grafting densities determined from %C and %S were in close agreement, thus indicating the complete removal of the surfactant template from the pores of the silicas prepared.

Table 2-1 Characteristics of saccharide-modified SBA-15 silicas

Saccharide Group	S_{BET}, m^2/g	V_{pore}, cm^3/g	R_{pore}, nm	%C	%S	Grafting density sacharide groups, μmole/m^2	
						from %C	from %S
Glucose	408	0.51	3.8	13.97	1.47	1.08	0.74
Maltotriose	341	0.45	3.3	17.75	0.73	0.52	0.45
Maltoheptaose	261	0.25	2.5	11.44	0.36	0.25	0.26

In order to evaluate the distribution of saccharides throughout the sample and their role in the formation of the pore structure, the silicas were subjected to calcination at 800 °C. For all the silicas, after the calcinations, the isotherms remained type IV, yet they were shifted up along the adsorption axis demonstrating an increase in the surface area and the pore volume (Figure 2-6). The observed changes were attributed to the "pore opening" due to removal of the saccharide groups (caused by calcination), which led us to conclude that the saccharide groups were largely concentrated within the pores. Table 2-2 shows the pore structure characteristics for saccharide-silicas after calcination.

Figure 2-6: Overlay of the N_2 adsorption-desorption isotherms of saccharide SBA-15 silicas and their calcinated materials

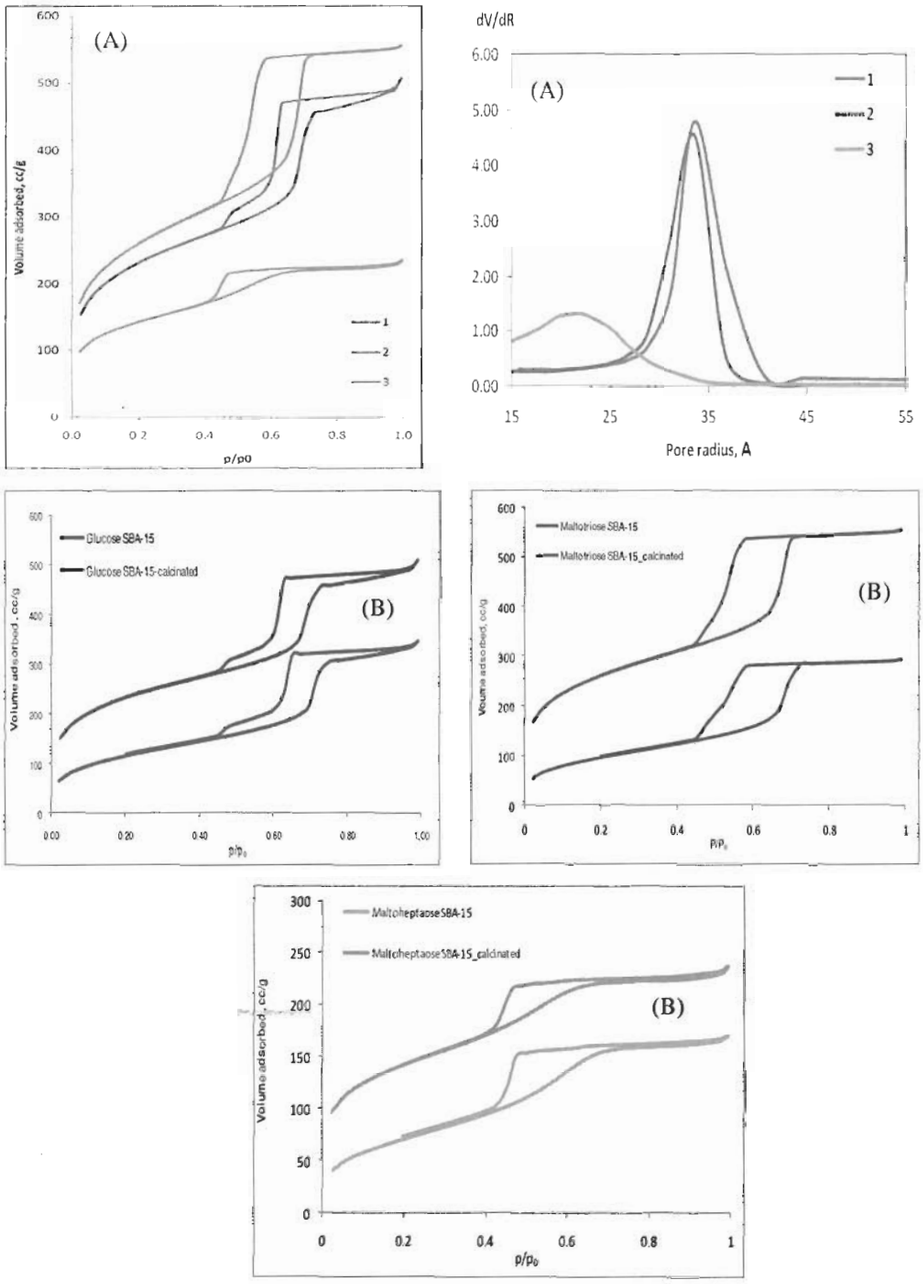

(A) Nitrogen adsorption-desorption isotherms (left) and pore-size distribution curves (right) for SBA-15 silicas modified with glucose (1), maltotriose (2), and maltoheptaose (3) after calcination at 800 °C. (B) Overlay of nitrogen isotherms of each adsorbent and its calcinated materials.

Table 2-2: The pore structure characteristics for saccharide-silicas after calcination at 800 °C

Saccharide group	S_{BET}, m^2/g	V_{pore}, cm^3/g	R_{pore}, nm
Glucose	513	0.75	3.6
Maltotriose	616	0.85	3.1
Maltoheptaose	345	0.35	2.0

TEM images of the saccharide SBA-15 materials demonstrated uniform, ordered pore structures and showed virtually no change as compared to bare SBA-15 type silicas (calcinated silicas). This data confirmed a preservation of the pore structure of the saccharide SBA-15 materials. The TEM images for the SBA-15 saccharide materials after calcination are presented in Figure 2-7.

Figure 2-7: TEM images for the SBA-15 saccharides after calcination

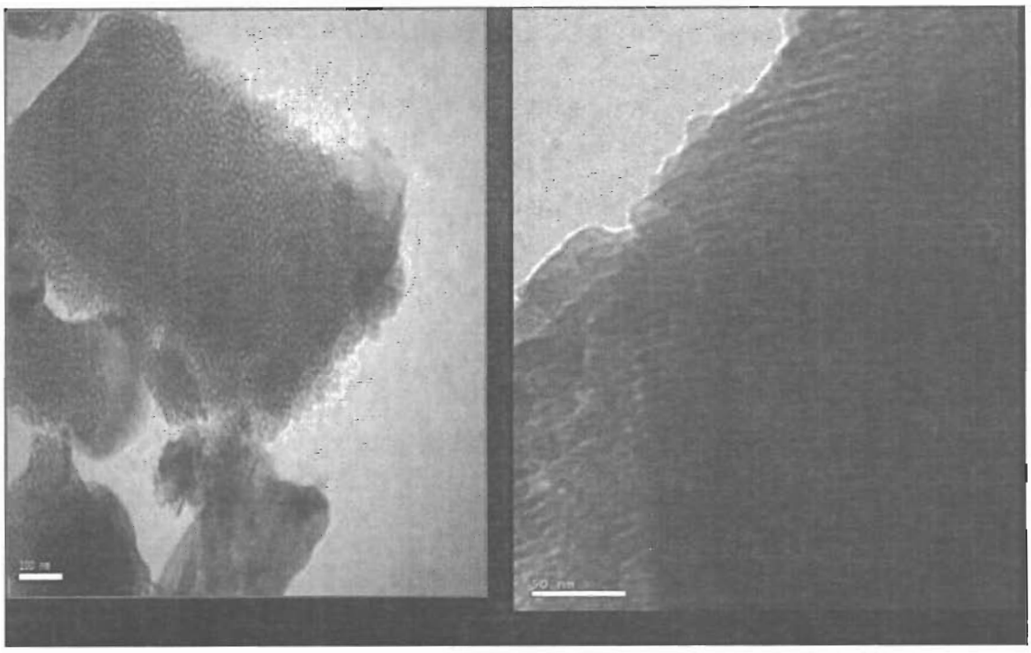

Glucose-SBA-15 (left) and maltotriose-SBA-15 (right) after calcination. Scale bar - 100 nm (left) and 50 nm (right).

Thermal properties of the prepared SBA-15 saccharide silicas

Thermal gravimetric analysis (TGA) determines the change in weight in relation to change of temperature. The thermal properties of these materials were assessed through TGA (Thermal Instruments) using temperatures ranging from 25-700 $^{\circ}$C, with a heating rate of 10 $^{\circ}$C/min in the flow of nitrogen (40 cm^3/min). The first weight loss feature (~4-6% loss) was observed below 100 $^{\circ}$C and was attributed to the desorption of weakly bound water. The main weight loss (~20-30%) was observed ~300-600 $^{\circ}$C, which was attributed to the degradation of the saccharide groups (Figure 2-8). The derivative TGA was also conducted on the SBA-15 saccharides. T_{MAX} (DTGA) is the onset of the weight loss and the temperature of the maximum rate of the weight loss. As it is demonstrated in

Figure 2-9, these materials are very stable up to T_{MAX} between 358.6 °C to 415.1 °C (the longer the saccharide the higher their thermal stability).

Figure 2-8: TGA plots for bare SBA-15 and SBA-15 modified with saccharides

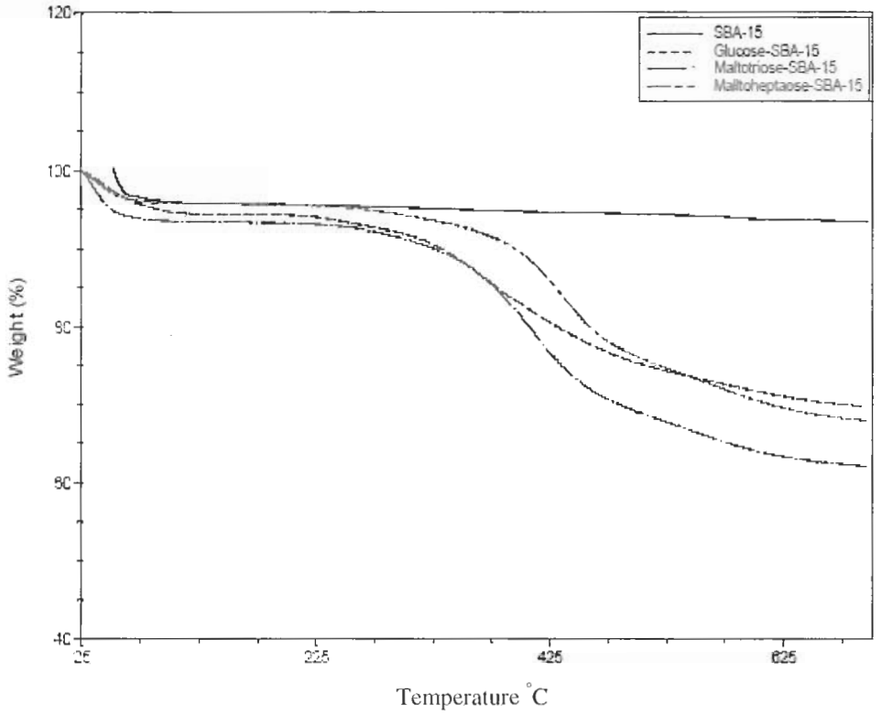

Figure 2-9: DTGA plots for SBA-15 modified with saccharides

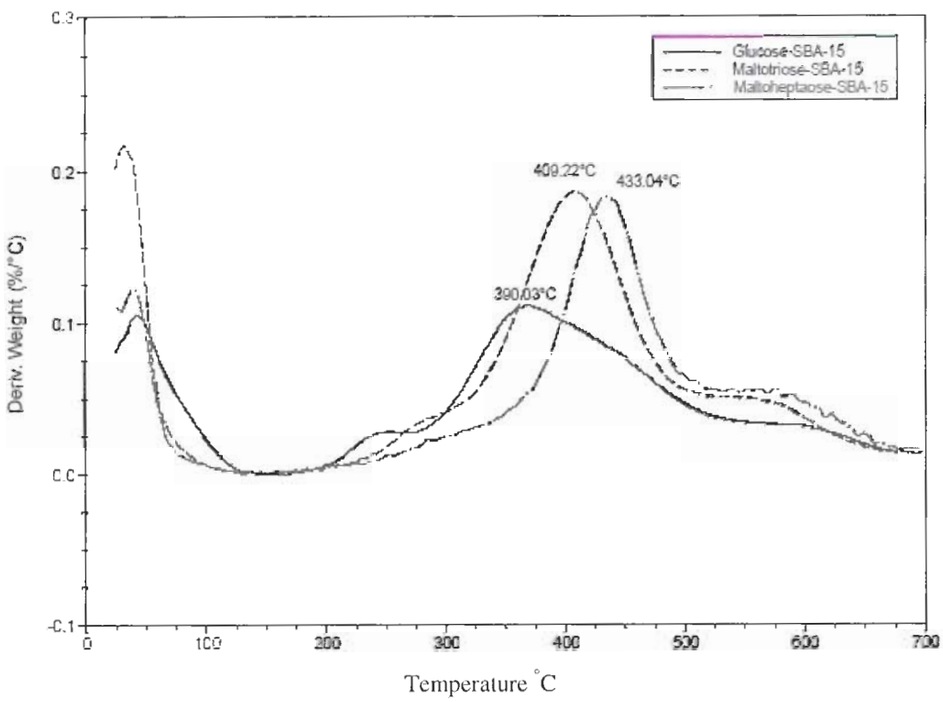

Column packing

Separately, the SBA-15 glucose and SBA-15 maltotriose materials were slurried in methanol and packed into a 4.6 × 50 mm stainless steel (Phenomenex) liquid chromatography column by the conventional method.[53]

Instrument and chromatography conditions

HPLC experiments were performed with an HP Agilent series 1050 series instrument, with a DAD detector interfaced to ChemStation software. The flow rate was kept between 0.8 to 1.2 mL/min. A combination of n-Hexane and ethanol was used as the mobile phase. The column temperature for these chromatographic experiments was performed at 35 °C. These two adsorbents were used for the separation of the

stereoisomers α/β-tetra-*O*-acetyl-phenylthio galactopyranoside or α/β–methyl glucopyranoside. The effect of the surface compositions of the thio saccharide silicas on the adsorption and separations of α/β-tetra-*O*-acetyl-phenylthio galactopyranoside was studied. As seen in Figures 2-10 for α/β tetra-*O*-acetyl-phenylthio-galactopyranose, the retention time is dependent on the surface composition; the larger the sugar ligand, the higher the retention. Both glucose- and maltotriose-SBA-15 adsorbents demonstrated very high stereoselectivity on the stated anomeric analytes. The selectivity is slightly higher using glucose SBA-15 than maltotriose-SBA-15 for the α/β tetra-*O*-acetyl-phenylthio galactopyranose.

Figure 2-10: Effect of surface composition of the saccharides-SBA-15 silicas on the adsorption and separation of anomeric α/β-tetra-*O*-acetyl-phenylthio galactopyranoside.

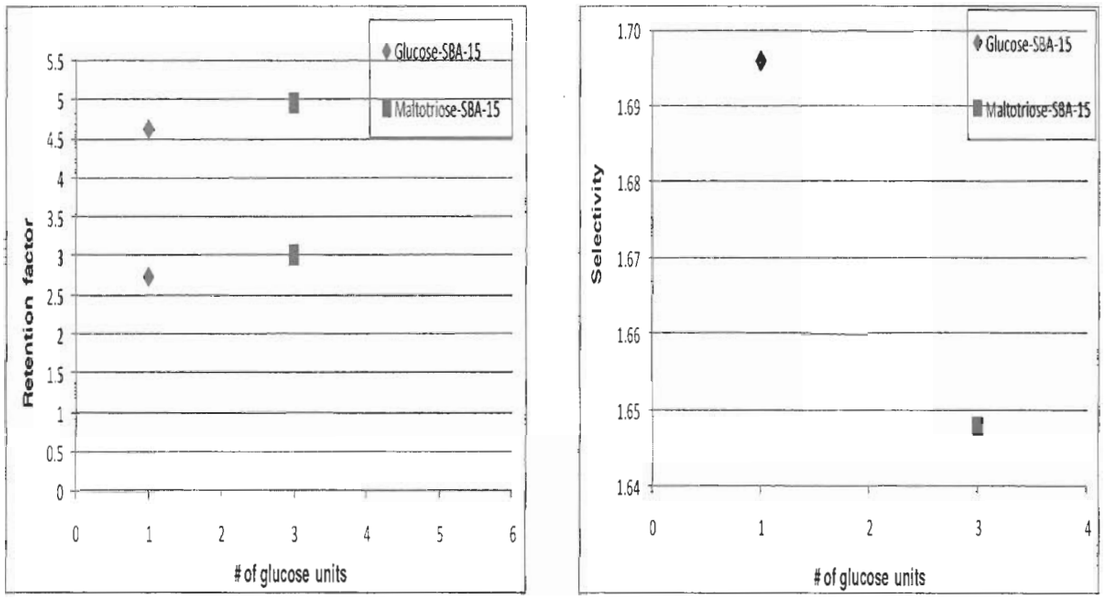

Retention factor ($k = t_R - t_0 / t_0$) (left) and selectivity ($\alpha = k_2 / k_1$) (right). Retention factor #1 is α and #2 is β

As it is demonstrated in Figure 2-11, a lack of chromatographic efficiency was also obvious. The synthesis of ordered porous material with stereoselective surfaces was the main goal of this work; the particle morphology was not controlled during the preparation. The silicas prepared were characterized with a broad distribution of particle sizes from ~0.1 to 20 μm. The size distribution can be improved by the particle size fractionation or through variation of the synthesis conditions (subject of future work).

Figure 2-11: Typical chromatograms for the separation of α/β- tetra-*O*-acetyl-phenylthio galactopyranoside

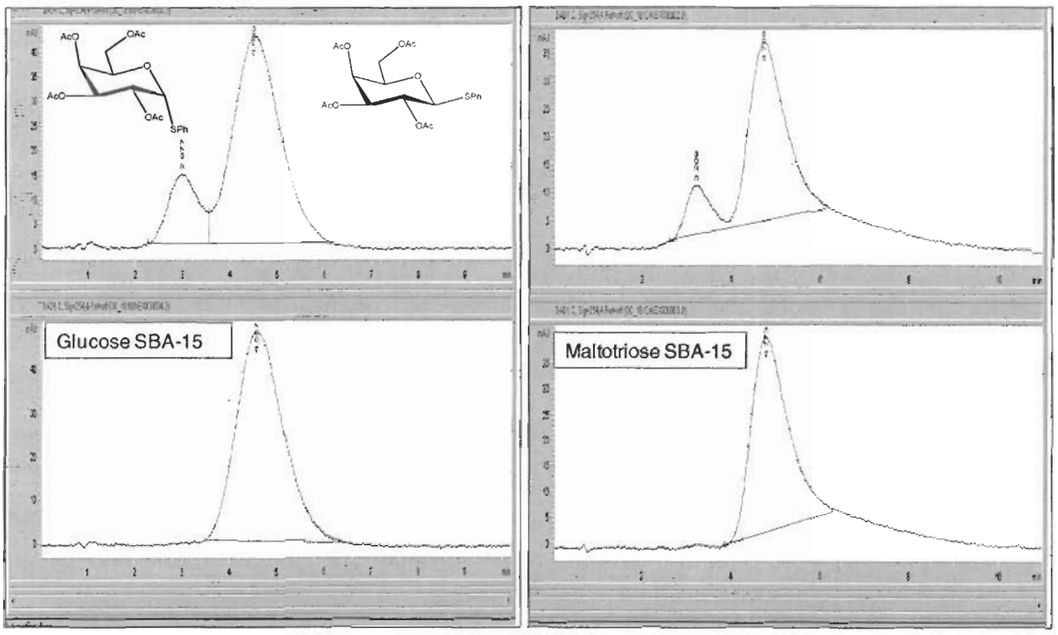

Mobile Phase: n-Hexane: ethanol. (94:6); 0.8 mL/ min; Column temp 35 °C. UV: 254 nm

Conclusions

The co-condensation "one-pot synthesis" method has gained much attention over the past decade. This is due to its simplicity, shortened preparation times, homogeneous distributions of functional groups, open pore volumes, and improved stability. Here tetraethyl orthosilicate (TEOS) and silane thio saccharides (analogs n=1, 3 and 7 glucose units) dissolved in ethanol were co-condensed using Pluronic P123 as a structure directing agent (template) under mild acidic conditions. We obtained novel chiral ordered mesoporous SBA-15 silicas with saccharide surfaces and high grafting densities. It was concluded that most of the saccharide groups were concentrated within the pores. This was demonstrated in nitrogen isotherms after the materials were calcinated. Furthermore, the co-condensation of TEOS with thio maltoheptaose was not suitable for preparing ordered mesoporous silica. It was observed by its nitrogen isotherm that maltoheptaose-SBA-15 materials had a wider pore size distribution. This disorder was recognized to the effect of the larger sized maltoheptaose moiety.

In addition, the solvent used to dissolve the silane thio saccharides was critical to prepare the saccharide mesoporous well ordered materials. As demonstrated in Addendum C, when acetonitrile was used instead of ethanol to dissolve the thio glucose, a very disordered mesoporous material was afforded. The materials prepared demonstrated high stereoselectivity in the HPLC separation of stereoisomers and this is reported for the first time to the best of our knowledge.

Addendum C (Nitrogen isotherms of glucose –SBA-15)

This supplement demonstrates the characterization of glucose SBA-15 silica by adsorption-desorption isotherms. It is notable that there is a very wide pore size distribution (PSD). This is attributed to the acetonitrile solvent used during the co-condensation reaction of TEOS with silane thio glucose. It seems that acetonitrile solvent inhibits the properties of the structure directing agent, P123 (Figure 2-12).

Figure 2-12: Nitrogen isotherms of the glucose-SBA-15 materials prepared using acetonitrile instead of ethanol to dissolve the thio glucose. (a) Pore size distribution.

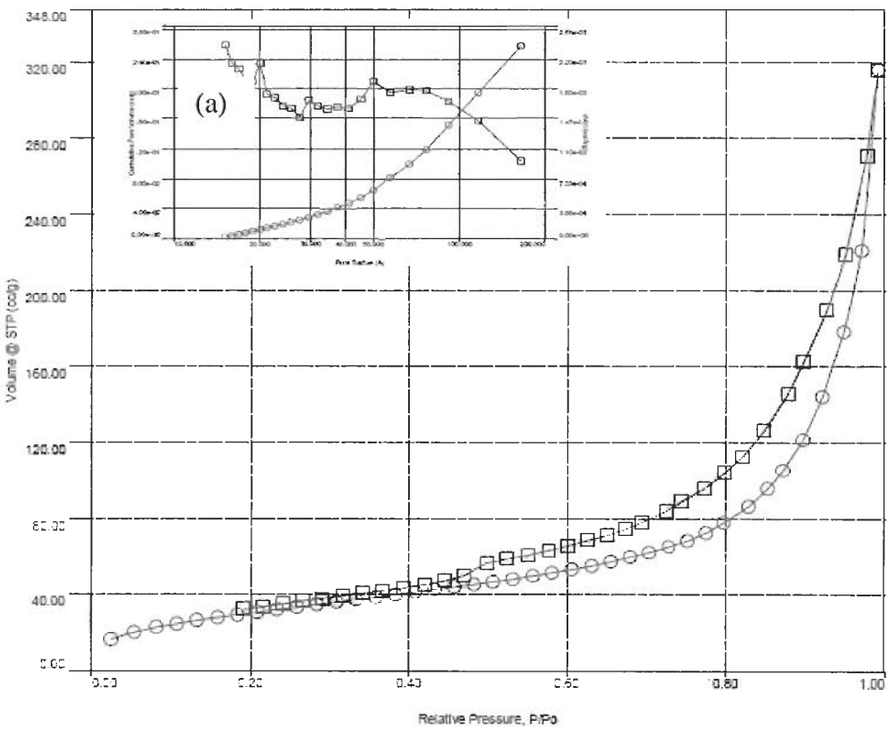

Chapter 3: Synthesis and characterization of new adsorbents with chemically-bonded saccharide surfaces for steroisomeric separation in reverse and normal phase high performance liquid chromatography

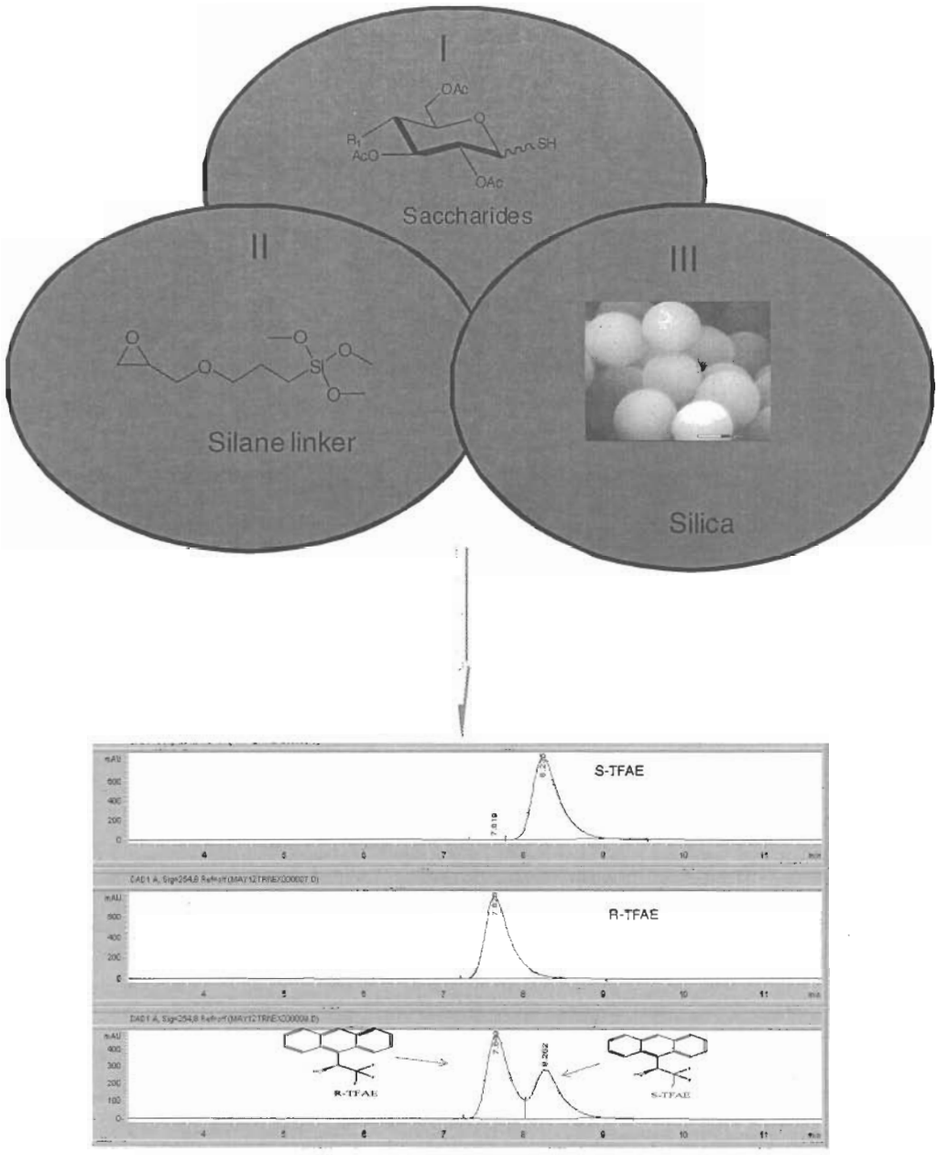

Abstract

Polysaccharide derivatives have been extensively used as chromatographic chiral selectors in chiral stationary phases (CSPs) for the separation of enantiomers by HPLC. There are two methods used to prepare CSPs using polysaccharides: coating and immobilization. CSPs prepared by coating the polysaccharide onto silica still represent the most popular approach. However, these CSPs have limited choices of chromatography solvents which limit their applicability. Polysaccharides chemically bonded onto silica overcome the disadvantages of the coating approach.

Here is described a synthesis of new classes of adsorbents with chemically bonded trimethoxysilyl-thio saccharides on the surfaces. The trimethoxysilyl-saccharides (n=1, 3, 7, and 13 glucose units) series were prepared and used as ligands. These ligands were immobilized onto silica with a novel, hydrolytically-stable carbon-sulfur bonding. This immobilization was conducted with a development of a new synthetic method to chemically bind a thio group on the anomeric carbon of the saccharide to silica. Two approaches were used to immobilize the saccharides; direct and surface chemical assembly.

In this study, three kinds of silicas were utilized: an inexpensive non-spherical porous silica, Aeorosil non porous fumed silica and spherical porous Prodigy silica. The non-spherical silica was used to study the chemistry of the surface modification. The Aeorosil silica was used to characterize the trimethoxysilyl-saccharides on the surface of silica by ^{1}H-NMR. The Prodigy silica was used for the final packing and stereoisomeric separations. The resulting new adsorbents were characterized by NMR, FTIR, TGA, nitrogen isotherms, and elemental analysis. Results indicate that direct immobilization is superior to the surface chemical assembly immobilization approach. These new

adsorbents prepared have been evaluated in the HPLC separations of various stereoisomers. A mechanism for the stereoisomeric chromatography separations of the analytes is proposed.

Introduction

Polysaccharides were some of the first materials used for chiral recognition. They have many chiral centers and they are relatively inexpensive. Their chiral recognition abilities were first observed in cellulose paper chromatography when a racemic amino acid gave two different spots using l-methyl-(β-phenylisopropyl)-amine as a solvent.[54-55] This discovery lead scientists to further investigate the use of sugars in enantioselective separations, with amylose being the most popular polysaccharide used. It was later discovered that polysaccharide derivatives showed very interesting chiral recognition properties which lead to their extensive use in enantiomeric separations.[56]

Microcrystalline triacetylcellulose (MCTA) and cellulose tribenzoate (CTB) were the first polysaccharide CSPs reported.[57-59] However, these first CPSs showed some abnormal physical properties such as poor efficiency and swelling in certain solvents. In order to solve these abnormalities, new CSPs based on adsorbing the polysaccharide derivatives onto aminopropyl-silica[60] were developed. These new CSPs are typically prepared by dissolving polysaccharide derivatives in tetrahydrofuran (THF) or in N,N-dimethylacetamide (DMA) and reacting them with a phenyl isocyanate or a benzoyl choride affording a carbamate or a benzoate. The disadvantage of the coating approach is that solvents such as THF or DMA cannot be used as mobile phase because these solvents could remove the polysaccharide chiral selector. Thus, these solvents are called prohibited solvents.[61] Though the prohibited solvents cannot be used as the mobile phase,

they could be very useful to resolve racemic mixtures, especially chiral components that cannot be separated by typical normal phase solvents.

Immobilizing polysaccharides on silica overcomes the limited used of solvents in chiral separation. Okamoto et al.[60,62] reported for the first time the immobilization of polysaccharides (amylose and cellulose) onto modified propyl amino silica. These novel CSPs were prepared by the reaction of the amino group on the surface of silica. Then a polysaccharide with a diisocynate acting as bond spacer was immobilized onto the amino modified silica. When comparing between immobilization with the coating approach, the authors noticed a decrease of enantioselectivity values. It was thought then that this issue was due to the lack of an ordered arrangement of the polysaccharide derivatives (chiral selectors) on the silica gel surface.

The immobilization of *tris* (4-vinylbenzoate) cellulose on amino modified silica by radical co-polymerization was reported in 1993.[63] In this approach, there was no spacer used and the amino silica was treated with acryloyl chloride. Then the polysaccharide derivative was reacted with the modified silica in the presence of a radical initiator. It was observed the CPSs were stable in solvents such as dichloromethane and tetrahydrofuran but they showed lower selectivity factors when compared with the coated approach.

All these immobilization approaches utilized modified amino silica for the preparation of CSPs with polysaccharides as chiral selectors. As described in Chapter 2, we have developed silica with saccharide surfaces by forming carbon-sulfur single bonds. Carbohydrates linked to silica in this fashion have not been reported in the literature to the best of our knowledge. The preparation of a series of peracetylated-1-thiol-

saccharides analogs (n=1, 3, 7, and 13 glucose units) were described in Chapter 1. These sugars were used as ligands on our new class of adsorbents in which a thiol group links peracetylated saccharides to silica through an epoxy-silane linker. Here we report the synthesis of structurally well-defined, saccharide CSPs using two post synthesis immobilization approaches: direct and surface chemical assembly.

The direct immobilization approach involved the reaction of the thiol saccharide with 3-glycidoxypropyl trimethoxysilane (GOPTMS). The syntheses of these trimethoxysilylated saccharides were described in Chapter 1. Then, the methoxy groups from the trimethoxysilylated saccharides react with the silanol groups of the silica. On the other hand, in the surface chemical approach, the GOPTMS was first reacted with silica. Then, this epoxy modified silica reacted with the thiol saccharide. In this study, three kinds of silicas were utilized: inexpensive non-spherical porous silica (Davisil), Aeorosil non-porous fumed silica and spherical porous Prodigy Phenomenex silica. The Prodigy silica was used for the final HPLC stereoisomer separations.

Experimental

Materials

Davisil silica with average pore diameter (D) of 15 nm, surface area 300 m^2/g. and Aerosil non-porous silica, surface area 200 m^2/g were obtained from Sigma Aldrich Chemical Company (St. Louis, MO, USA). Prodigy silica (D: 15 nm), surface area 325 m^2/g was donated from Phenomenex. Stereoisomer analytes (Figure 3-1) were obtained from Sigma Aldrich. All other chemicals and solvents were of analytical or HPLC grade.

Figure 3-1: Structures of stereoisomers used for chromatographic separations.

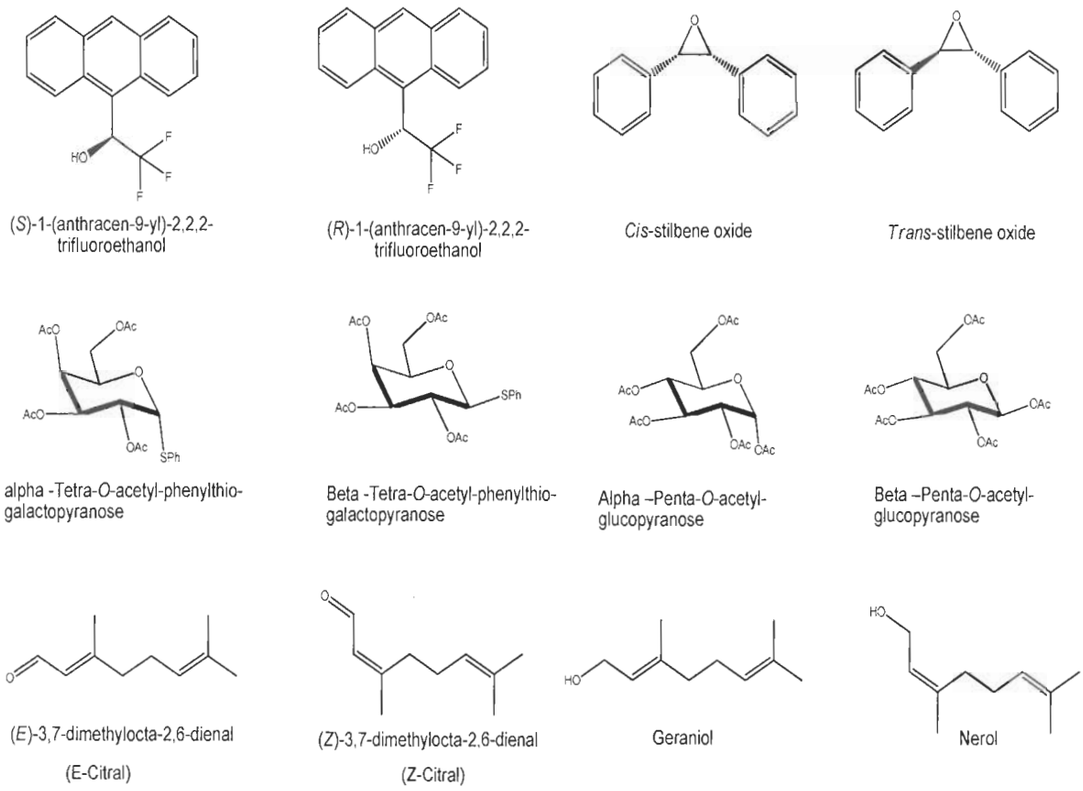

Synthesis of peracetylated-1-thiol-saccharides and their silylated derivatives.

The syntheses of thiol-saccharides and their silylated derivatives were described in detail in Chapter 1.

Synthesis of silica thio glucose and silica thio maltotriose via surface chemical assembly method

Briefly, the silica (Davisil or Aerosil) was first activated by reacting it with the GOPTMS linker affording an epoxy-activated silica. Then thiol glucose and thiol maltotriose were reacted with the epoxy group of the activated silica under mild basic conditions to facilitate the ring opening. In a typical synthesis, silica (500 mg) was transfered into a scintillation vial and deionized water (20 mL) was added at ambient temperature. After the silica was dispersed, GOPTMS (0.5 g, 2.1 mmol) was added. After 48 hours, the epoxy activated silica was collected and thoughly washed (to remove excess GOPTMS) with deionized water followed by the addition of acetone. The material was dried at 60 °C.

In separate vials, thiol glucose and thiol maltotriose (400 mg) were dissolved in acetonitrile (6 mL). The epoxy-activated silica (0.5 g) was transferred into each vial of the dissolved saccharide together with 10 mM aqueous dibasic potassium phosphate (2 mL). The vial was agitated with a mechanical shaker at ambient temperature for 48 hours. The crude saccharide silica was collected and thoroughly washed (to remove excess thio saccharide and byproducts) with deionized water followed by the addition of acetone. The material prepared was dried at 60 °C. The synthetic scheme for the preparation of saccharide silica by surface chemical assembly is shown in Figure 3-2.

Figure 3-2: Surface chemical assembly approach

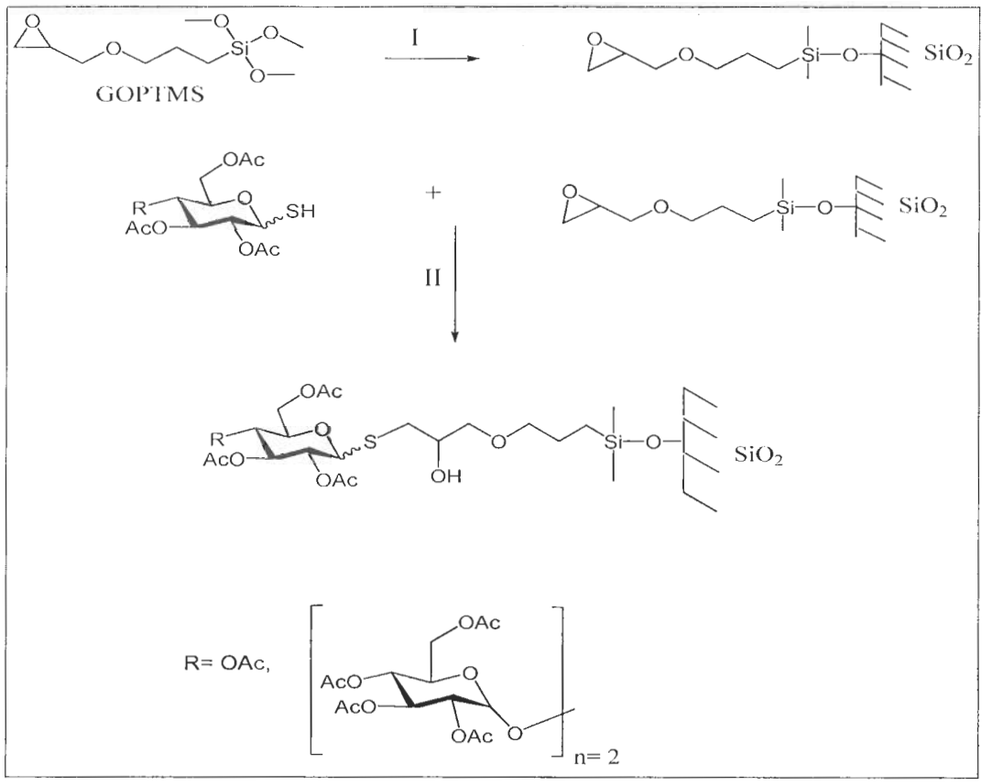

(I) DI water/silica; (II) acetonitrile, 10 mM K_2HPO_4 in aqueous solution.

Synthesis of silica thio saccharides (analogs n=1, 3, 7, 8 and 13) via direct immobilization

The first step in the direct immobilization approach is the conversion of the thiol saccharide to its silylated derivatives. This conversion was described in detail in Chapter 1. The peracetylated-1-thiol-saccharides were reacted with the GOPTMS (2-4 equivalents) in acetonitrile (30 mL) containing aqueous 10 mM dibasic potassium phosphate (3:1 ratio). The reaction was completed within 10 to 12 hours. The crude products from the reactions were then extracted with ethyl acetate and concentrated *in vacuo* affording the trimethoxysilylated thio saccharides. In a typical synthesis, silica (500 mg) was transfered into a scintillation vial and warm deionized water (7 mL) was added. After the silica was dispersed, trimethoxysilylated thio saccharides (700 mg) (previously dissolved in 3 mL acetonitrile) was added. The reaction was conducted at 60-70 $^{\circ}$C for 3-7 days (temperature/reaction time was dependant on the size of the saccharide). After hydrolysis and polycondensation, adsorbents with chemically bonded trimethoxysilylated thio saccharides were obtained. Then the modified silicas were filtered off and washed succesfully with acetonitrile, distilled water, and acetone to remove byproducts and salts and dried at 60 $^{\circ}$C for one day. Refer to Figure 3-3 for the synthesis of derivatized saccharide silicas.

Figure 3-3: Synthesis of derivatized saccharide silica via direct immobilization

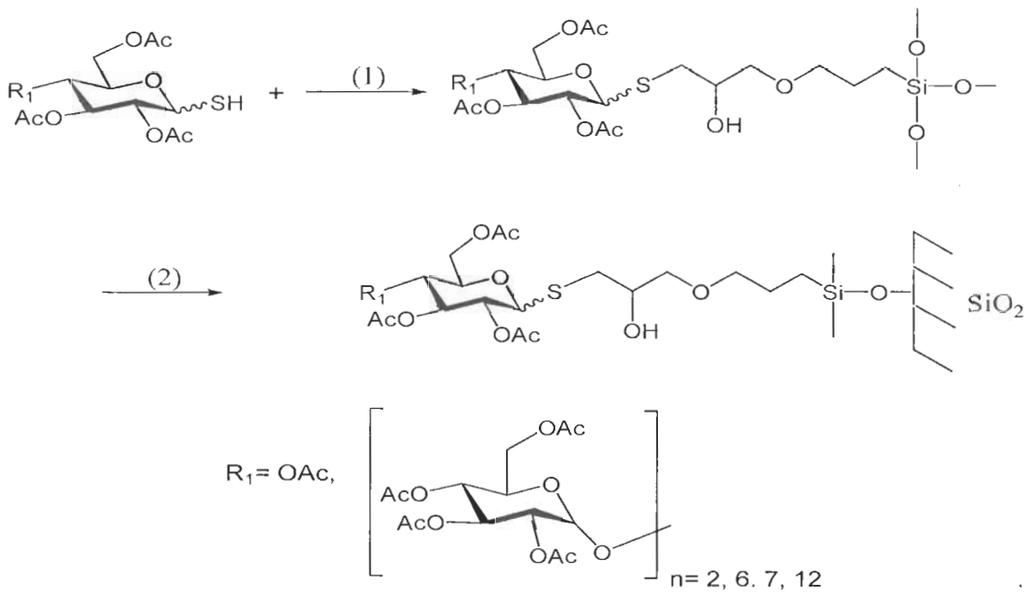

(1) GOPTMS, acetonitrile, 10 mM K_2HPO_4 in water, RT; (2) acetonitrile, HPLC water/silica, at 60-70 °C.

Note: The reaction of the trimethoxysilylated thio saccharides with Davisil and Aerosil can also be conducted at ambient temperature. However, when the saccharides were reacted with the Prodigy silica warm conditions (temperature, 60-70 °C) were needed.

Characterization

Elemental analyses

Carbon analyses were performed with a Perkin Elmer 2400 CHN Analyzer. Elemental Analyses was performed by Robertson Microlit Laboratories (Madison, NJ) using the ASTM method.

Infrared spectroscopy

Infrared spectra were recorded with a Perkin Elmer Spectrum One FTIR instrument using a mercury cadmium telluride detector. The spectra were obtained using a Harrick Seagull accessory (reflectance mode, 45° angle of incidence, 128 scans, and resolution 4 cm^{-1}).

Nitrogen isotherms

Nitrogen adsorption-desorption isotherms (77K) were obtained to determine the surface characteristics of the porous silica; isotherms were acquired using an Autosorb-1 analyzer (Quantachrome Instruments, Boynton Beach, FL, USA). Refer to Chapter 2 for parameters used for the nitrogen isotherms experiments.

Thermal gravimetric analyses

Thermal analyses of the saccharide silicas after modification was performed in nitrogen using a TA Instruments Hi-Res 2950 Thermogravimetric Analyzer using a heating rate of 10 °C/min.

NMR experiments

The ^{1}H-NMR experiments were conducted using a Bruker 600 MHz spectrometer with a cryoprobe. The use of the cryoprobe reduced the signal to noise ratio and increased the sensitivity of the Aerosil saccharide samples.

Results and Discussion

FT IR Spectra-Silica saccharides

Figure 3-4 shows an overlay of the spectra for glucose- and maltotriose- modified silicas. It compares the surface chemical assembly and direct immobilization approaches using Davisil silica. Peaks at ~2920, 2850 cm^{-1} (C-H stretches), and ~1760 cm^{-1} (C=O stretch). A broad peak at ~3200-3300 cm^{-1} was O-H stretching from the surface water. Peaks appeared to be with higher intensities when the direct immobilization approach is used. Based on the elemental analyses (Tables 3-1 and 3-2) the higher intensity of the peaks was due to higher grafting density when the direct immobilization approach was used.

Figure 3-5 demonstrates an overlay of the spectra for maltotriose-, and maltoheptaose-Aerosil. Peaks have the same pattern as indicated above. Both, maltotriose- and maltoheptaose- fumed silica have similar peaks intensities.

These experiments were done to understand the chemistry of saccharide silica and they were not used for chromatographic separations.

Figure 3-4: FTIR spectra comparing surface chemical assembly and direct immobilization approaches

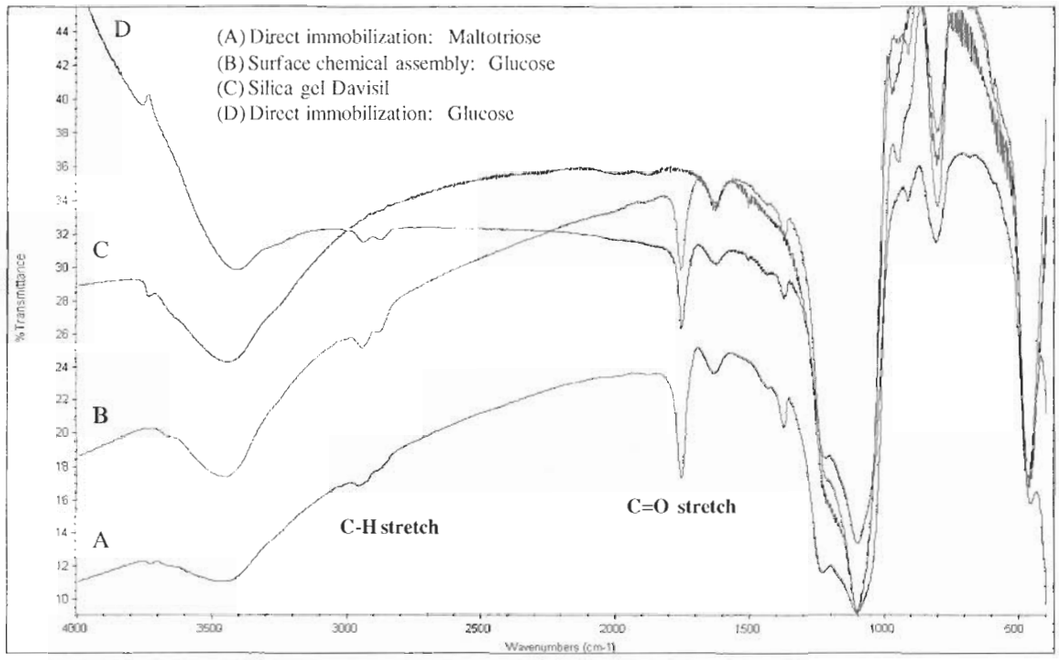

Figure 3-5: FTIR spectra of the Aerosil silica with bonded saccharides prepared by direct immobilization

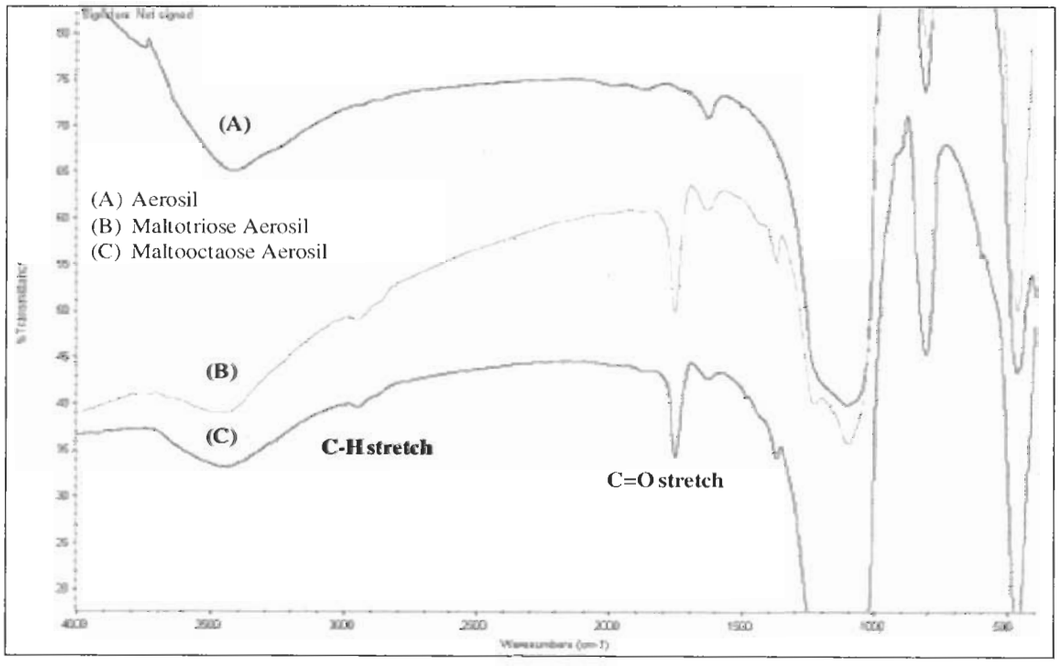

Modification of Prodigy silica saccharides

The modifications of Prodigy trimethoxysilylated thio saccharides were monitored by FT-IR. The Prodigy silica saccharides were prepared following the direct immobilization approach. Prodigy silica is a spherical particle shape and it is one of the best for high pressure liquid chromatography (HPLC). Figure 3-6 shows an overlay of the spectra for glucose-, maltotriose-, maltoheptaose-, and maltodecatriose modified silicas. Peaks at ~2920, 2850 cm^{-1} (C-H stretches), and ~1760 cm^{-1} (C=O stretch) were attributed to methyl, methylene, and carbonyl groups in the acetylated saccharides. Peaks at ~1000-1100 cm^{-1} were attributed to Si-O stretches from silica matrix. A broad peak at ~3200-3300 cm^{-1} was O-H stretching from the surface water. A positive peak at 3750 cm^{-1} (SiO-H stretch) was attributed to the removal of the silanol groups due to reaction with saccharide silanes.

Figure 3-6: Infrared spectra for bare Prodigy and saccharide Prodigy silicas

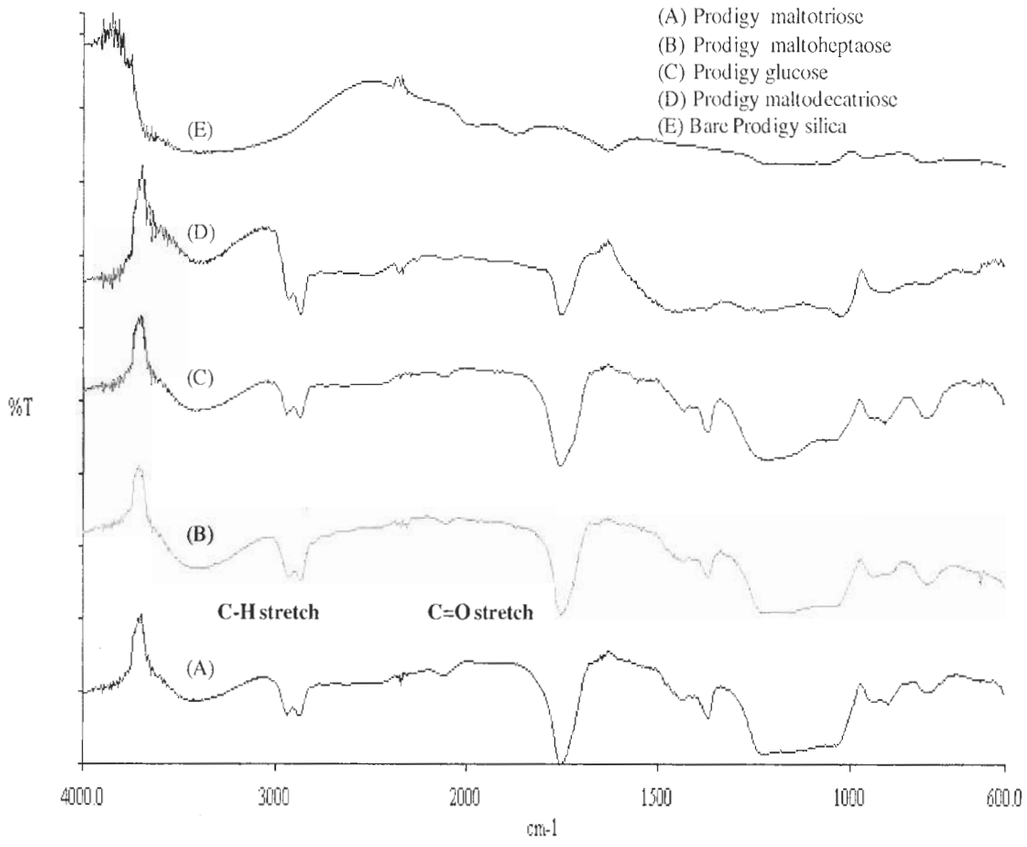

^{1}H-NMR experiments (Aerosil silica saccharides)

^{1}H-NMR was another unique technique used in this thesis to characterize the adsorbents with saccharide surfaces. Aerosil silica was used as a solid support and to the best of our knowledge, this techique has never been performed before to characterize saccharides bonded on silica. Aerosil silica is a non-porous material and ready dispersed when organic solvent is used. Figure 3-7 shows the ^{1}H-NMR overlay spectra of fumed silica saccharides in chloroform-D_3. There are three major resonances observed clearly in the ^{1}H-NMR experiments: two resonances from the protons from the silane linker and the resonance observed for the methyl protons from the acetate groups. As observed in the trimethoxysilylated thio glucose, the protons from the linker are labeled as 1 and 2 (Figure 3-7) at 0.50 ppm and 1.55 ppm respectively and protons from the acetate groups at ~ 2.0 ppm. These ^{1}H-NMR experiments lead us to believe that the saccharide had some mobility on the silica matrix and this is important for stereoisomer separation.

Figure 3-7: ^{1}H-NMR spectra of modified saccharide fumed silica

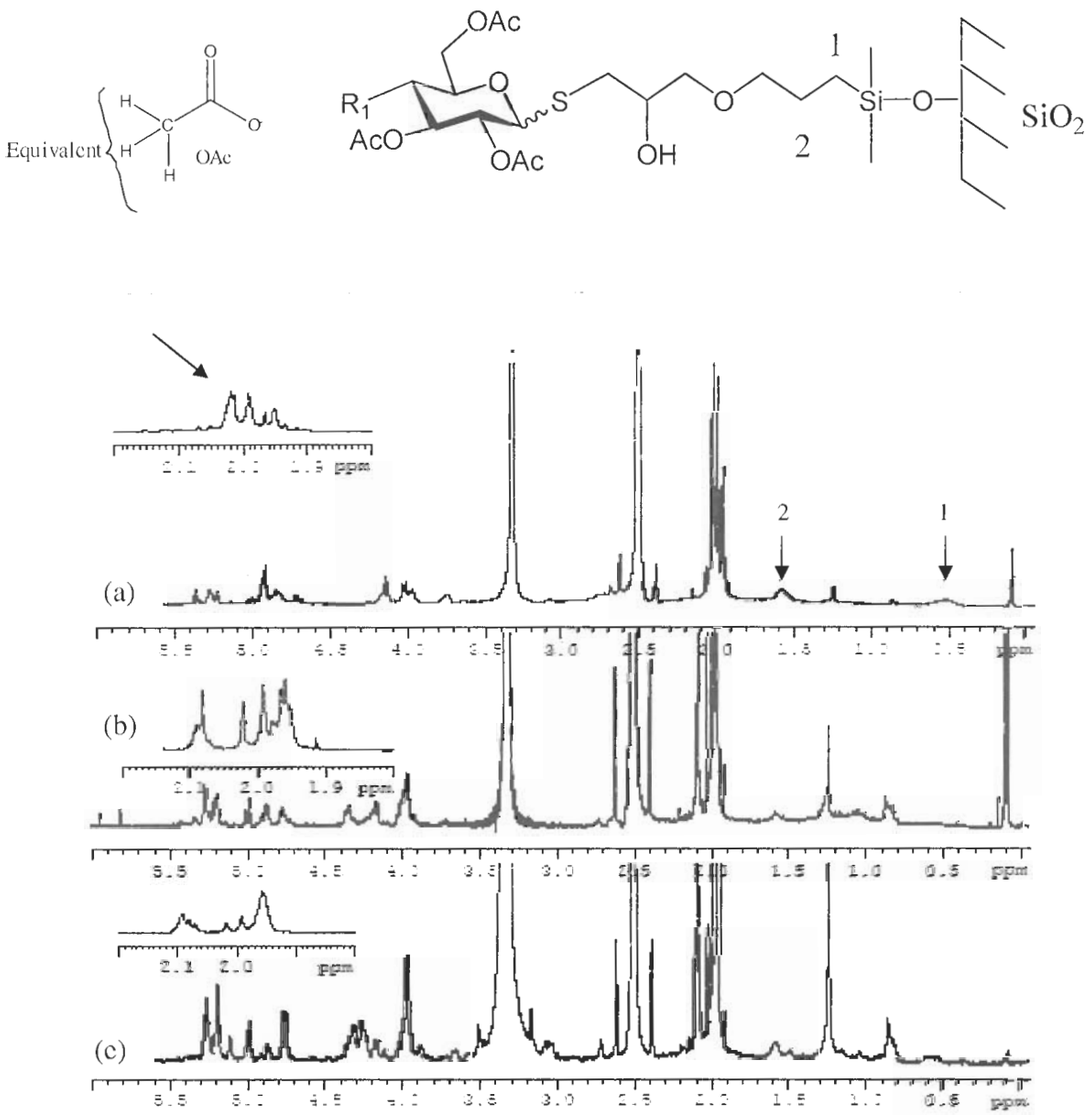

(a) Silane glucose; (b) silane maltotriose; (c) silane maltooctaose. Bruker 600 MHz ($CDCl_3$)

Grafting density of silica saccharides

Carbon and sulfur analyses of adsorbents with chemically bonded trimethoxysilylated thio saccharides were performed by Robertson Microlit Laboratories (Madison, NJ). Table 3-1 and Table 3-2 compare the grafting density between the surface chemical assembly and the direct immobilization approaches to the syntheses of the adsorbents. Based on this data, it was concluded that direct immobilization was superior to the surface chemical assembly approach. Thus the modifications of the Prodigy silicas were conducted using the direct immobilization approach. Table 3-3 shows the grafting density of the Prodigy saccharide materials used for final column packing and stereoisomeric chromatographic separations.

The grafting densities of the derivatized saccharide monolayers were calculated using the following formulas.[64]

$$\rho = \frac{6 \times 10^5 (\%C)}{[1200nc - MW \times (\%C)} \times \frac{1}{S\ (BET)} \times \#\ of\ Glc \quad (1)$$

$$\rho = \frac{6 \times 10^5 (\%S)}{[3200ns - MW \times (\%S)} \times \frac{1}{S\ (BET)} \times \#\ of\ Glc \quad (2)$$

MW is the molecular weight of the saccharide-silane group, *ns* and *nc* the numbers of sulfur or carbon atoms in the grafted group. %C and %S are the weight percent carbon and sulfur in these materials and the S (BET) is the nitrogen isotherm surface area of bare silica. # of *Glc* is the number of glucose units bonded onto silica. Equations 1 and 2, then provides the surface concentration (grafting density, ρ) as the number of each silane-saccharide silane group repeat glucose unit per 1 nm^2 of the silica surface.

In theory, the grafting density of these adsorbents based on carbon and sulfur should be in the same ratio. However, this was not the case. In the surface chemical

assembly, the grafting density of the carbon is higher than the sulfur. It was suspected that some epoxy groups on the surface of the silica did not reacted completely with the thiol saccharides. In addition, the grafting density of the carbon is slightly higher than sulfur in the direct immobilization approach. This is due to utilization of crude trimethoxysilylated thio saccharides during the modification of silica. These silane saccharides are about 80% pure materials. It was believed then that unreacted GOPTMS was also on the surface of the silica. For the Prodigy silica, it was thought that the silane byproducts exhibited a negligible effect on the stereoisomeric separations.

Table 3-1: Elemental and grafting density data of the materials from the surface chemical assembly approach

Adsorbent	*Carbon*	*Hydrogen*	*Sulfur*	*# of Glc units/nm²*	
Davisil silica	*%*	*%*	*%*	From C %	From S %
Epoxy-activated silica	8.79	1.87	NA	3.2	NA
Glucose- silica	12.9	2.10	1.0	1.21	0.72
Maltotriose-silica	14.29	2.20	0.45	1.95	0.93
Maltoheptaose-silica	9.20	1.28	< 0.05	NA	NA

Table 3-2: Elemental and grafting density data of Aerosil saccharides prepared via direct immobilization approach

Adsorbent *Aerosil silica*	*Carbon* %	*Hydrogen* %	*Sulfur* %	*# of Glc units/nm²* From C %	From S %
Glucose silica	8.60	1.04	0.90	1.52	1.11
Maltotriose silica	8.48	1.11	0.50	2.01	1.89
Maltoheptaose silica	9.74	1.25	0.18	2.25	1.54
Maltooctaose silica	8.23	1.21	0.27	2.16	1.84

Table 3-3: Elemental and grafting density data of Prodigy saccharide materials

Adsorbent *Prodigy*	*Carbon* %	*Hydrogen* %	*Sulfur* %	*# of Glc units/nm²* From C %	From S %
Glucose silica	11.14	1.48	1.27	1.23	1.00
Maltotriose silica	14.01	2.09	0.75	2.20	1.85
Maltoheptaose silica	11.69	2.12	0.33	1.90	1.83
Maltodecatriose silica	5.61	1.08	0.08	0.84	0.70

Nitrogen isotherms (Prodigy silica saccharides)

The nitrogen adsorption and desorption isotherms for the adsorbents with chemically bonded trimethoxysilylated thio saccharides and bare Prodigy silica are shown in Figure 3-8. The profile of all isotherms in the capillary condensation region is similar to each other, indicating minor changes in the pore size distribution. Addendum D shows a graph of the pore size distribution of the bare prodigy silica and the Prodigy saccharides. The total specific pore volume, *C* constant and specific surface area, decreased after modification of Prodigy silica gel. This decrease was more obvious as the size of the saccharide group increased (Table 3-4). The decrease of pore volume and surface area are thought to be due to the large concentration of saccharides within the pores on the modified Prodigy. The Prodigy saccharides show a low increase at low relative pressure values. This indicates minimal nitrogen adsorption interactions with a slightly hydrophobic surface. In addition, the hysteresis loop for the Prodigy saccharides has lower p/p_s than the bare Prodigy. This demonstrates that the Prodigy saccharides pore sizes are smaller when compared with the bare Prodigy.

The *C* constant is measured using the Brunauer-Emmett-Teller (BET) equation. The *C* constant gives important information of the materials surface energy. As it is observed in Table 3-4, the *C* constant from the bare Prodigy silica is very high indicating a high surface energy. Once the Prodigy silicas are modified with saccharides the surface energy is decreased. This was expected since silica wants to reduce its surface energy and the organic saccharide groups have very low surface energies. The *C* constant can also give information regarding the hydrophobicity of materials. A typical C18 stationary phase has a *C* constant of about 22.[65] The *C* constants from the Prodigy

saccharides were 51-57, which indicates these materials are less hydrophobic than a typical C18 silicas.

The surface area of these porous materials are determined using BET theory to the nitrogen adsorption isotherm.[66] The BET equation measures the amount of nitrogen molecules taken in the first monolayer and it is multiplied by the area of a nitrogen (assumed to be 16.2 $Å^2$)[53] molecule occupies on the adsorbent surface. This value is divided by the mass of the adsorbent sample. The resulting surface areas are then corrected per 1 g of silica based on the weight loss obtained from TGA by the following equation:

$$Sc = \frac{S\ (BET)}{(100 - \%W)}$$

Sc is the corrected surface area per 1 of silica. $\%W$ is the percent weight loss of the bonded saccharides silica.

Figure 3-9 demonstrates that as the number of glucose residues increases the surface area decreases. This also indicates that the pores in the adsorbents are occupied with the derivatized saccharides.

Table 3-4 Data from the nitrogen isotherm experiments

Adsorbent	*Surface area (m^2/g)*	*Total PV (cc/g)*	*Ave Pd (Å)*	*C constant*
Bare Prodigy	310	1.2	154	579
Glucose silica	275	0.8	136	56
Maltotriose silica	261	0.6	130	57
Maltoheptaose silica	241	0.6	134	51
Maltodecatriose silica	148	0.5	141	53

Figure 3-8: Nitrogen adsorption isotherms on Prodigy adsorbents with chemically bonded saccharides.

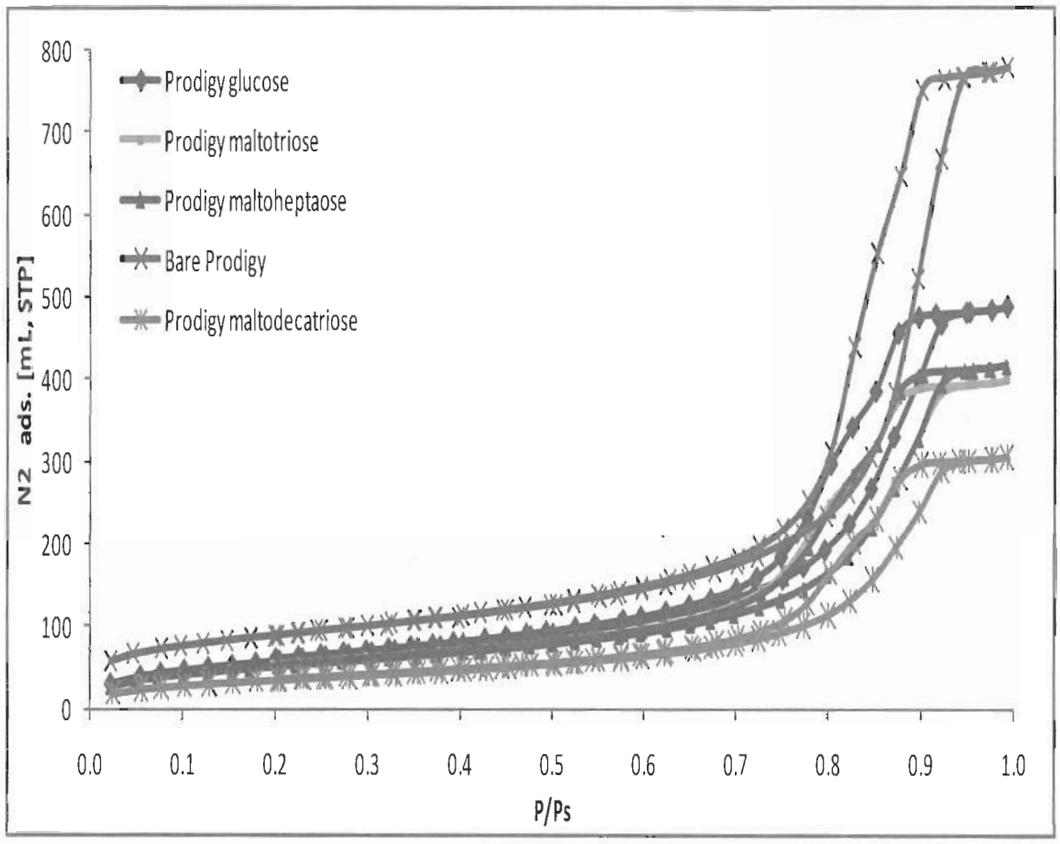

Figure 3-9: Surface area of the bare Prodigy and corrected surface areas of the Prodigy adsorbents with chemically bonded saccharides

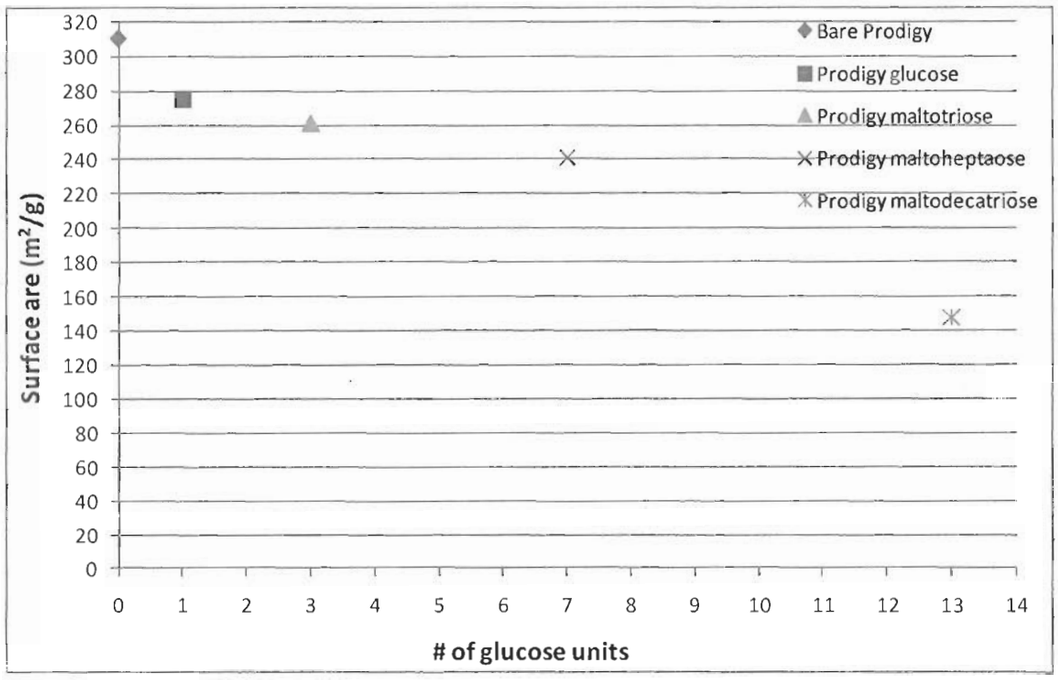

TGA analyses (Silica saccharides)

Thermal properties of the prepared silicas were assessed through TGA using a temperature range of 25-700 °C, a heating rate of 10 °C/min in a flow of nitrogen (40 cm^3/min). The first weight loss feature (~1-2% loss) was observed below 100 °C and was attributed to the desorption of weakly bound water. The main weight loss (~11-27%) was observed ~250-600 °C, and was attributed to the degradation of the saccharide groups (Figure 3-10).

Figure 3-10: Thermal properties of the Prodigy adsorbents with chemically bonded saccharides

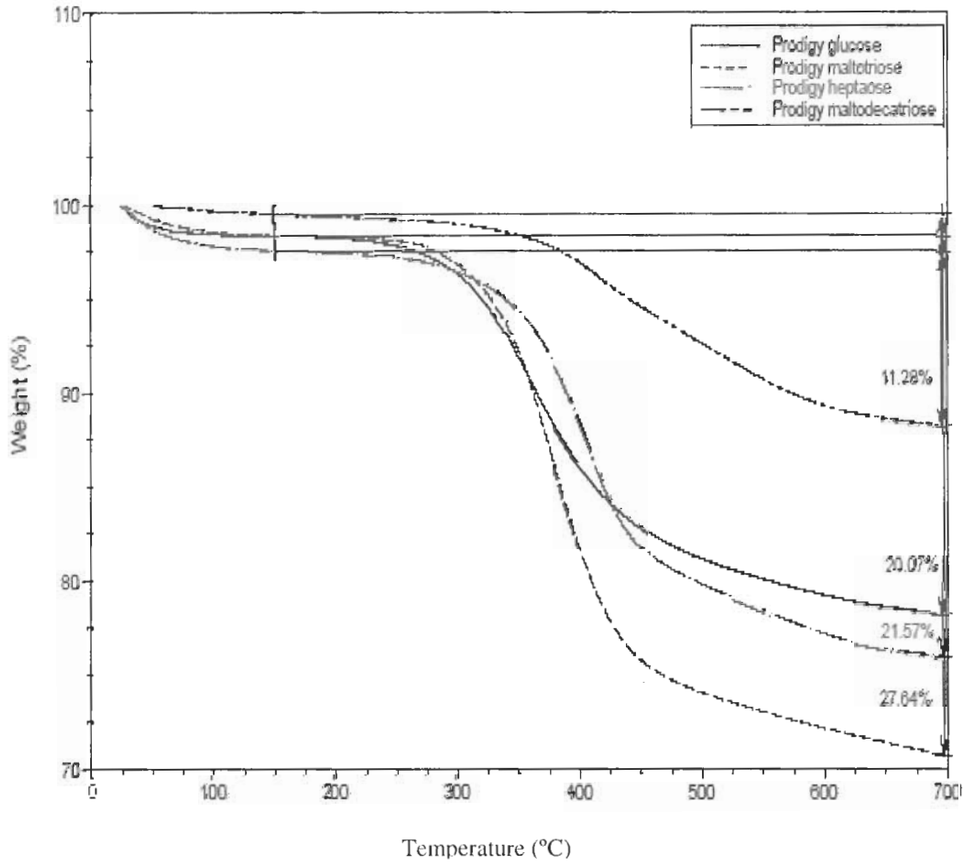

In addition, TGA can give information where the weight loss is most apparent. This is done by a derivative weight loss curve. It is clearly observed in Figure 3-11 that the larger the saccharides the higher the temperature in which the weight loss is most apparent.

Figure 3-11: DTGA plots of the Prodigy adsorbents with chemically bonded saccharides

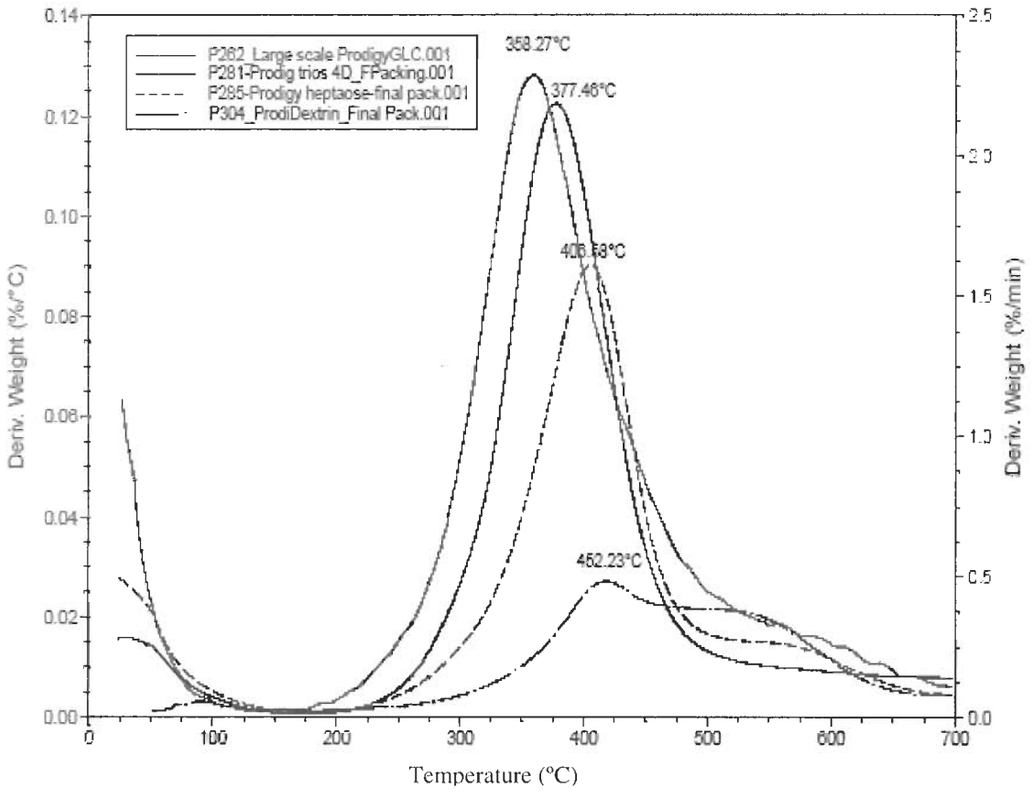

Reaction kinetics of the Prodigy silica glucose

In order to monitor and determine the reaction kinetics for Prodigy silica and the trimethoxysilylated saccharide, TGA was used. This reaction was conducted using the direct immobilization approach. In a typical experiment, a small portion silica was taken out at different times during the reaction (Figure 3-12). The portion of silica was washed with water, acetonitrile and acetone and the weight loss was measured by TGA. There was only 2 % weight loss between the 9 hour and the 22 hour experiments, which indicated that the reaction was going very slowly. Thus, an additional 30% of the original concentration of the derivatized glucose was added to the reaction. After 36 hours, the reaction was again re-measured by TGA and the data indicated a higher concentration of the bonded saccharide. After 48 hours, a portion of silica saccharide was analyzed once again by TGA and the weight loss indicated completion of the reaction. Figure 3-12 demonstrates the reaction kinetics of Prodigy silica with trimethoxysilated thio glucose at 60 °C using TGA.

Figure 3-12: Reaction kinetics for the preparation Prodigy silica saccharides by TGA.

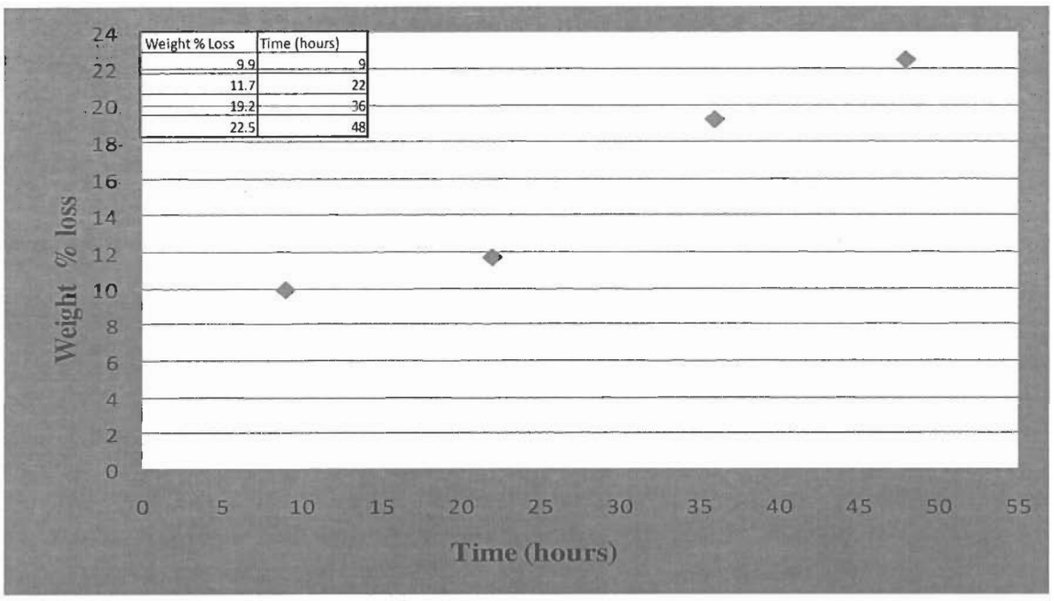

Column packing

Each Prodigy silica saccharide was slurried in methanol and packed into a 4.6 × 100 mm stainless steel liquid chromatography column by the conventional method. [53]

Our main goal was just to verify stereoselectivity of new adsorbents under HPLC conditions using small size of each adsorbent batch. Thus the packing procedure was not optimized and the maximum packing efficiency was not achieved.

Chromatographic experiments

Chromatographic separations using well-defined saccharide structures as ligands allowed us to explore and give more insight into the separation mechanism between our novel adsorbents and stereoisomeric compounds. As reported[67-69] in the literature, there are many intermolecular interactions between the adsorbing sites of the CSPs and the

analytes. These intermolecular interactions are hydrogen bonding, Π- Π interactions, steric effects, and dipole-dipole interactions. It is suspected that these same kind of intermolecular interactions drive the stereoisomer separations of our new adsorbents (Prodigy saccharides). Figure 3-13 illustrates these possible intermolecular interactions using Prodigy maltotriose as example.

Figure 3-13: Demonstration of potential intermolecular interactions between TFAE and Prodigy maltotriose.

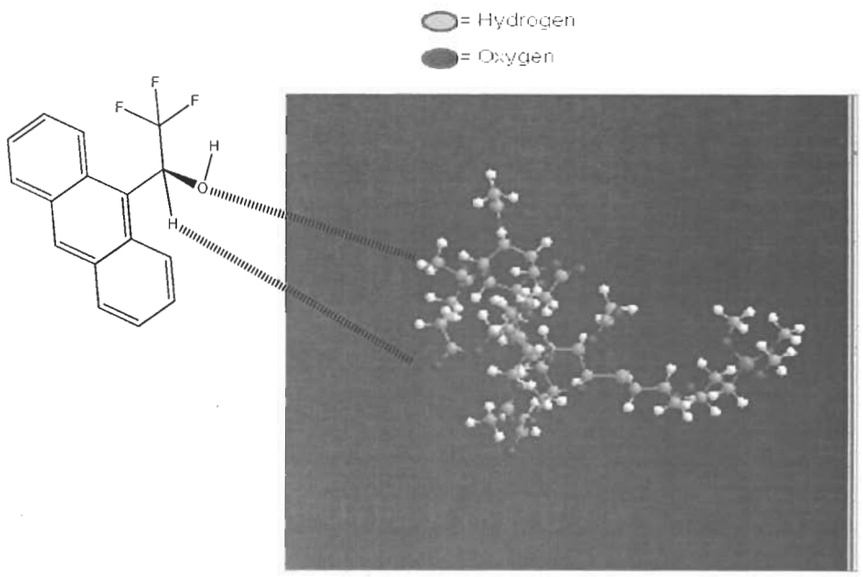

Stereoisomer separations using normal phase mode

Normal phase mode was used for stereoisomer chromatographic separation of ((S/R)-2,2,2-trifluoro-1-(9-anthryl)-ethanol (TFAE), α/β-2,3,4,6-tetra-*O*-acetyl-phenylthio-D-galactopyranose and α/β-1,2,3,4,6-penta-*O*-acetyl-D-glucopyranose. For the TFAE, the adsorbents with chemically bonded maltotriose gave the best enantioselectivity. Surprisingly, the maltoheptaose and maltodecatriose gave almost no selectivity on this TFAE chiral analyte. It is suspected that the major chiral recognition was not from the asymmetric derivatized saccharides with many chiral binding sites but was from Pirkle-type recognition. In Pirkle-type CSPs, the chiral recognition involves dipole-dipole, hydrogen bonding, π-π and steric interactions.[70-71]

It appears that these intermolecular interactions involving our saccharide chiral selectors and the TFAE played a special role in the chiral discrimination. Furthermore, the electron-withdrawing group on TFAE might enhance the enantioselectivity. Figure 3-14 shows an example of the TFAE chromatographic chiral stereoselectivity using the adsorbent with chemically bonded silane thio maltotriose.

Figure 3-14: Chromatograms for the adsorbent enantioselectivity of ((S/R)-2,2,2-trifluoro-1-(9-anthryl)-ethanol using Prodigy silica maltotriose

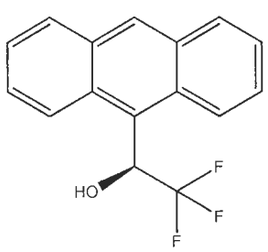

(*S*)-1-(anthracen-9-yl)-2,2,2-trifluoroethanol

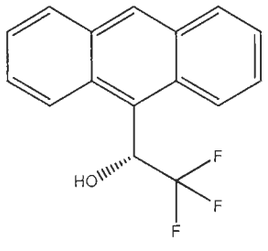

(*R*)-1-(anthracen-9-yl)-2,2,2-trifluoroethanol

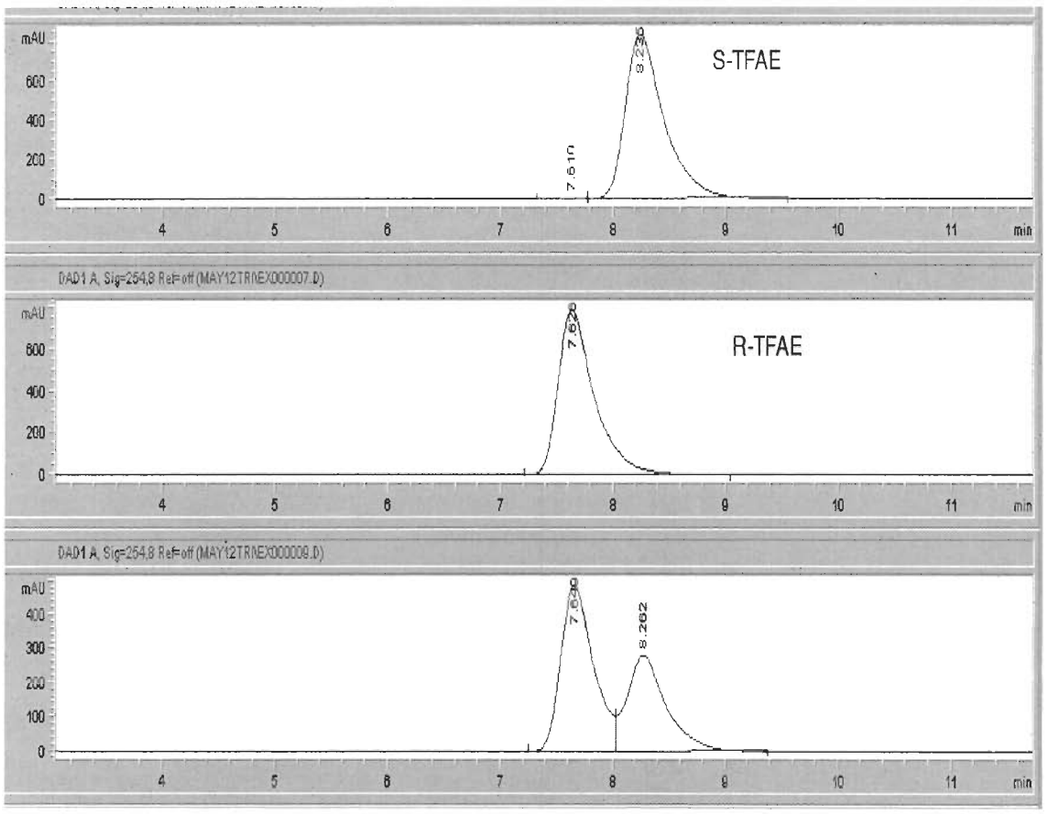

Mobile phase: n-Hexane-$CHCl_3$-IPA (84:15:1); 1.0 mL/ min; column temp 25 °C. UV: 254 nm.

In addition, the effect of the surface composition (trimethoxysilated thio saccharide ligands) on the adsorption and separations of anomeric α/β-2,3,4,6-tetra-*O*-acetyl-phenylthio-D-galactopyranose and α/β-1,2,3,4,6-penta-*O*-acetyl-D-glucopyranose were studied. As seen in Figure 3-15 for the galactopyranose isomeric mixture, the retention time is dependent on the surface composition; the larger the ligand, the higher the retention. However, this trend was not observed on the adsorption with chemically bonded maltodecatriose. This was probably due to either low grafting density (refer to Table 3-3) or the slow mobility of the maltodecatriose due to its bulk in this matrix. However, the stereoselectivity of the adsorbent with chemically bonded derivatized maltodecatriose was similar or better for both anomeric analytes. Figure 3-16 and Figure 3-17 show retention factors and selectivity for α/β-2,3,4,6-tetra-*O*-acetyl-phenylthio-D-galactopyranose and α/β-1,2,3,4,6-penta-*O*-acetyl-D-glucopyranose, respectively. It was suspected that hydrogen bonding, π-π interactions and Van der Waal's forces are the stronger chemical interactions on the anomeric separations using these novel adsorbents. Table 3-5 summarizes the data obtained for the stereoisomers separation using normal phase mode.

Figure 3-15: Effect of surface composition on the separation of α/β-2,3,4,6-tetra-*O*-acetyl-phenylthio galactopyranose

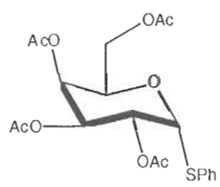

α- galactopyranose

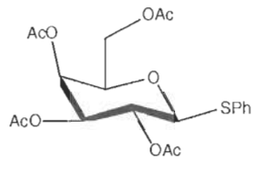

β- galactopyranose

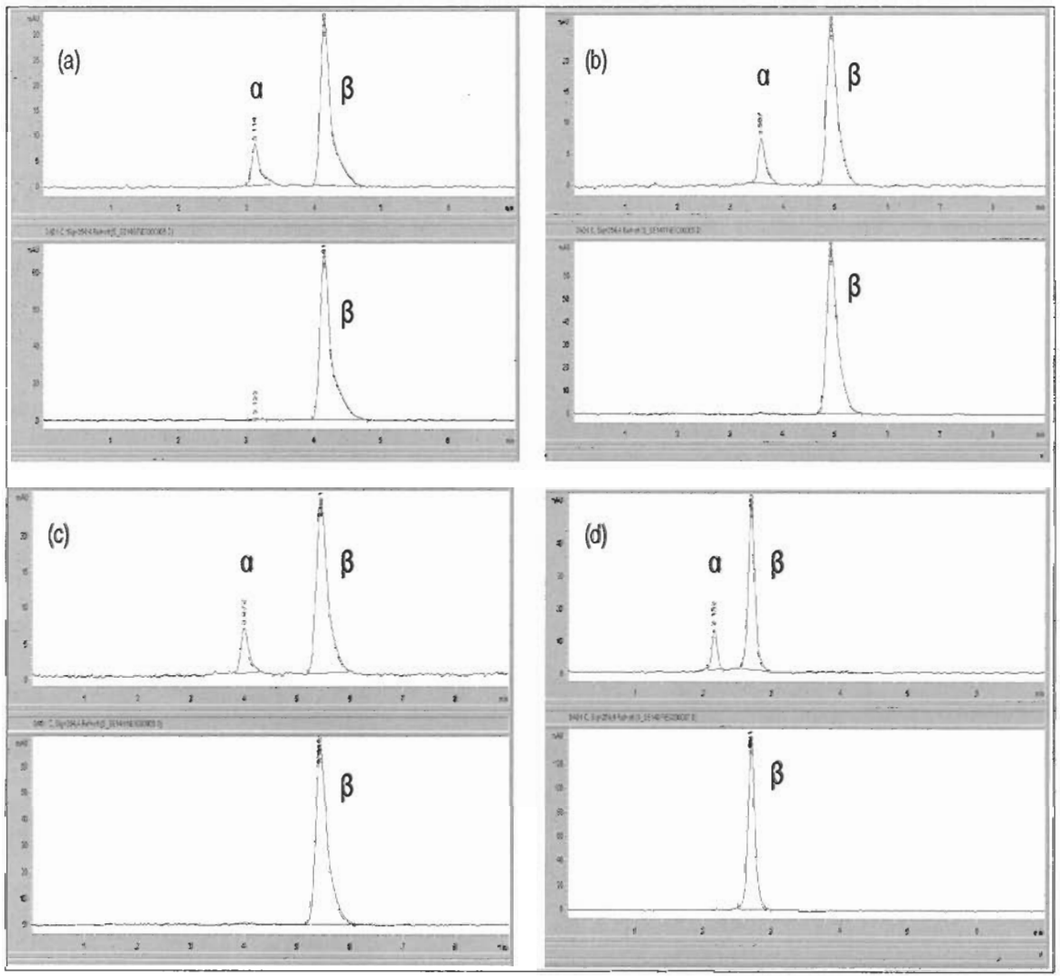

Adsorbents: (a) Prodigy glucose; (b) Prodigy maltotriose; (c) Prodigy maltoheptaose; (d) Prodigy maltodecatriose. Mobile phase: n-Hexane:ethanol (90:10); 1.0 mL/ min; Column temp 30 °C. UV: 254 nm

Figure 3-16: Effect of surface composition in the retention factor and selectivity for α/β-2,3,4,6-tetra-*O*-acetyl-phenylthio-D-galactopyranose.

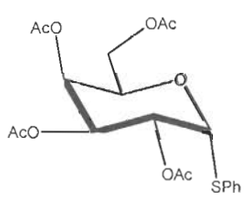

α- galactopyranose

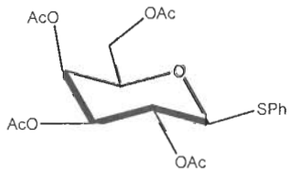

β- galactopyranose

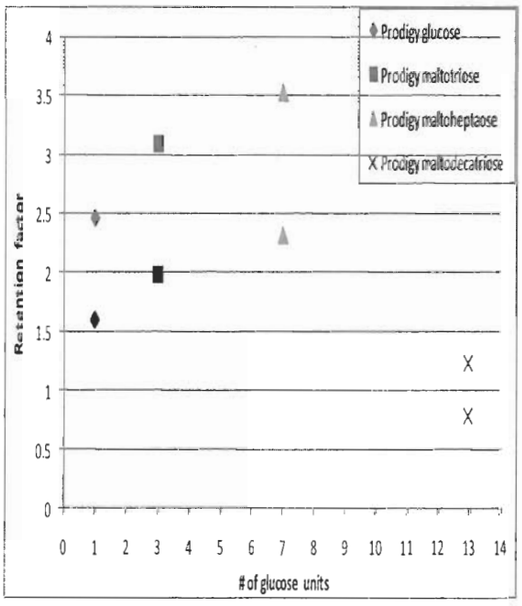

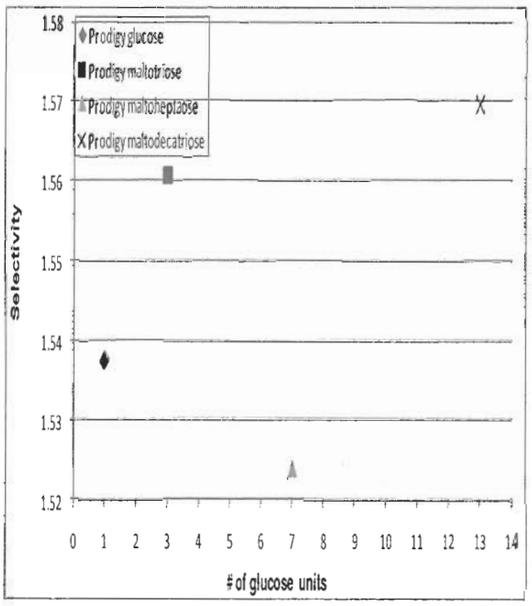

Mobile phase: n-Hexane :ethanol (90:10); 1.0 mL/ min; Column temp 30 °C. UV: 254 nm. Retention factor ($k = t_R - t_0 / t_0$) (left) and selectivity ($\alpha = k_2 / k_1$) (right). Retention factor #1 is α and #2 is β

Figure 3-17: Effect of surface composition on the retention factor and selectivity for α/β-1,2,3,4,6- penta-*O*-acetyl –D-glucopyranose

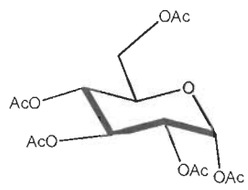

α- glucopyranose

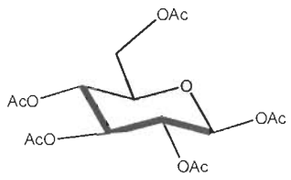

β- glucopyranose

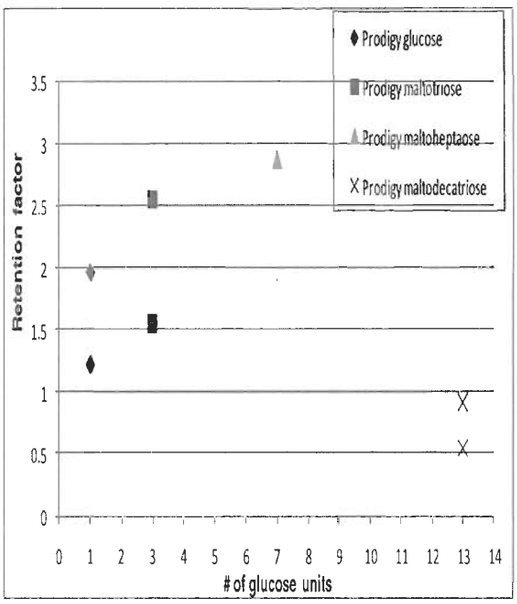

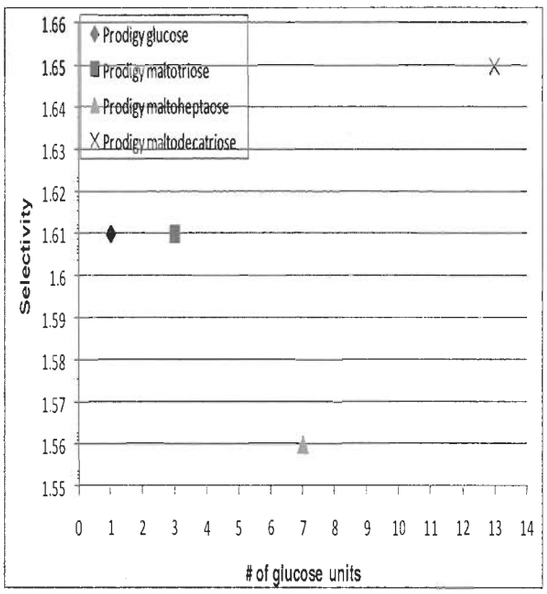

Mobile phase: n-Hexane:ethanol (90:10); 1.0 mL/ min; Column temp 30 °C. UV: 225 nm. Retention factor ($k = t_R - t_0 / t_0$) (left) and selectivity ($\alpha = k_2 / k_1$) (right). Retention factor #1 is α and #2 is β

Table 3-5: Summary of stereoisomer separations by normal phase mode

Stereoisomer	*Adsorbent*	*K1*	*K2*	*α*
[a]TFAE	Glucose	4.35	4.69	1.05
K1 (S) and *K2* (R)	Maltotriose	4.41	4.84	1.10
[b]TA-*O*-acetyl-phenylthio-galactopyranose	Glucose	1.60	2.46	1.54
	Maltotriose	1.98	3.09	1.56
K1 (α) and *K2* (β)	Maltoheptaose	2.31	3.52	1.52
	Maltodecatriose	0.79	1.24	1.57
[b]Penta-*O*-acetyl-glucopyranose	Glucose	1.22	1.96	1.61
	Maltotriose	1.55	2.56	1.61
K1 (α) and *K2* (β)	Maltoheptaose	1.84	2.87	1.56
	Maltodecatriose	0.54	0.92	1.65

[a] n-Hexane:$CHCl_3$:IPA (84:15:1), 1.0 mL/ min, column temp 25 °C. UV: 254 nm.

[b] n-Hexane:EtOH (90:10), 1.0 mL/ min, column temp 30 °C. UV: 254 nm.

Chromatographic results using reverse phase mode

There are reports in the literature discussing the separation of *trans/cis* stilbene using derivatized polysaccharide CSPs in only the normal phase mode.[72-73] Our new adsorbents showed stereoselectivity for *trans/cis* stilbene oxide using normal and reversed phase modes. In fact, a higher selectivity was observed when the reverse phase mode was utilized with our saccharide Prodigy silicas. Thus, in this study, the effect of the saccharide surface composition on the adsorption and chromatographic separation of *trans/cis* stilbene oxide was conducted by reverse phase HPLC. As shown in Figure 13-18 and Figure 13-19, increasing the size of the saccharide ligand increased the retention time/retention factor of the *trans/cis* stilbene oxide analyte. As in the normal phase mode, the adsorbent with the maltodecatriose did not follow this pattern. We speculate that this is most likely due to either not enough grafting on the surface or because a saturation point is reached and the larger ligand is not freely mobile. Even though the retention factors of the adsorbent with chemically bonded maltodecatriose are lower than with the other adsorbents, this ligand has the highest selectivity. Figure 13-17 demonstrates that by increasing the size of the saccharide ligand the stereoselectivity for the separation of stilbene oxide increases.

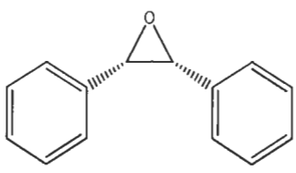

Cis-stilbene oxide

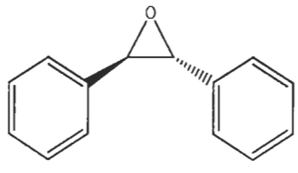

Trans-stilbene oxide

Figure 3-18: Effect of surface composition on the separation of *cis/trans-* stilbene oxide

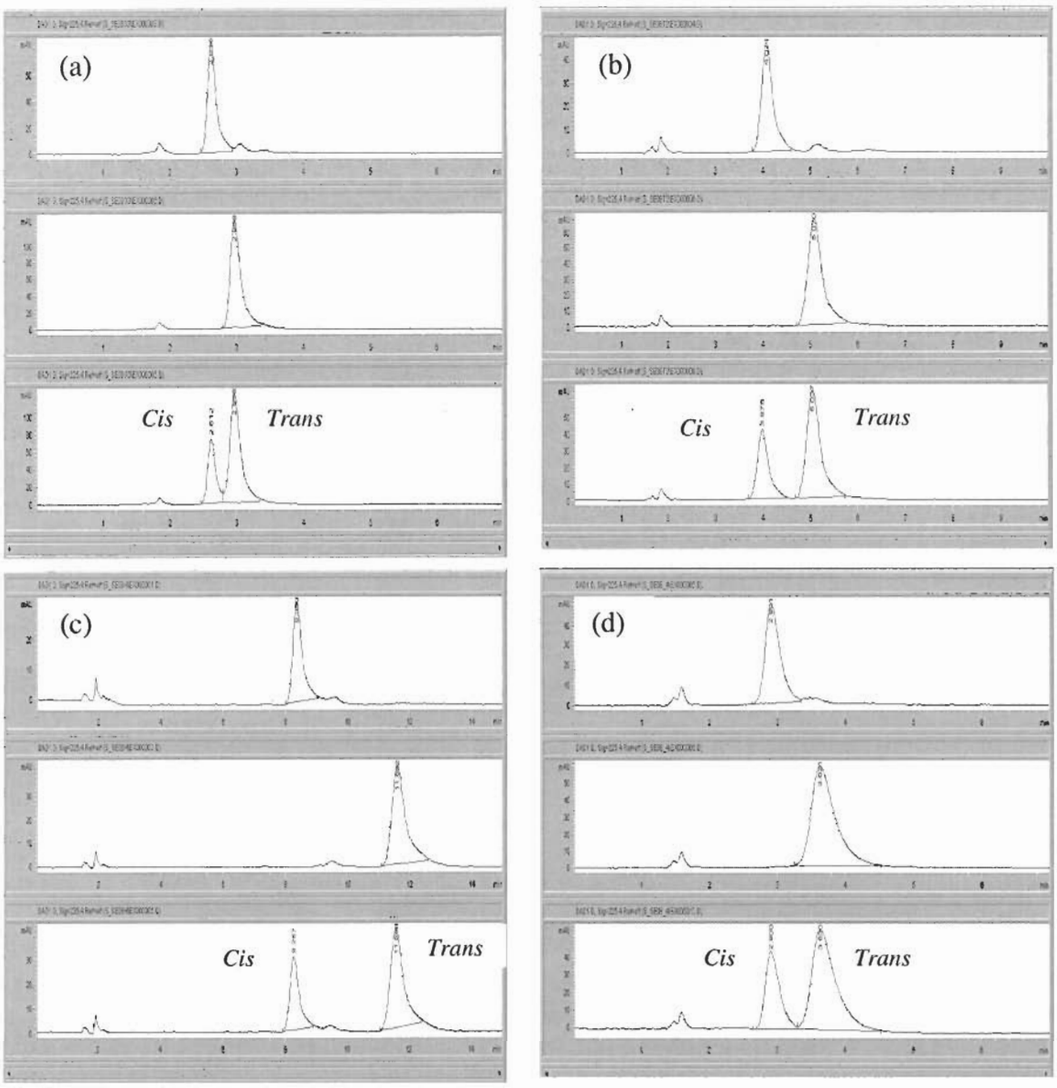

Adsorbents: (a) Prodigy glucose; (b) Prodigy maltotriose; (c) Prodigy maltoheptaose; (d) Prodigy maltodecatriose. Mobile phase: water: acetonitrile (70:30); 0.8 mL/ min; Column temperature 30 °C. UV: 225 nm

Figure 3-19: Effect of surface composition in the retention factor and selectivity for *cis/trans*- stilbene oxide

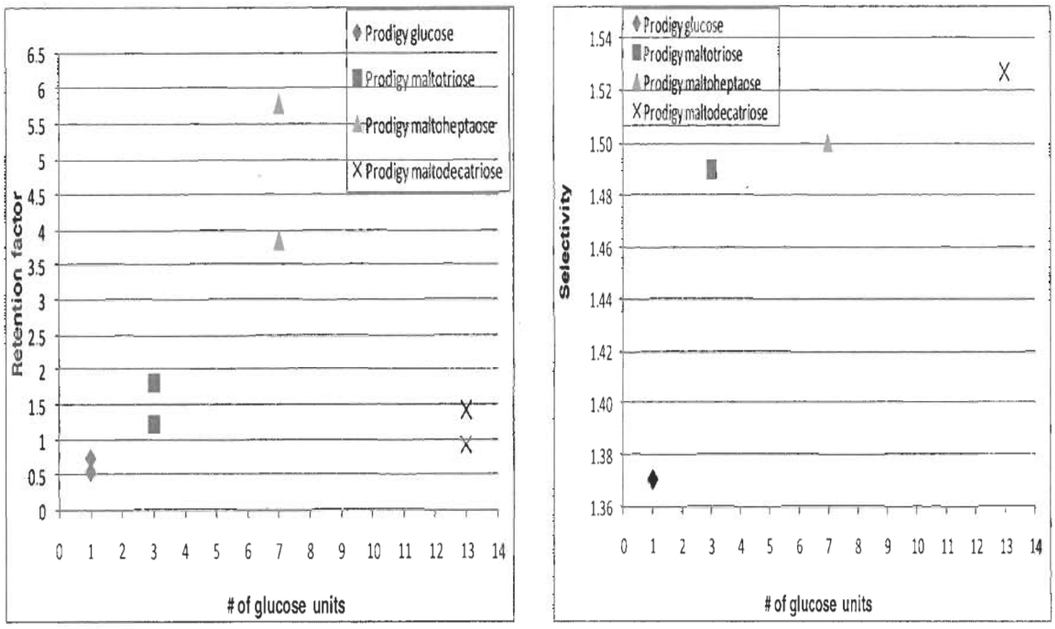

Mobile phase: water: acetonitrile (70:30); 0.8 mL/ min; Column temperature 30 °C. UV: 225 nm. Retention factor ($k = t_R - t_0 / t_0$) (left) and selectivity ($\alpha = k_2 / k_1$) (right). Retention factor #1 is *Cis* and #2 is *trans*

Our new adsorbents exhibited stereoselectivity with several terpenoid compounds such as *E/Z*-citral, nerol and geraniol. *E/Z*-citral mixtures were separated on the adsorbents with chemically bonded maltoheptaose and maltotriose. Almost no separation was observed with derivatized glucose and maltodecatriose. Nerol and geraniol showed acceptable selectivity using only the adsorbent with bonded maltoheptaose. Data suggests that the major chemical interactions involved in these separations are due to steric effects and π-π interactions. Since the maltoheptaose is one of the largest ligands used in this study, steric effects and π-π interactions are stronger. Table 3-6 summarizes the data obtained for the separation of stereoisomers using reverse phase mode.

Table 3-6: Summary of stereoisomer separations by reverse phase mode

Stereoisomer	*Adsorbent*	*K1*	*K2*	*α*
[a]Citral	Maltotriose	4.41	4.84	1.10
*K*1 (E)	Maltoheptaose	2.86	3.24	1.13
*K*2 (Z)				
[b]Nerol (*K*1)	Maltoheptaose	4.18	4.44	1.06
Geraniol (*K*2)				
[c]Stilbene Oxide	Glucose	0.54	0.74	1.37
*K*1 (*Cis*)	Maltotriose	1.21	1.80	1.49
*K*2 (*Trans*)	Maltoheptaose	3.86	5.79	1.50
	Maltodecatriose	0.93	1.42	1.53

[a] Water:acetonitrile (90:10), flow rate 0.9 mL/ min, column temp 45 °C. UV: 220 nm.

[b] Water:acetonitrile (95:5), flow rate 0.9 mL/ min, column temp 45 °C. UV: 220 nm.

[c] water: acetonitrile (70:30); 0.8 mL/ min; Column temp 30 °C. UV: 225 nm

Conclusions

New classes of adsorbents with chemically-bonded trimethoxysilyl-thio saccharides on their surfaces have been synthesized. The trimethoxysilyl-saccharide (analogs n=1, 3, 7 and 13 glucose units) series were prepared and used as chiral selectors. These ligands were immobilized onto silica *via* post-synthesis grafting. The post-synthesis reaction was conducted using two approaches: direct immobilization and surface chemical assembly. Results indicate that the direct immobilization method is superior to the surface chemical assembly approach. The resulting new adsorbents were characterized by NMR, FTIR, TGA, nitrogen isotherms, and elemental analyses.

These new adsorbents have been evaluated in the HPLC separations of various stereoisomers. These stationary phases can be used in either normal or reverse phase modes because the saccharides were chemically bonded not coated onto silica gel. We hypothesize that in the normal phase, hydrogen bonding, π-π, and Van der Waals interactions play an important role in the stereoisomeric separations. While in reverse phase, it was suspected that steric effects, π-π and hydrogen bonding dominate the chemical interactions enhancing the diastereomer separations. The adsorbent with chemically-bonded maltodecatriose had the lowest retention factor among all the ligands. However, its selectivity was similar or better than the smaller saccharides.

Addendum D (TGA graph)

This supplement provides reaction kinetics for the preparation of Prodigy silica glucose monitored by TGA

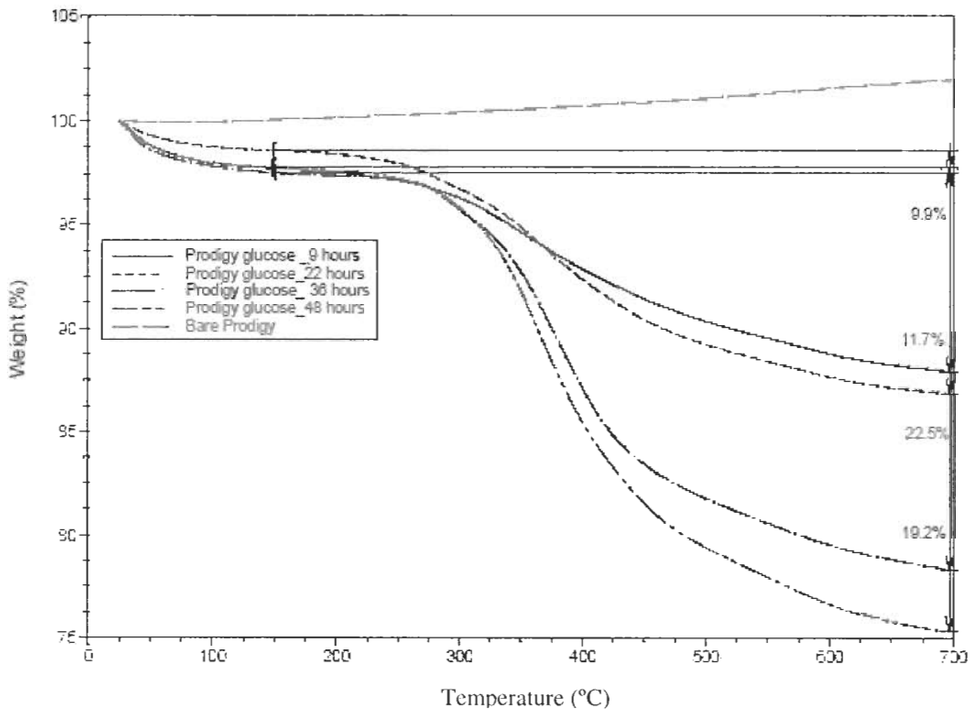

Addendum E (Chromatogram)

This supplement provides a typical chromatogram for the stereoisomeric *E/Z*-citral separations using Prodigy maltoheptaose stationary phase.

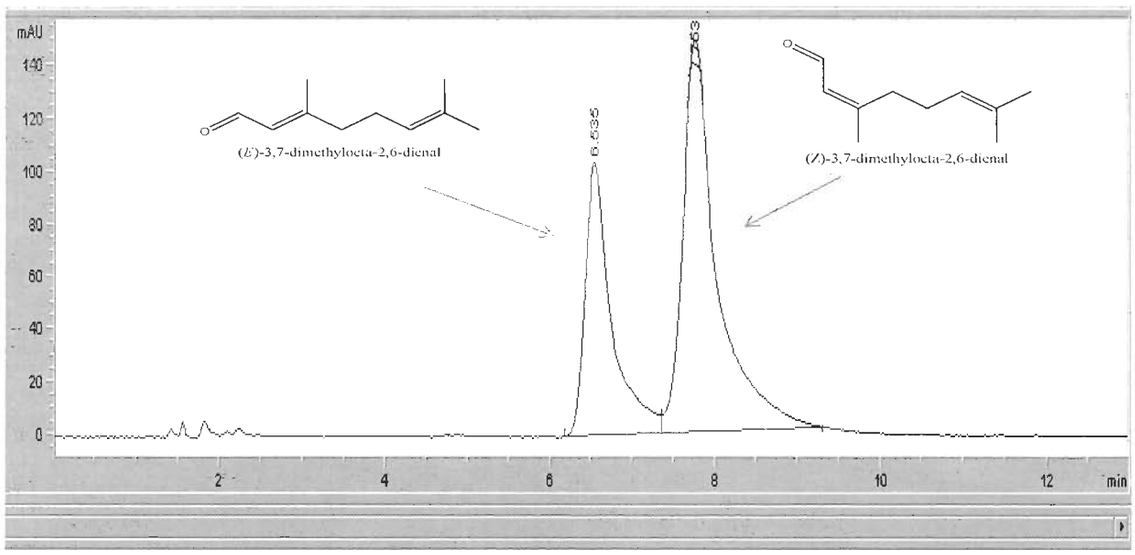

Mobile phase: Water: acetonitrile (90:10); 0.9 mL/min; Column temp 45 °C. UV: 220nm

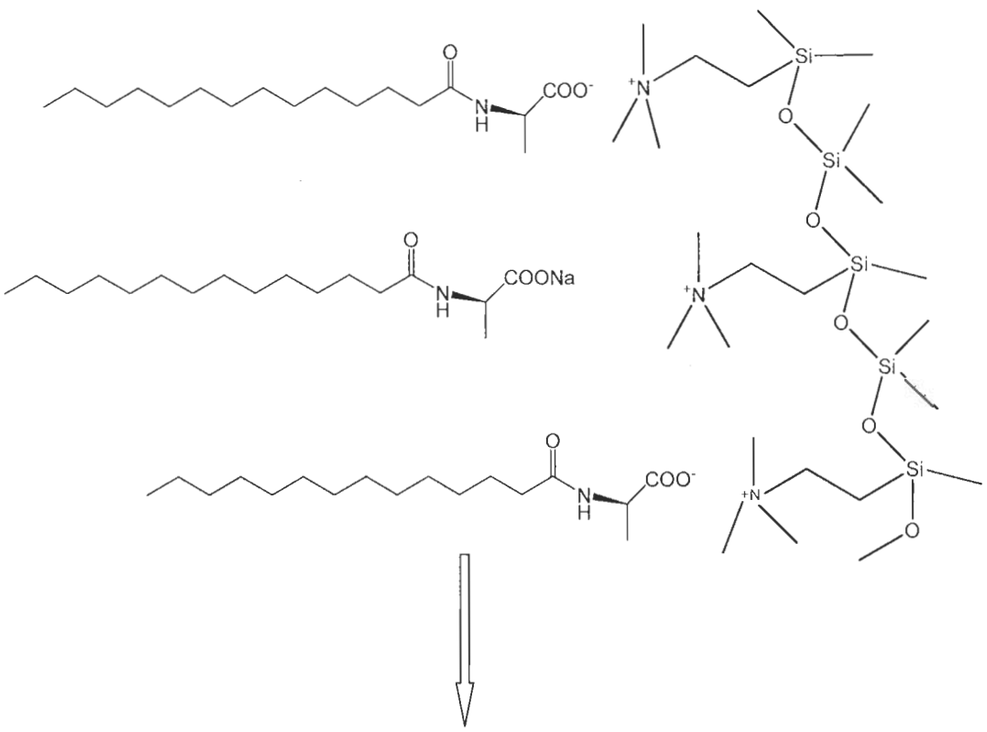
O
N
H
COO⁻
+N
Si
O
COONa

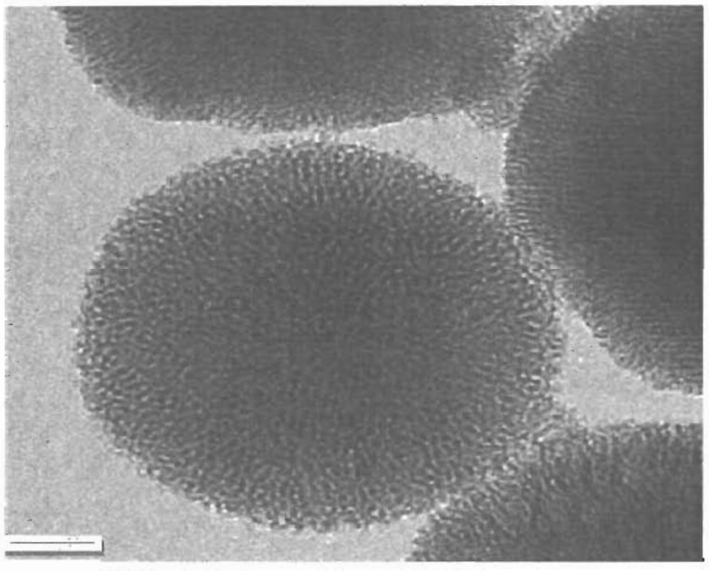
50 nm

Introduction

Since the development of well ordered mesoporous structures with large surface areas, [74-75] scientists have become very interested in these materials. These mesoporous silicas have potential applications in areas such as adsorption, chromatography, catalysis and sensors.[76-79] Mesoporous silicas have been prepared by using alkaline (M41S families) and acidic (SBA types materials) conditions.[80-84] In the M41S families, mesoporous MCM-41 material was first reported and it has been studied extensively since then.[74-75] Typically, MCM-41 has pore diameters between 2-10 nm with a highly ordered 2D hexagonal arrangement of mesoporous silica. In the SBA types, SBA-15 material has been widely studied. SBA-15 also has a well-ordered structure with a hexagonal pattern of pores.

The mesoporous well-ordered structures are formed by using surfactants as templates and tetraethyl orthosilicate TEOS, as an inorganic precursor. Recently, there have been many reports in the literature on the synthesis of mesoporous materials using anionic surfactants as templates.[85-90] The electrostatic attraction interaction between the anionic surfactant and the cationic silica surface was reported to be important for the synthesis of mesoporous silica.

Anionic chiral surfactants based on an amino acid as a head group are interesting molecules because they could lead to the formation of helical porous materials. Helical porous materials are attractive due to their potential application in chiral chromatography and stereoselective catalyst reactions. Recently, the formation of chiral mesoporous silicas[91-92] using N-myristoyl–D/L-alanine as a templates, TEOS (silica precursor) and N-trimethoxysyl-propyl-N,N,N-trimethylamonium (TMAPS) as a co-structure directing agent (CSD) were reported. These chiral porous silicas were reported to be left and right

handed helical particles. It was suggested that the helical porous was directed by the L and D alanine chiral surfactants.

On the other hand, the transformation of a silica structure to a different silica material has been deeply studied in the last decade. This phase transformation is called pseudomorph. [93] The main goal of the pseudomorphic transformation of silica is to change its surface characteristics by treating the material with alkaline conditions and high temperature. Under these conditions the silica materials take a structure mimicking the added template. These new materials could also be used for applications such as chromatography or catalysis reactions. For example, one reported had successfully demonstrated the transformation of a broad pore-diameter and spherical particle silica material to a well-ordered spherical MCM-41 mesoporous material.[93] Other literature[94-95] reported the successful synthesis of MCM-48 mesoporous materials by pseudomorphic transformation of MCM-41 parent silica. Since MCM-48 has a highly branched porous structure, it could be used for ion chromatography and catalytic reactions.

In this chapter, the synthesis of novel silica structures by co-condensation and pseudomorphic transformation was demonstrated. The co-condensation material was prepared by using N-myristoyl-L-alanine (C_{14}-L-Alan) as a template, TEOS (silica precursor) and TMAPS (CSD) were used under alkaline conditions. The trimethoxy groups of TMAPS covalently bound the silicon atoms of the TEOS to afford cationic groups on the silica surface. At the same time, the negative group of the C_{14}-L-Alan interacted with the positively charged ammonium site resulting in new silica materials (C_{14}-L-Alan-silicas). The pseudomorphic transformation was conducted using Prodigy and SBA-15 silicas, TMAPS and C_{14}-L-Alan - template. In addition, the chitosan

oligosaccharide was used as a chiral template with SBA-15 silica at pH=9.5 and 10.5. The pore order and structure of the materials prepared were characterized by TEM and N_2 adsorption.

Experimental

Materials

Tetraethyl orthosilicate, N-myristoyl chloride, L-Alanine, TMAPS and chitosan oligosaccharide were obtained from Sigma Aldrich Chemical Company (St. Louis, MO, USA). All other chemicals and solvents were of analytical or HPLC grade. Prodigy silica (average diameter: 15 nm), surface area 325 m^2/g was donated from Phenomenex. SBA-15 was prepared in our laboratories.

Synthesis of C_{14}-L-Alan chiral anionic surfactant

The C_{14}-L-Alan surfactant was prepared by condensation/acetylation of L-Alan with N-myristoyl chloride following the procedure reported in the literature.[96] In a typical reaction, L-Alan (1.3 g, 14.6 mmol) was dissolved in a mixture of 1 M NaOH aqueous (11 mL), 10% $NaHCO_3$ (11 mL) and THF (11 mL). N-myristoyl chloride (3.5 g, 14.2 mmol) was dissolved in THF (20 mL). While stirring in an ice bath (2-5 °C) N- myristoyl chloride in THF was added dropwise to the mixture. The reaction mixture was left stirring at room temperature for 2-3 hours. The organic solvent was concentrated *in vacuo* and the remaining solution (about 27 mL) was acidified with 2 N HCl (20 mL). The crude product was extracted with dichloromethane (2X, 40 mL). The organic layer was dried (Na_2SO_4), filtered, and concentrated *in vacuo* to afford crude C_{14}-L-Alan as a white solid. The product was further purified by recrystallization from benzene affording

a pure solid C_{14}-L-Alan chiral surfactant (2.3 g, 7.7 mmol, 53% yield). ^{1}H-NMR and ^{13}C-NMR data were consistent with the literature values reported.[91] The synthetic scheme of the preparation of C_{14}-L-Alan surfactant is demonstrated in Figure 4-1.

Figure 4-1: Synthesis of C_{14}-L-Alan ionic chiral surfactant

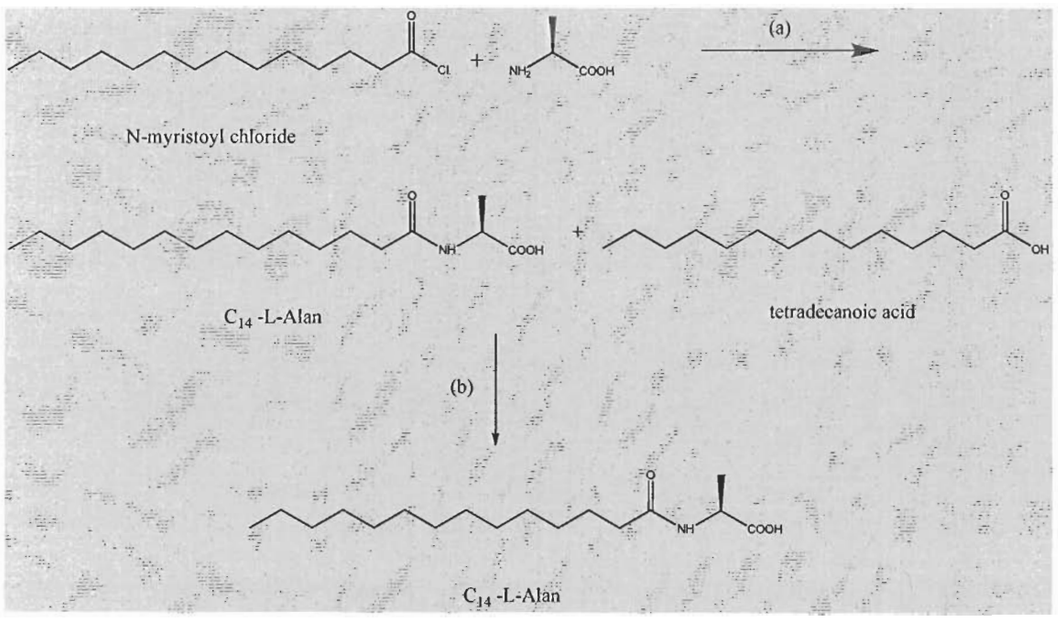

(a) 1M NaOH/$NaHCO_3$/THF at 2-5 °C, 2 N HCl, dichloromethane (b) Recrystallization from benzene

Synthesis of C_{14}-L-Alan-mesoporous silica

Briefly, this chiral mesoporous silica was prepared by co-condensation of TEOS with TMAPS and C_{14}-L-Alan surfactant as a template under alkaline conditions. In a typical synthesis, C_{14}-L-Alan (0.13 g, 0.43 mmol) was dissolved in water (14 mL). A mixture of TEOS (0.6 g, 2.9 mmol), TMAPS (90 mg, 50% methanol), 0.1 M NaOH (430 μL) and 0.1 M HCl (370 μL) (to partially neutralized the salt) was added to the template. The mixture was allowed to react at 33 °C with stirring for about 7 minutes and placed on the bench for 2 hours at room temperature. Then, the mesoporous material was cured at 80 °C for 17 hours. The product was recovered by centrifugal separation and dried overninght at 60 °C. All the organic moities were removed by calcination at 600 °C for 12 hours. The calcinated silica was labeled as C_{14}-L-Alan-MS.

Pseudomorphic transformation: Prodigy Silica- C_{14}-L-Alan surfactant

The surface characteristic of silica was changed by treating the materials at a variety of high temperatures and aging under alkaline conditions.

Series A (4X reactions): Separately, C_{14}-L-Alan surfactant (0.36 g. 2.0 mmol) was dissolved in 0.2 M NaOH (10 mL) and in 1 M HCl (200 μL) at 35 °C for one hour (clear solution is observed). Prodigy silica (0.4 g) was added to the template and placed on the bench for 20 hours at room temperature. Then, the reaction mixture was cured at a variety of temperatures (90 °C, 110 °C and 125 °C) for 1 day. The product was recovered by centrifugal separation and dried overninght at 60 °C. All the organic moities were removed by calcination at 600 °C for 12 hours. The calcinated materials were label as C_{14}-L-Alan- Prodigy.

Series B (2X reactions): Separately, C_{14}-L-Alan surfactant (0.36 g, 2.0 mmol) was dissolved in 0.2 M NaOH (10 mL) and in 1 M HCl (200 μL) at 35 °C for one hour (clear solution is observed). Prodigy silica (0.4 g) and TMAPS (0.2 g, 50% methanol) was added to the template and placed on the bench for 20 hours at room temperature. Then, the reaction mixture was cured at 125 °C for 1 and 3 days. The product was recovered by centrifugal separation and dried overnight at 60 °C. All the organic moities were removed by calcination at 600 °C for 12 hours. The calcinated samples were labeled as C_{14}-L-Alan- Prodigy- 2

Pseudomorphic transformation: SBA-15 Silica chiral ionic surfactant

The pseudomorphic transformation of SBA-15 was conducted using a variety of high temperatures, aging and chiral surfactants under alkaline conditions.

Series A (3X reactions): Separately, C_{14}-L-Alan surfactant (0.36 g. 2.0 mmol) was dissolved in 0.2 M NaOH (10 mL) and in 1 M HCl (200 μL) at 35 °C for one hour (clear solution is observed). SBA-15 silica (0.4 g) and TMAPS (0.2 g, 50% methanol) was added to the template and placed on the bench for 20 hours at room temperature. Then, the reaction mixture was cured at 125 °C for a variety of days (1, 2 and 3 days). The product was recovered by centrifugal separation and dried overnight at 60 °C. All the organic moities were removed by calcination at 600 °C for 12 hours. The calcinated samples were labeled as C_{14}-L-Alan-SBA-15.

Series B (3X reactions): Separately, C_{14}-L-Alan surfactant (0.18 g, 1.0 mmol) was dissolved in 0.2 M NaOH (5 mL) at 35 °C for one hour (clear solution is observed). SBA-15 silica (0.2 g) and TMAPS (0.1 g, 50% methanol) was added to the template. The reaction was adusted to a pH of 9.8, 10.8 or 11.8 and each reaction was placed on

the bench for 20 hours at room temperature. The reaction mixture was cured at 80 °C for 14 hours. The product was recovered by centrifugal separation and dried overnight at 60 °C. All the organic moities were removed by calcination at 600 °C for 12 hours. The calcinated samples were labeled as C_{14}-L-Alan-SBA-15-2.

Series C (2X reactions): Individually, C_{14}-L-arginine (0.32 g, 0.8 mmol) or C_{16}-L-arginine (0.34 g, 0.8 mmol) surfactant was dissolved in 0.2 M NaOH (10 mL) at 35 °C for one hour (clear solution is observed). SBA-15 silica (0.4 g) was added to the template and placed on the bench for 3 hours at room temperature. Then, the reaction mixture was placed in an oven at 75 °C for 17 hours. The product was recovered by centrifugal separation and dried overnight at 60 °C. All the organic moities were removed by calcination at 600 °C for 12 hours. The calcinated samples were labeled as C_{14}-L-Arg-SBA-15 and C_{16}-L-Arg-SBA-15.

Series D (2X reactions): Individually, chitosan oligosaccharide (0.4 g, ~ 0.08 mmol) was dissolved in 0.1 N HCl (5 mL) at 30 °C for one hour (clear solution is observed). SBA-15 silica (0.4 g) was added to the template and adjuted to pH=9.5 and pH=10.5 with 1 N NaOH. The reaction mixture was placed under static conditions at 30 °C for 20 hours and cured at 80 °C for 8 hours. The product was recovered by centrifugal separation and dried overnight at 60 °C. All the organic moities were removed by calcination at 600 °C for 12 hours. The calcinated samples were labeled as chitosan-SBA-15.

Characterization

Nitrogen isotherms

Nitrogen adsorption-desorption isotherms (77K) were obtained to determine the surface characteristics of silica; isotherms were acquired using an Autosorb-1 analyzer

(Quantachrome Instruments, Boynton Beach, FL, USA). Refer to Chapter 2 for the nitrogen isotherms parameters. Prior to analysis, the materials were degassed at 100 °C overnight using the out-gassing port of the instrument.

NMR experiments

The ^{1}H-NMR experiments were conducted using a Bruker 500 MHz NMR spectrometer.

Results and Discussion

NMR experiments: Synthesis of C_{14}-L-Alan chiral anionic surfactant

^{1}H-NMR (500 MHz, $CDCl_3$) was one of the techniques used to monitor the synthesis of C_{14}-L-Alan. Figure 4-2a demonstrates the ^{1}H-NMR spectrum of the crude C_{14}-L-Alan surfactant (before recrystallization). As can be observed in Figure 4-2a, the tetradecanoic acid byproduct is very significant in this batch. It is suspected that the N-myristoyl chloride is hydrolyzed during the reaction with alanine producing the tetradecanoic acid byproduct. The amount of the byproduct was estimated to be around 60%. This estimation was done by comparing the integration ratio between the product at 2.24 ppm (2H, t, -CH2-COO) and byproduct at 2.36 ppm (2H, t, -CH2-COO). Figure 4-2b demonstrates a significant increase of the product and subsequent decrease of the byproduct after recrystallization.

Figure 4-2: ^{1}H-NMR experiment for the synthesis of C_{14}-Alan

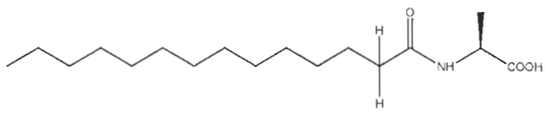

C_{14} -L-Alan 1

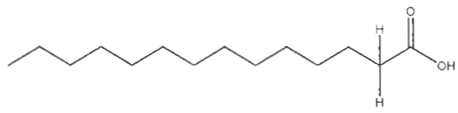

tetradecanoic acid 2

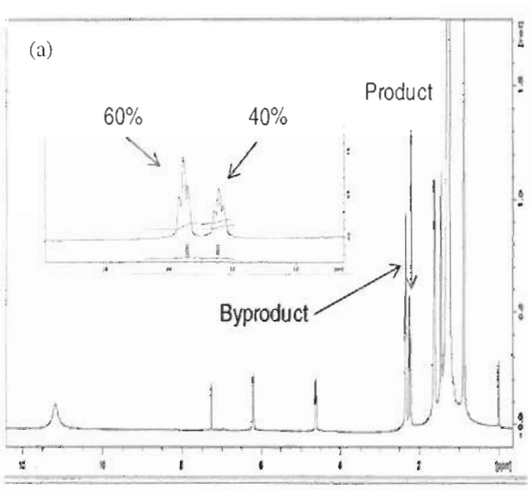

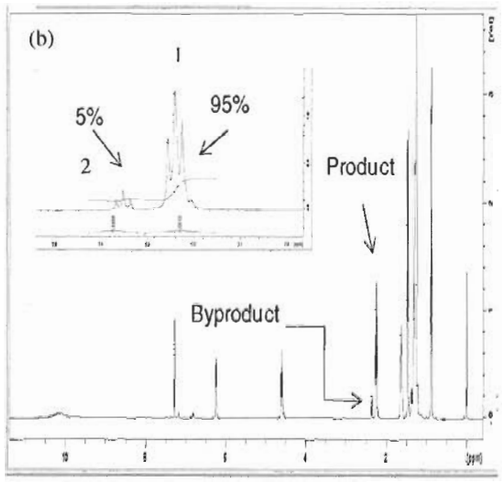

(a) Crude C_{14}-L-Alan (b) C_{14}-L-Alan after recrystallization from benzene, Varian 500 MHz ($CDCl_3$).

Characterization of C_{14}-L-Alan-MS by TEM

Figure 4-3 shows the transmission electron microscope (TEM) image of the calcinated C_{14}-L-Alan-MS. This material shows an ordered porous structure in some regions and the particle was surrounded by channel with different orientations. Disordered pores were also present in other regions. It is suspected that this different orientation blocks of the inner pore system might be the caused for the low surface area and pore volume (Figure 4-4, and Table 4-1).

Figure 4-3: TEM image of C_{14}-L-Alan-MS

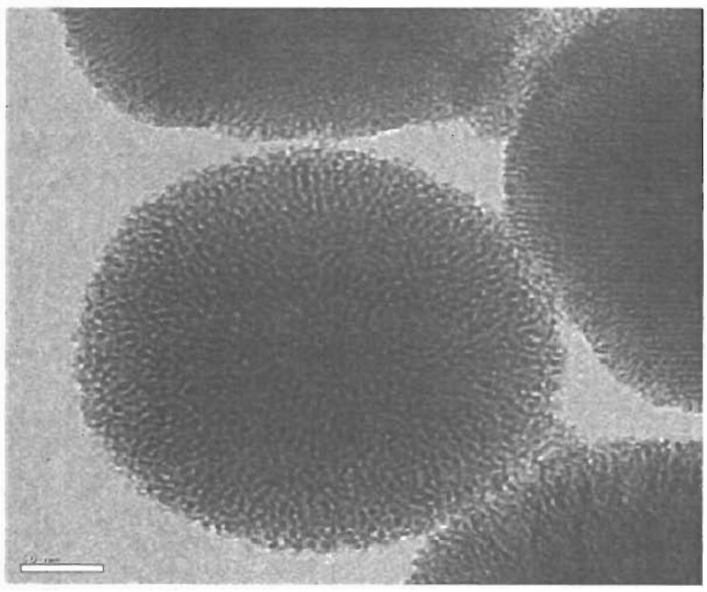

50 nm

Nitrogen isotherms of C_{14}-L-Alan-MS

The C_{14}-L-Alan-MS was further characterized by nitrogen adsorption-desorption isotherms (Figure 4-4). The isotherms were type IV isotherms with a capillary condensation hysteresis at ~0.5-0.95 p/p_s indicating mesoporous materials.[49] The isotherm shows an uptake at ~0.37 p/p_s and another uptake starting at 0.9 p/p_s. This nitrogen isotherm suggested present of small pores with mean pore radius of ~ 1.8 nm and some large pores or voids. Table 4-1 shows the surface area and pore volume of the material C_{14}-L-Alan-MS.

Figure 4-4: Nitrogen isotherm of C_{14}-L-Alan-MS

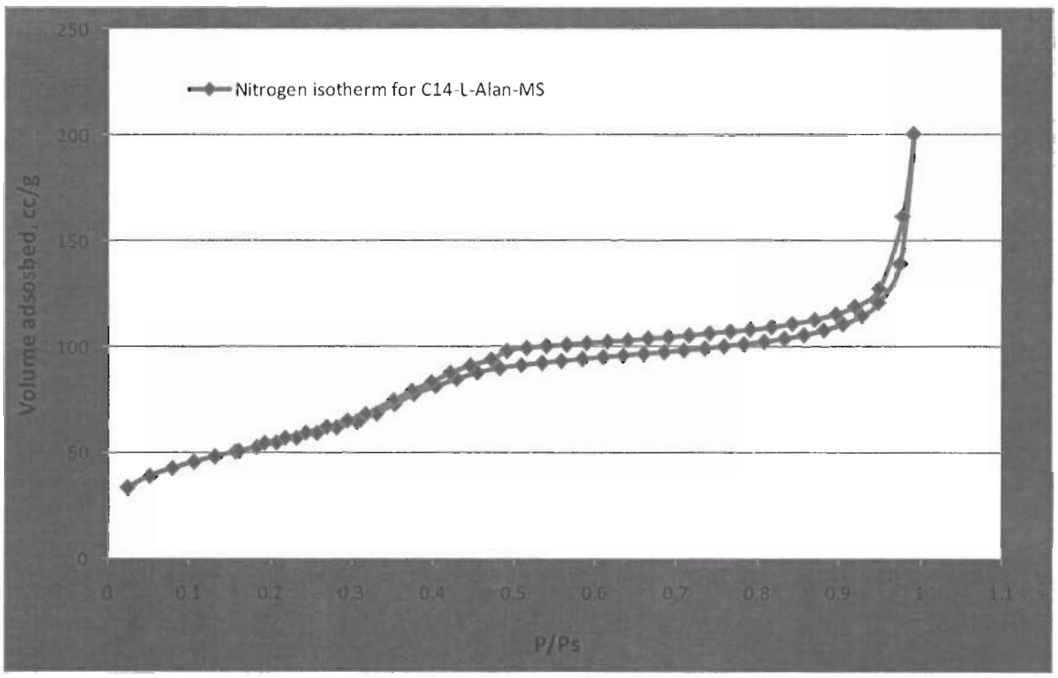

Nitrogen isotherms of C_{14}-L-Alan-Prodigy (Series A)

The goal here was to transform Prodigy silica to a chiral mesoporous structure. Figure 4-5 shows the nitrogen isotherms of the C_{14}-L-Alan-Prodigy (Series A) silica materials. All the materials had type IV isotherms with capillary condensation hysteresis at ~0.8-0.95 p/ps. A broad pore size distribution is observed for all the materials (treated and parent silicas). The pore size of the treated silicas increases: Higher temperature, the larger pores. In addition, the treated materials show a noticeable decrease of surface area and pore volume as the temperature increases. Based on the nitrogen isotherms data, it is unclear whether we are be able to conclude that the parent Prodigy silica was transformed to chiral mesoporous materials with these conditions.

Figure 4-5: Nitrogen isotherm of C_{14}-L-Alan-Prodigy and its parent silica

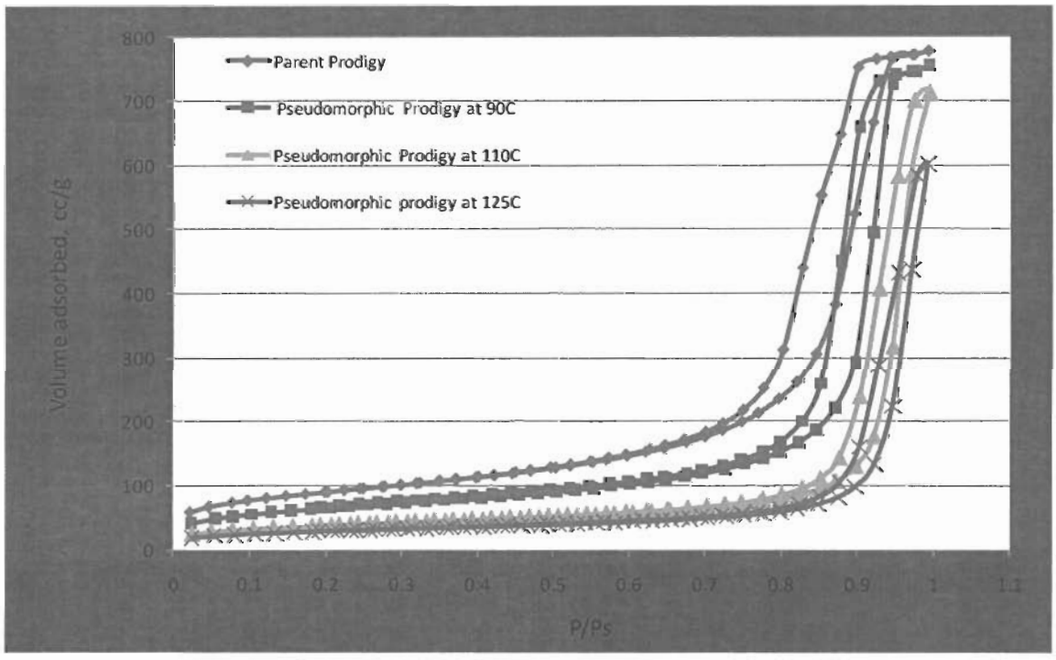

Nitrogen isotherms of C_{14}-L-Alan-Prodigy2 (Series B)

The C_{14}-L-Alan-Prodigy2 materials were synthesized to study the effect of TMAPS in the pseudomorphic transformation process. All the materials had type IV isotherms with capillary condensation hysteresis at ~0.8-0.95 p/ps as C_{14}-L-Alan-Prodigy materials. Figure 4-6 (a) compares the nitrogen isotherms of two materials that were treated with and without TMAPS at 125 °C for 1 day. Data suggests that in the presence of TMAPS the parent silica is more stable than without TMAPS. The material treated with TMAPS for one day at 125 °C does not show significant differences in surface area and pore volume when compared with the parent silica. Figure 4-6 (b) compares two of the C_{14}-L-Alan-Prodigy2 materials (TMPS for 1 and 3 days at 125 °C). Aging at 125 °C for longer times did not have a major impact on the subjected Prodigy silica (Figure 4-6 (b)). Table 4-1 shows the surface areas and pore volumes of all the Prodigy treated materials

Table 4-1 N_2 isotherm data of the C_{14}-L-Alan-MS and Prodigy silicas

Adsorbent	*Surface area (m^2/g)*	*Total PV (cc/g)*	*Ave Pd (Å)*
C14-L-Alan-MS	120	0.2	**40**
Parent Prodigy	310	1.2	**154**
Prodigy at 90°C_1D	226	1.1	200
Prodigy at 110°C_1D	130	1.1	340
Prodigy at 125°C_1D	100	0.4	140
Prodigy at 125°C_1D (TMAPS)	215	0.9	174
Prodigy at 125°C_3D (TMAPS)	163	0.7	164

Figure 4-6: Nitrogen isotherm of C_{14}-L-Alan-Prodigy2 and its parent silica

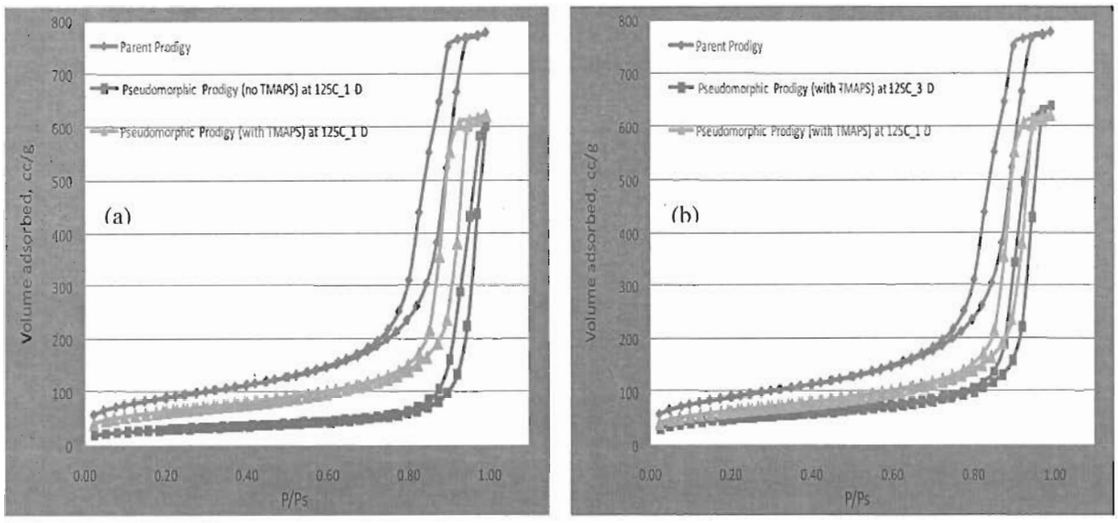

(a) C_{14}-L-Alan-Prodigy/ C_{14}-L-Alan-Prodigy2: 1 day at 125 °C without and with TMAPS

(b) C_{14}-L-Alan-Prodigy2: For 1 and 3 days at 125 °C with TMPAS.

Characterization of C_{14}-L-Alan-SBA-15 and C_{14}-L-Alan-SBA-15 C_{14}-L-Arg-SBA-15 by TEM

TEM was performed on all the subjected SBA-15 materials. The TEM images for all these materials prepared with a variety of chiral surfactants, temperatures and high pH conditions formed fiber-type structures with the pore structure resembling that of parent SBA-15 silica. In summary, based on the morphology, it appears that those fibers are broken into smaller parts from the original SBA-15 with these conditions. In addition, the type of surfactant (C_{14}-Alan, C_{14}-Arg and C_{16}-Arg) does not affect the outcome of the reaction. Within the range studied, time and temperature of treatment do not appear to play an important role when SBA-15 was used as the parent silica. However, the chiral surfactants seem to be important, as without them no changes were observed. Figure 4-7

shows typical TEM images using C_{14}-L-Alan-SBA-15 treated for 3 days (4-7 (a)) and C_{14}-L-Arg-SBA-15 (4-7 (c)).

Figure 4-7: TEM images C_{14}-L-chiral surfactants-SBA-15 and their parent silica

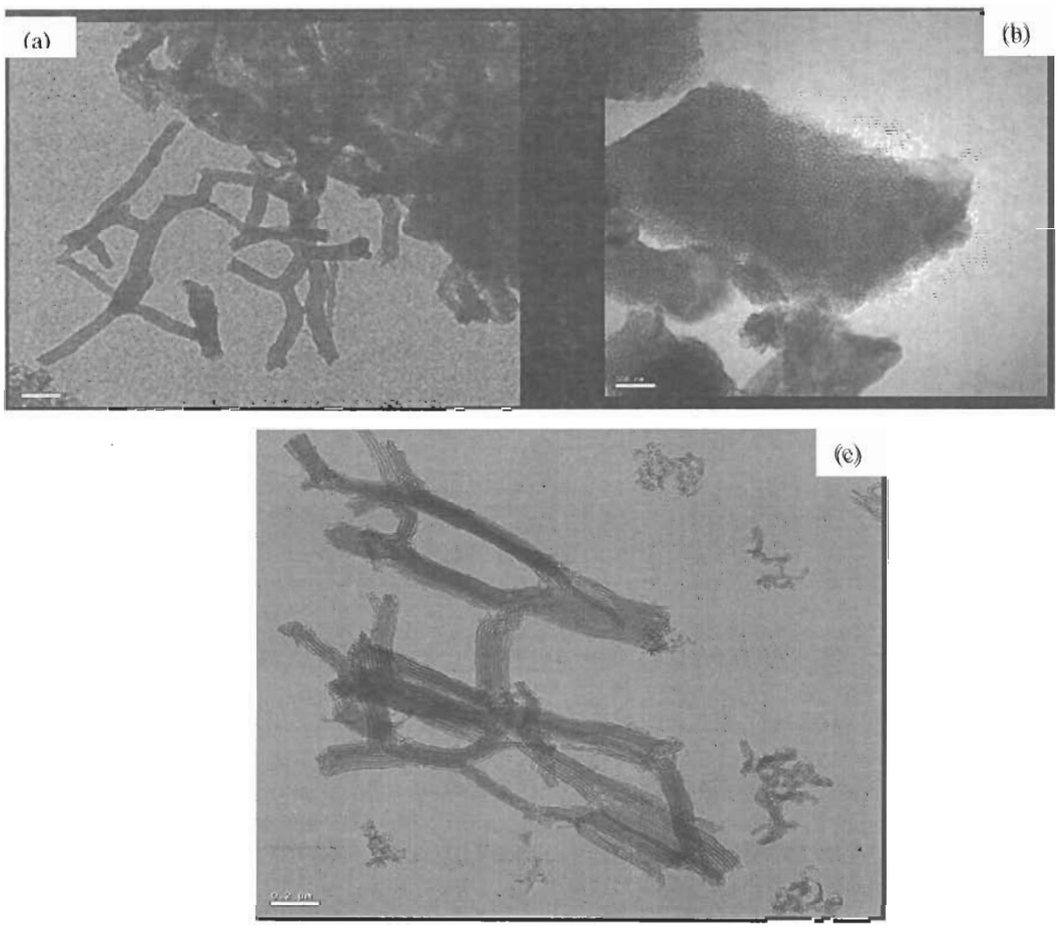

(a) C_{14}-L-Alan-SBA-15-3 days at 125 °C (b) Parent SBA-15 silica

(c) C_{14}-L-Arg-SBA-15-8 hours at 80 °C

Nitrogen isotherms of C_{14}-L-Alan-SBA-15 (Series A, 3D)

The structure of C_{14}-L-Alan-SBA-15 (3 days at 125 °C) was further characterized by nitrogen adsorption-desorption isotherms (Figure 4-8). The isotherms were type IV isotherms. There was a noticeable change in the structure of the treated material versus the parent SBA-15 silica (Figure 4-8). The treated mesoporous silica showed an increase of pore diameter and pore volume, yet the surface area decreased. It is interesting to observe that the C_{14}-L-Alan-SBA-15 material had transformed into a similar nitrogen isotherm shape as the spherical Prodigy silica. Figure 4-9 demonstrates the nitrogen isotherms of the C_{14}-L-Alan-SBA-15 and a parent Prodigy silica.

Figure 4-8: Nitrogen isotherms of C_{14}-L-Alan-SBA-15 and its parent silica

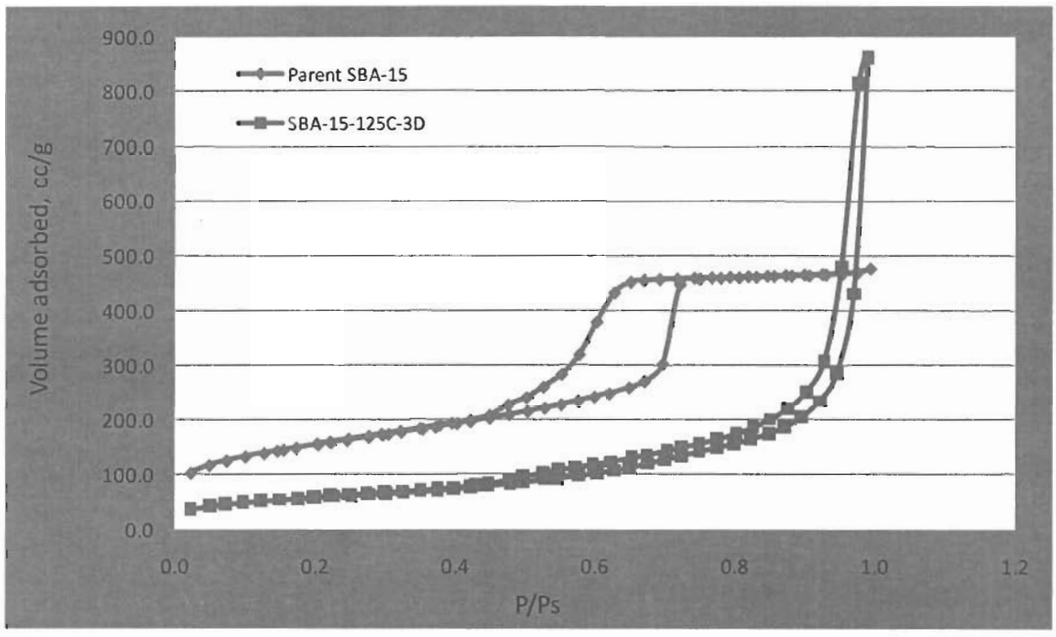

Figure 4-9: Nitrogen isotherms of C_{14}-L-Alan-SBA-15 and Prodigy silicas

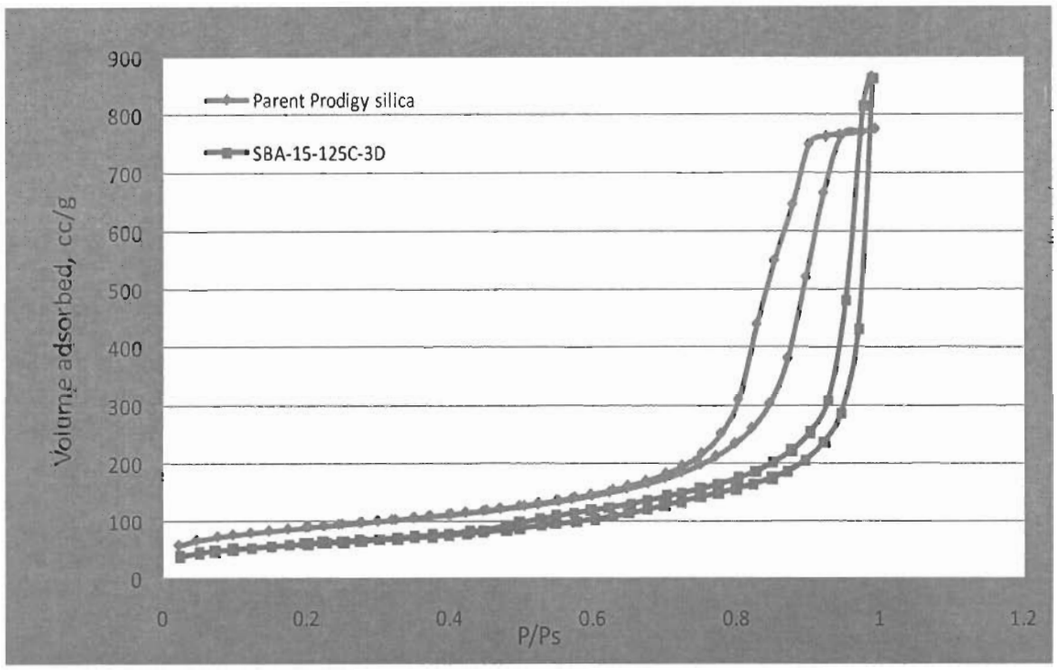

Nitrogen isotherms of Chitosan-SBA-15

Figure 4-10 shows the nitrogen isotherm of the chitosan-SBA-15 (pH=9.5) and its parent SBA-15 silica. The surface area and the pore volume of the chitosan-SBA-15 silica demonstrated substantial decreases but the isotherms remained type IV. The capillary condensation hysteresis for both materials were quite different The pore size distribution (PSD) curves were symmetrical and narrow showing uniform pores with mean radii of ~3.3, for parent SBA-15 while for Chitosan-SBA-15 broad pore size distribution was observed. The transformation using chitosan as a chiral template and SBA-15 as the parent silica was obvious. However, this material still needs to be characterized by TEM to further evaluate the ordered porous structure. Also the role of pH on the

transformation needs to be investigated. This is subject to future work. Table 4-2 summarizes the nitrogen isotherm data of all the treated SBA-15 silica materials.

Figure 4-10: Nitrogen isotherms of Chitosan-SBA-15 and its parent silica

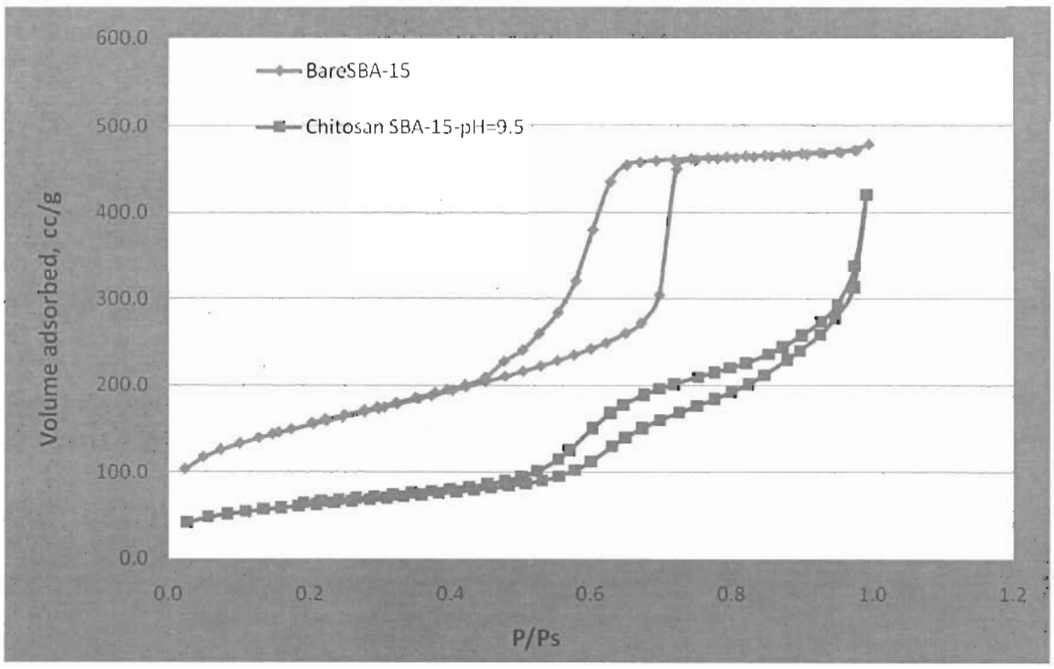

Table 4-2 Nitrogen isotherms of SBA-15 treated materials

Adsorbent	*Surface area (m^2/g)*	*Total PV (cc/g)*	*Ave Pd (Å)*
C14-L-Alan-SBA-15-3D	195	0.4	86
Chitosan_SBA-15_8 hours (pH=10.5)	120	0.2	73
Chitosan_SBA-15_8 hours (pH=9.5)	190	0.4	82

Conclusions

Unique chiral mesoporous silicas were successfully synthesized by co-condensation and pseudomorphic transformation methodologies with templated chiral surfactants. In this report, TEOS was co-condensed with TMAPS as a co-structure directing agent affording silica modified with quaternized amino site surfaces and templated with the chiral anionic L-alanine (C_{14}-L-Alan). The negative charge of the chiral template (C_{14}-L-Alan) is believed to interact with the positive quaternized amino, contributing to the formation of unique silicas with helical porous structures. The pseudomorphic transformation methodology was studied in this report as well. Spherical Prodigy and SBA-15 silicas (parent silicas) and C_{14}-L-Alan and chitosan (porous directing templates) were used in the pseudomorphic transformation. It was demonstrated by the nitrogen isotherm technique that the C_{14}-L-Alan template did not have a significant effect on the formation of mesoporous silica when Prodigy silica was treated with alkaline and high temperature conditions. Under the same conditions, SBA-15 silica was transformed to a different mesoporous structure. TEM images on the subject SBA-15 materials show interesting fiber-type structures. It appears by TEM that the chiral surfactants play an important role when used with SBA-15 silica, as without them no changes were observed.

References

(1) Philips, D. J.; Bell-Alden, B.; Cava, M.; Grover, E. R.; Mandeville W. H.; Mastico, R.; Sawlivich, W.; Vella, G.; Weston A. *J. Chromatogr.* **1991,** *536*, 95-106.

(2) Marra, A.; Moni, L.; Pazzi, D.; Corallini, A.; Bridi, D.; Dondoni, A. *Org. Biomol. Chem.* **2008**, *6*, 1396-1409

(3) Varki, A. *Glycobiology* **1993**, *3*, 97.

(4) Glycosciences Status and Perspective, Gabius, H-J., Gabius, S., Eds.; Chapman and Hall: Weinheim, 1997.

(5) Okamoto, Y.; Ohashi, T.; Kaida, Y.; Yashima, E. *Chiralit.* **1993,** *5*, 616-621.

(6) Okamoto, Y.; Kawashima, M.; Yamamoto, K.; Hatada, K. *Chem.Lett.* **1984**, 739-742.

(7) Okamoto, Y.; Kawashima, M.; Hatada, K. *J. Chromatogr.* **1986**, *363*, 173-186.

(8) Chankvetadze, B.; Yashima, E.; Okamoto, Y. *Chem. Lett.* **1992**, 617-620.

(9) Chankvetadze, B.; Yashima, E.; Okamoto, Y. *J. Chromatogr. A* **1994**, *670*, 617-620.

(10) Okamoto, Y.; Aburatani, R.; Hatada, K. *J. Chromatogr.* **1987**, *389*, 39-49.

(11) Stalcup, A. M.; Williams, K. L. *J. Chromatogr.* **1995,** *695*, 185-193.

(12) Kano, K.; Minami, K.; Horiguchi, K. *J. Chromatogr A* **1995,** *694*, 307-313.

(13) Weller, O.; Schulze, J.; König, W. A. *J. Chromatogr.* **1987,** *403*, 263-270.

(14) Schulze, J.; König, W.A. *J. Chromatogr.* **1986,** *355*, 165-175.

(15) Aburatani, R.; Okamoto, Y.; Hatada, K. *Bull. Chem. Soc. Jpn.* **1990,** *63*, 3606-3610.

(16) Lai, X. H.; Ng, S.C. *J. Chromtogr. A* **2004**, *1031*, 135.

(17) Zhou, Z. M.; Fang, M.; Yu, C. X. *Anal. Chim. Acta* **2005**, *539*, 23.

(18) Johnston, B. D.; Pinto, B. M. *J. Org. Chem.* **2000**, *6*, 4607-4617.

(19) Zhichao, P.; Dong, H.; Caraballo, R.; Ramstrom, O. *Eur. J. Org. Chem.* **2007,** 4927.

(20) Gamblin, P. D.; Philippe, G.; Kanteren, S.; Oldham, N. J.; Fairbanks, A. J.; Davis, B. G. *Angew.Chem.* **2004,** *116*, 845-851.

(21) Aldrich Library of ^{1}HNMR Spectra; Aldrich Chemical; Beil. 17,V,6,368; Merk 14, 60.

(22) Aldrich Library of ^{1}H, ^{13}C and FTIR Spectra; Aldrich Chemical; Beil. 2, IV,6, 359; FT-IR 2 (1), 1112:D / FT-IR 1 (1), 625:C / FT-NMR 1 (1), 1057:C / IR-Spectra (3), 372:D / IR-Spectra (2), 331:B / RegBook 1 (1), 763:B / Sigma FT-IR 1 (1), 1147:A / Structure Index 1, 118:D:7

(23) Farkas, E.; Janossy, L.; Harangi, J.; Kandra, L.; Liptak, A. *Carbohydr. Res.* **1997,** *303*, 407-415.

(24) Beck, J. S.; Vartuli, J. C.; Roth,W. J.; Leonowicz, M. E.; Kresge, C. T.; Schmitt, K. D.; Chu, C. T. W.; Olson, D. H.; Sheppard, E. W.; McCullen, S. S. B.; Higgins, J. B.; Schlenker, J .L. *J. Am. Chem. Soc.* **1992**, *114*, 10834–10843.

(25) Kresge, C. T.; Leonowicz, M. E.; Roth, W. J.; Vartuli, J.C.; Beck, J. S. *Nature* **1992,** *35,* 710–712.

(26) Ryoo, R.; Kim, J. M.; Ko, C. H.; Shin, C.H. *J. Phys. Chem.* **1996,** *100,* 17718–17721.

(27) Inagaki, S.; Koiwai, A.; Suzuki, N.; Fukushima,Y.; Kuroda, K. *Bull. Chem. Soc. Jpn.* **1996,** *69,* 1449–1457.

(28) Zhao, D.; Feng, J.; Huo, Q.; Melosh, N.; Frederickson, G.H.; Chmelka, B.F.; Stucky, G.D. *Science* **1998**, *279*, 548–552.

(29) Feng, X.; Frywell, G. E.; Wang, L.Q.; Kim, A.Y.; Liu, J.; Kemner, K.M. *Science* **1997**, *276*, 923–926.

(30) Wei, Q.; Chen, H. Q.; Nie, Z. R.; Hao, Y. L.; Wang, Y. L.; Li, Q. Y.; Zou, J. X. *Mater. Lett.* **2007,** *6,* 1469-1473.

(31) Mercier, L.; Pinnavaia, T. J. *Chem. Mater.* **2000,** *12,* 188.

(32) Beaudet, L.; Hossain, K. Z.; Mercier, L. *Chem. Mater.* **2003**, *15*, 327.

(33) Wei, Q.; Nie, Z. R.; Hao, Y. L.; Chen, Z. X.; Wang, W.; Zou, J. X. *Mater. Lett.* **2005**, *59*, 3611–3615.

(34) Burleigh, M. C.; Markowitz, M. A.; Spector, M. S.; Gaber, B. P. *J. Phys. Chem. B* **2001**, *105*, 9935.

(35) Hall, S. R.; Davis, S. A.; Mann, S. *Langmuir* **2000**, *16*, 1454

(36) Huh, S.; Wiench, J. W.; Yoo, J.-C.; Pruski, M.; Lin, V. S.-Y. *Chem. Mater.* **2003**, *15*, 4247.

(37) Walcarius, A.; Etienne, M.; Lebeau, B. *Chem. Mater.* **2003**, *15,* 2161–2173.

(38) Chong, A. S. M.; Zhao, X. S. *J. Phys. Chem B* **2003**, *107*, 12650–12657.

(39) Melero, J.A.; Stucky, G.D.; Grieken, R.; Morales, G. *J. Mater. Chem.* **2003,** *12,* 1664.

(40) Shen, J.G.G.; Herman, R.G.; Klier, K.; *J. Phys. Chem. B* **2006**, *106*, 9975.

(41) Che, S.; Liu, Z.; Ohsuna, T.; Sakamoto, K.; Terasaki, O.; Tatsumi, T. *Nature* **2004**, *429*, 281.

(42) Gabashvili, A.; Medina, Dana D.; Gedanken, A.; Mastai, Y. J. *Phys. Chem. B* **2007**, *111*, 11105-11110.

(43) Jin, H.; Qiu, H.; Sakamoto, Y.; Shu, P.; Terasaki, O.; Che, S. *Chemistry-A European Journal* **2008**, *14*, 6413-6420.

(44) Guo, Z.; Du, Y.; Chen, Y.; Ng, S.-C.; Yang, Y. *J. Phys. Chem. C* **2010**, *114*, 14353-14361.

(45) Burkett, S. L.; Sims, S.D.; Mann, S. *Chem. Commun.* **1996**, 1367.

(46) Macquarrie, D.J. *Chem. Commun.* **1996**, 1961.

(47) Sayari, A.; Hamoudi, S. *Chem. Mater.* **2001**, *13*, 3151.

(48) Hunks, W.J.; Ozin, G.A. *J. Mater. Chem.* **2005**, *15*, 3716.

(49) Dash, S.; Mishra, S.; Patel, S.; Mishra, B. *Adv. Colloid Interface Sci.* **2008,** *140,* 77

(50) Lämmerhofer, M. *J. Chromatogr. A* **2010**, *1217*, 814-856.

(51) Zhao, D.; Huo, Q.; Feng, J.; Chmelka, B.F.; Stucky, G.D. *J. Am. Chem. Soc.* **1998**, *120*, 6024.

(52) Gregg, S.J., Sing K. S. W., Adsorption, Surface Area and Porosity. Academic Press, London 1982.

(53) Kazakevich,Y., Lobruto, R., HPLC for pharmaceutical scientists. Hoboken, Jersey: John Wiley & Sons, Inc, 2007.

(54) Dent, C.E. *J. Biochem.* **1948,** *4,* 169.

(55) Kotake, M.; Sakan, T.; Nakamura, N.; Senoh, J. *J. Am. Chem. Soc.* **1951**, *73*, 2973

(56) Franco, P.; Senso, A.; Olivero, L.; Minguillo, C. *J. Chromatogr. A* **2001**, *906*, 155-170.

(57) Rimbock, K.H.; Kastner, F.; Mannschreck, A. *J. Chromatogr.* **1896**, *351*, 346.

(58) Francotte, E.; Wolf, R. M. *Chirality* **1991**, *3*, 43.

(59) Francotte, E.; Wolf, R. M. *J. Chromatogr.* **1992**, *595*, 63.

(60) Okamoto, Y.; Aburatani, R.; Miura, S.; Hatada, K. *J. Liq.Chromatogr.* **1987,** *10*, 1613.

(61) Subramanian,G., Chiral Separation Technique. Canterbury, Kent: Wiley-VCH, Inc, 2007.

(62) Yashima, E.; Fukaya, H.; Hatada, K. ; Okamoto, Y. *J. Chromatogr. A* **1994,** *677*, 11.

(63) Santarelli, X.; Muller, D.; Jozefonvicz, J. *J. Chromatogr.* **1988,** *443*, 55.

(64) Kazakevich Y. V.; Fadeev, A. Y. *Langmuir* **2002,** *18*, 317.

(65) Giaquinto, A.; Liu, Z.; Batch, A.; Kazakevich Y. V. *Anal. Chem.* **2008**, *80*, 6358.

(66) Brunauer, S.; Emmet, P. H.; Teller, E. *J. Am. Chem. Soc.* **1938,** *60*, 309.

(67) Yamamoto, C.; Okamoto, Y. *Methods of Mol. Biol.* **2004,** *243,* 173.

(68) Yamamoto, C.; Yashima, E.; Okamoto, Y. *Bull. Chem. Soc. Jpn.* **1999,** *72,* 1815

(69) Yashima, E. *J. Chromatogr. A* **2001,** *906*, 105.

(70) Welch, C. W. *J. Chromatogr.* **1994,** *666*, 3.

(71) Cleveland, T. *J. Liq. Chromatogr.* **1995,** *18*, 649.

(72) Chankvetadze, L.; Chankvetadze, S.; Sidamonidze, E.; Yashima, E.; Okamoto, Y. *J. Chromtogr. A* **1997**, *787*, 67.

(73) Toga, Y.; Tachibana, K.; Ichida, A. *J. L. Chromtogr. & Related Technologie* **2003**, *26*, 3235.

(74) Inagaki, S.; Koiwai, A.; Suzuki, N.; Fukushima, Y.; Kuroda, K. *Bull. Chem. Soc. Jpn.* **1996**, *69*, 1449.

(75) Kresge, C. T.; Leonowicz, M. C.; Roth, W. J.; Vartuli, J. C.; Beck, J. C. *Nature* **1992**, *259*, 710.

(76) Sayari, A. *Chem. Mater.* **1996,** *8*, 1840.

(77) Murakami, Y.; Yashima, S.; Okubo, T.; Maruyama, S. *Chem. Phys. Lett.* **2003,** *375,* 393.

(78) Joo, S.H.; Choi, S. J.; Oh, I.; Kwak, J.; Liu, Z.; Terasaki, R.; Ryoo, O. *Nature* **2001,** *412,* 169.

(79) Hoffmann, F.; Cornelius, M.; Morell, J.; Fröba, M. *Angew. Chem. Int. Ed.* **2006,** *45,* 3216.

(80) Monnier, A.; Margolese, D. I.; Schuth, F.; Huo, Q.; Kumar, D.; Maxwell, R. S.; Stucky, G. D.; Krishnamurty, M.; Petroff, P.; Firouzi, A. M.; Chmelka, B. F. *Science* **1993,** *261,* 1299.

(81) Hou, Q. S.; Margolese, D. I.; Ciesla, U.; Feng, P.; Gler, T. E.; Sieger, P.; Leon, R.; Petroff, P. M.; Schuth, F.; Stucky, G. D. *Nature* **1994,** *368,* 317.

(82) Hou, Q. S.; Margolese, D. I.; Stucky, G. D. *Chem. Mater.* **1996,** *8,* 1147.

(83) Mann, S. *Nature.* **1988,** *332,* 119.

(84) Che, S.; Lim, S.; Kaneda, M.; Yoshitake, H.;Terasaki, O.; Tatsumi, T. *J. Am. Chem. Soc.* **2002,** *124,* 13962.

(85) Yokoi, T.; Yoshitake, H.; Tatsumi, T. *Chem. Mater.* **2003,** *15,* 4536.

(86) Che, S.; Garcia-Bennett, A. E.; Yokoi, T.; Sakamoto, K.; Kunieda, H.; Terasaki, O.; Tatsumi, T. *Nature Mater.* **2003,** *2,* 801.

(87) Garcia-Bennett, E.; Terasaki, O.; Che, S.; Tatsumi, T. *Chem. Mater.* **2004,** *16,* 813.

(88) Garcia-Bennett, A. E.; Che, S.; Miyasaka, K.; Sakamoto, Y; Tatsumi, T.; Ohsuna, T.; Liu, Z.; Terasaki, O. *Stud. Surf. Sci Catal.* **2005,** *156,* 11.

(89) Garcia-Bennett, A. E.; Kupferschmidt, Y.; Sakamoto, Y.; Che, S.; Terasaki, O. *Angew. Chem. Int. Ed.* **2005,** *44,* 5317.

(90) Gao, C.; Sakamoto, Y.; Sakamoto, K.; Terasaki, O.; Che, S. *Angew. Chem. Int. Ed.* **2006,** *45,* 4295.

(91) Yokoi, T.; Yamataka, Y.; Yoichiro, A.; Sato, S.; Kubota, Y.; Tatsumi, T. *Micropor. Mesoport. Mat.* **2007,** *103,* 20.

(92) Che, S.; Liu, Z.; Ohsuma, T.; Sakamoto, K.; Terasaki, O.; Tatsumi, T. *Nature* **2004,** *429,* 281.

(93) Martin, T.; Galarneau, A.; Di Renzo, F.; Fajula, F.; Plee, D. *Angew. Chem. Int. Ed.* **2002,** *41,* 2590.

(94) Xia, Y.; Mokaya, R. *J. Mater. Chem.* **2003,** *13,* 3112.

(95) Landry, C.; Tolbert, S. H.; Gallis, K. W.; Monnier, A.; Stucky, G. D.; Norby, P.; Hanson, J. C. *J. Mater. Chem.* **2001,** *13,* 1600.

(96) Gerova, M.; Rodrigues, F.; Lamere, J.F.; Dobrev, A.; Forgues, S. F. *J. Colloid Interface Sci.* **2008,** *319,* 526.